APPLICATIONS OF BOX-JENKINS METHODS OF TIME SERIES ANALYSIS TO THE

RECONSTRUCTION OF DROUGHT FROM TREE RINGS

by

David Michael Meko

A Dissertation Submitted to the Faculty of the

DEPARTMENT OF HYDROLOGY AND WATER RESOURCES

In Partial Fulfillment of the Requirements
For the Degree of

DOCTOR OF PHILOSOPHY
WITH A MAJOR IN HYDROLOGY

In the Graduate College

THE UNIVERSITY OF ARIZONA

1 9 8 1

STATEMENT BY AUTHOR

This dissertation has been submitted in partial fulfillment of requirements for an advanced degree at The University of Arizona and is deposited in the University Library to be made available to borrowers under rules of the Library.

Brief quotations from this dissertation are allowable without special permission, provided that accurate acknowledgment of source is made. Requests for permission for extended quotation from or reproduction of this manuscript in whole or in part may be granted by the copyright holder.

SIGNED: _____

ACKNOWLEDGMENTS

I owe thanks to many people who directly or indirectly made this work possible. Dr. Charles W. Stockton was especially helpful in providing support from the outset. As my dissertation advisor and employment supervisor the past five years, he helped greatly in encouraging new approaches to old problems. The tree-ring data used in this study are the result of field collections and laboratory analyses by workers from the Laboratory of Tree-Ring Research at The University of Arizona. What are "data from the files" to me represent years of diligent work by others. Dr. C. W. Stockton, W. R. Boggess, Dr. D. R. Davis, Dr. S. Ince, Dr. V. C. Lamarche, Jr., and Dr. E. S. Simpson kindly reviewed the manuscript.

TABLE OF CONTENTS

TABLE OF CONTENTS—Continued

Page

LIST OF ILLUSTRATIONS

LIST OF ILLUSTRATIONS--<u>Continued</u>

LIST OF TABLES

LIST OF TABLES--<u>Continued</u>

ABSTRACT

The lagged responses of tree-ring indices to annual climatic or hydrologic series are examined in this study. The objectives are to develop methods to analyze the lagged responses of individual tree-ring indices, and to improve upon conventional methods of adjusting for the lag in response in regression models to reconstruct annual climatic or hydrologic series. The proposed methods are described and applied to test data from Oregon and Southern California.

Transfer-function modeling is used to estimate the dependence of the current ring on past years' climate and to select negative lags for reconstruction models. A linear system is assumed; the input is an annual climatic variable, and the output is a tree-ring index. The estimated impulse response function weights the importance of past and current years' climate on the current year's ring. The identified transfer function model indicates how many past years' rings are necessary to account for the effects of past years' climate.

Autoregressive-moving-average (ARMA) modeling is used to screen out climatically insensitive tree-ring indices, and to estimate the lag in response to climate unmasked from the effects of autocorrelation in the tree-ring and climatic series. The climatic and tree-ring series are each prewhitened by ARMA models, and crosscorrelation between the ARMA residuals are estimated. The absence of significant crosscorrelations implies low sensitivity. Significant crosscorrelations at

lags other than zero indicate lag in response. This analysis can also aid in selecting positive lags for reconstruction models.

An alternative reconstruction method that makes use of the ARMA residuals is also proposed. The basic concept is that random (uncorrelated in time) shocks of climate induce annual random shocks of tree growth, with autocorrelation in the tree-ring index resulting from inertia in the system. The steps in the method are (1) fit ARMA models to the tree-ring index and the climatic variable, (2) regress the ARMA residuals of the climatic variable on the ARMA residuals of the tree-ring index, (3) substitute the long-term prewhitened tree-ring index into the regression equation to reconstruct the prewhitened climatic variable, and (4) build autocorrelation back into the reconstruction with the ARMA model originally fit to the climatic variable.

The trial applications on test data from Oregon and Southern California showed that the lagged response of tree rings to climate varies greatly from site to site. Sensitive tree-ring series commonly depend significantly only on one past year's climate (regional rainfall index). Other series depend on three or more past years' climate. Comparison of reconstructions by conventional lagging of predictors with reconstructions by the random-shock method indicate that while the lagged models may reconstruct the amplitude of severe, long-lasting droughts better than the random-shock model, the random-shock model generally has a flatter frequency response. The random-shock model may therefore be more appropriate where the persistence structure is of prime interest. For the most sensitive series with small lag in response, the choice of reconstruction method makes little difference in properties of

the reconstruction. The greatest divergence is for series whose
impulse response weights from the transfer function analysis do not die
off rapidly with time.

CHAPTER 1

INTRODUCTION

Purpose and Scope

Statistical analysis of climatic and hydrologic data is hampered by the short duration of many historical rainfall and streamflow time series. Statistics from the relatively short historical record may be misleading as indicators of expected conditions, especially when the long-term climatic record contains appreciable persistence or trends (Kilmartin 1976). At the same time, persistence and trends, and their proper specification, are of great importance to the design of reservoirs (Henry and Cassidy 1978, Lettenmaier and Burges 1978).

Considerable work in recent years has been directed toward developing stochastic simulation models that duplicate reasonably well the long-term persistence properties found in geophysical time series (Mandelbrot and Wallis 1968; O'Connell 1971; Rodriguez-Iturbe, Mejia, and Dawdy 1972; Hipel and McLeod 1978; and others). Stockton and Boggess (1979) have proposed that the reliability of estimates of long-term persistence can be improved by using hydrologic series which have been augmented or extended back in time with tree rings. This approach is valid, however, only if the persistence in tree-ring reconstructions faithfully mirrors the persistence in climate. As argued by Matalas (1962), biological memory processes in the tree itself may build persistence into tree-ring data.

1

An important function of a tree-ring reconstruction model is
therefore to adjust for, or to remove, the effects of nonclimatic
persistence--persistence not found in the driving climatic variables--
from the tree-ring data. The purpose of this study is to illustrate the
use of modern time series methods to analyze the nonclimatic persistence
in tree-ring series and to adjust for nonclimatic persistence in
reconstruction models.

The reconstruction models in modern tree-ring studies have
ranged in complexity from standard multiple linear regression (Meko,
Stockton, and Boggess 1980) to multivariate techniques such as canonical
regression with predictors and predictands both transformed beforehand
into new sets of orthogonal variables (Blasing and Fritts 1976, Stockton
and Meko 1975).

In general, the reconstruction model acts as a filter in space
and time to transform the tree-ring series into the predicted climatic
series. For example, a simple model to reconstruct annual precipitation
from tree rings at two sites is

$$Y_t = a_0 + b_1 X_{t,1} + b_2 X_{t-1,1} + b_3 X_{t,2} + b_4 X_{t-1,2} \qquad (1.1)$$

where Y_t is the predicted rainfall in year t; $X_{t,i}$ is the tree-ring
variable at the ith site in year t; a_0 is a regression constant; and
b_1, b_2, b_3, b_4 are the regression coefficients. The filtering in space
results from the weighting of tree rings from two different locations:
the larger-scale climatic variations common to both sites are empha-
sized, and the local climatic variations are smoothed out. The filtering
in time results from including tree rings from years other than year t

as predictors of climate in year t. The need for filtering in time arises from the lag in the trees' response, which causes a climatic anomaly in year t to be reflected not only in the ring-width anomaly for year t, but also to some extent in the ring-width anomalies for one or more subsequent years (Fritts 1976, p. 27).

This study concentrates on the lagged response of tree rings to an annual climate variable, and the related problem of lagging of tree rings in regression models to reconstruct the climatic variable. Some specific questions that are addressed are: (1) How many lags should be included in the regression model? (2) Does this number vary among tree-ring sites? and (3) Can lagging be dispensed with in favor of an alternative technique?

The answers to these questions are tied to the lagged responses of the individual tree-ring series to the climatic variable. Techniques that have proven useful in other fields in studying the lagged response in stochastic systems are Box-Jenkins time series and transfer-function modeling. For example, in the biological sciences, autoregressive-moving-average (ARMA) time series modeling was used by Kuehl, Buxton, and Briggs (1976) to clarify the lagged relationship between a climate variable and boll retention in cotton. Transfer-function modeling has been used to study the lagged responses in economic (Wallis 1977, Bruggeman and O'Neill 1980, Zellner and Palm 1974) and hydrologic (Sharma 1980, Whitehead 1979) systems.

ARMA and transfer-function modeling are applied to the problem of lagged response of tree rings to climate in this study. The approach taken is to model the responses of individual tree-ring series in two

test regions to annual rainfall indices in the regions. One region is centered in Southern California, the other in Northern Oregon. The results of the modeling are used to select lags for reconstruction models, and the regional precipitation indices are reconstructed using the selected lag models.

In addition, an alternative reconstruction method is proposed and tested. This method makes use of ARMA modeling to "prewhiten" or remove the autocorrelation from the tree-ring series and the rainfall index before regressing the one on the other to estimate the reconstruction equation. In this method, nonclimatic persistence is treated at the prewhitening stage, and no lags are included in the regression equations.

Finally, the regressions and long-term reconstructions by this alternative method are compared with those by the lagged-tree-ring method, and the advantages and disadvantages of each method are discussed.

Background

Persistence in the annual time series of the climatic variables governing growth is one possible source of persistence in tree-ring data. Lagging schemes would be unnecessary in reconstruction models if this were the only source of persistence. The autocorrelation in many tree-ring series is too great, however, to be attributed to climate alone (Stockton 1975), suggesting that additional persistence—referred to as nonclimatic persistence in this study—is built into the tree-ring series either by the biological system of the trees or by outside influences.

Sources of Nonclimatic Persistence

The most obvious source of nonclimatic persistence in tree-ring data is error in removal of the growth trend when converting annual ring widths to tree-ring indices. This indexing procedure, called standard-ization, is accomplished by fitting a mathematical function to the ring-width series and dividing the measured ring widths by the corresponding value of the function, which may be an exponential, a polynomial, a straight line (Stokes and Smiley 1968), or a spline function (Cook 1981). The mathematical curve is intended to represent the underlying trend of decreasing ring width with increasing tree age. This is only a mathe-matical approximation, however, and it is often a matter of judgment which curve to fit. An inappropriate choice of curve, or any substantial deviation of the true "age trend" from the selected curve, may build autocorrelation into the tree-ring index.

The age trend is only one of many possible sources of nonclimatic persistence. Natural cycles in biological processes may tend to build a periodicity into tree-ring indices. For example, many species tend to produce heavy seed crops at intervals of several years (Harlow and Harrar 1968). Stored photosynthate may consequently be channeled into cone growth at the expense of ring growth at similar intervals. Fires (Keen 1937) and insect infestation (Keen 1937, Murrow and La Marche 1978) may also induce surges and depressions of growth lasting several years. The same may be said of any other factor that alters the vitality of the tree or the competition from neighboring trees for moisture and light (Fritts 1976, p. 244).

Nonclimatic persistence can also arise from the distribution of the effects of a climate anomaly over several years by carryover in the biological response of the tree. For example, a very dry year may cause roots to die back, needles to drop, and stored food to be depleted such that the vitality of the trees and their capacity for photosynthesis is lowered for several subsequent years (Fritts 1976, p. 26).

Soil moisture storage may also build in nonclimatic persistence. A soil moisture anomaly affecting tree growth at the end of the growing season in year t may linger to affect ring width in year t+1. Soil moisture capacity, drainage properties of the soil, rooting depths of trees, and the selected annual climatic variable are likely to determine the size of this effect.

Careful selection of tree-ring sites and fitting of growth curves can possibly eliminate some of the effects mentioned above, and minimize the nonclimatic persistence in tree-ring indices; but persistence due to carryover in the biological response is not likely to be amenable to these measures.

Lagging Schemes in Tree-Ring
Reconstructions

Early workers in dendroclimatology recognized the need for considering nonclimatic persistence in interpreting tree rings. Schulman (1956, p. 39) cautioned against deriving relationships between rainfall and tree rings without recognizing the "carry over effect of excessive or deficient rainfall of earlier years, especially following extensive wet or dry periods." He found that the response of trees to a wet year sometimes lagged by more than a year, especially if the period preceding

the wet year was very dry, and attributed the lag to a "weakened vitality" of trees following a severe extended drought.

Fritts (1962), in multiple linear regression analysis of ring widths against climatic, water-balance, and prior-growth variables, found statistically significant correlation between earlywood width in year t and the preceding year's latewood width. Further work by Fritts (1965, 1974) indicated that as many as three preceding years' growth were significantly correlated with the current year's growth. In a study of 127 coniferous sites in western North America, Fritts (1974) found that ring growth on the average was directly correlated with the width of rings formed in the preceding season, and less with rings for two or three previous years.

Soon after the adoption of multivariate statistical techniques in tree-ring reconstructions (Fritts et al. 1971), several different methods for adjusting for nonclimatic persistence in reconstruction models were developed. All of these included lagged tree-ring indices in one form or another as predictors of a climate variable or a set of climate variables.

In discussing the various lagging schemes, it is convenient to use matrix notation to designate a generalized N-years by M-variables predictor matrix

$$_N\tilde{W}_M = \begin{bmatrix} W_{1,1} & W_{1,2} & \cdots & W_{1,M} \\ W_{2,1} & W_{2,2} & & \cdot \\ & \cdot & \cdot & \cdot \\ & \cdot & & \cdot & \cdot \\ & \cdot & & & \cdot & \cdot \\ W_{N,1} & & \cdot & \cdot & W_{N,M} \end{bmatrix} \tag{1.2}$$

where each column is a time series of a predictor variable and each row represents an observation or year. The M variables may be tree-ring indices or orthogonal transformations of tree-ring indices; and the predictor matrix may be calibrated with the climate variables by multiple linear regression (Draper and Smith 1966), principal components regression (Cooley and Lohnes 1971), or canonical regression (Glahn 1968), depending on the design of the problem. The focus of this study, however, is the method of including lags.

The most straightforward lagging scheme is stepwise multiple linear regression of the climate variable on the lagged tree-ring indices (Douglas 1976, 1980; Meko, Stockton, and Bogess 1980). The columns in the predictor matrix (1.2) are tree-ring indices, current and lagged, from several sites. These predictors are determined by stepwise regression from some larger pool of potential predictors, again made up of lagged tree-ring indices.

A shortcoming of this scheme is that the pool of potential predictors becomes uncomfortably large as the number of tree-ring sites increases, and as more lags are considered. The danger of spurious inflation of the multiple correlation coefficient (squared) (R^2) is consequently great (Rencher and Pun 1980).

Another shortcoming is the multicolinearity or intercorrelation of the predictors in the regression equation. Multicolinearity is inherent in the model itself, since the tree-ring indices are presumably correlated with one another and also autocorrelated. Multicolinearity can lead to regression equations whose coefficients are illogical in sign and magnitude, and consequently useless in interpreting the

relative importance of the various predictors (Cooley and Lohnes 1971, p. 56).

For example, in the drought study of Meko, Stockton, and Boggess (1980), several of the weights in the final regression equation were illogical given the physical system. A rational equation would have positive coefficients on lags 0 and +1, and negative coefficients on lag -1: the positive weights on years t and t+1 would imply high growth in those years associated with wet conditions in year t. The negative weights on t-1 would imply that the estimated wetness of year t indicated by rings t and t+1 should be reduced if the ring for year t-1 had also been wide. The weights were logical through the first seven steps of the stepwise procedure, but were illogical for four of the final five steps. Evidently, multicolinearity was important in the final regression equation. It should be noted that in the case of negative lags, the sole reason for a predictor to enter the regression is multicolinearity, since there obviously is no cause-effect relationship between the climate in year t and the tree rings from previous years. The critical question is whether the physically unrealistic model resulting from effects of multicolinearity leads to unreliable long-term reconstructions. The only sure way to guard against this possibility is by careful verification with independent data (Cooley and Lohnes 1971, p. 57).

One final drawback to the stepwise regression approach in adjusting for persistence is the uncertainty in selection of lags to include for the initial set of potential predictors. Assumption of a very small number of lags (e.g., t-1, t) may reduce the likelihood of

artificial inflation of R^2 mentioned earlier, but runs the risk of un-
satisfactorily accounting for persistence in tree-ring series that may
have a large lag in their response to climate. Assumption of a large
number of lags, on the other hand, may allow for more flexibility in
adjusting for persistence, but runs the risk of artificially inflating
R^2.

Stepwise regression on lagged tree rings is clearly not practical
when the number of tree-ring sites is large. It is also cumbersome if
the predictand set consists of more than one variable. Orthogonal trans-
formations have proven useful in these situations to emphasize large-
scale patterns of tree-growth anomalies, reduce the set of predictors
and predictands to some tractable number of transformed variables, and
eliminate the risk of multicolinearity.

The method of combining lagging with orthogonal transformation
has varied from study to study. The first method, used by Stockton
(1971, 1975) to reconstruct annual streamflow, defines a set of p
orthogonal tree-ring variables

$$z_{t,1}, \; z_{t,2}, \; z_{t,3} \; \cdots \; z_{t,p} \tag{1.3}$$

by transforming the _lagged_ tree-ring indices. Each new variable $z_{t,i}$
is a linear combination weighting the tree-ring indices both in space
and in time. Some subset M of the p transformed variables then serves
as the predictors in the generalized predictor matrix (Eq. 1.2). The
M variables to be used as predictors are selected to maximize the per
cent variance explained R^2 of the climatic data.

This method avoids the problems of multicolinearity, since the predictor variables are orthogonal to one another. It also facilitates treatment of large masses of data by transforming cumbersome tree-ring and climatic data sets into manageable subsets of predictors and predictands. The lagging scheme is very restrictive, however, in linking the adjustment for persistence to the covariation of the tree-ring indices in space. While orthogonal transformations on unlagged tree-ring indices can be interpreted as preferred modes of spatial variation of tree growth—which may be related to similar spatial patterns in climate—the transformations on lagged data do not lend themselves to physical interpretation. Conceptually, they are hybrids of covariance in space and persistence in time. There is no logical reason to expect such hybrid modes of variation to exist.

Another problem is that the number of lags to include on the tree-ring indices is uncertain. The number must be either assumed or arrived at by trial-and-error reconstructions using different numbers of lags. The problems with assuming a number of lags were mentioned before. The drawback of trial-and-error reconstructions is that if enough models are tried, the criteria of a "good" model are likely to be satisfied eventually by chance alone. The model may yield a high R^2 and even good agreement with independent data, if the independent data had already been brought into play in comparing the different reconstructions; but the long-term reconstruction generated by the model may be unreliable.

A second lagging scheme in models with orthogonally transformed variables is to transform the underlined unlagged tree-ring indices, and lag the resulting transformed variables in the predictor matrix (Stockton and

Meko 1975, Fritts 1976). The tree-ring indices are transformed into a set of K orthogonal variables:

$$Z_{t,1}, \ Z_{t,2}, \ Z_{t,3}, \ \cdots, \ Z_{t,k} \tag{1.4}$$

where each variable is a linear combination weighting the tree-ring indices in space but not in time.

A subset of the orthogonal variables is then lagged in the prediction matrix (Eq. 1.2). For example, if the model includes two orthogonal variables, lagged t-1, t, t+1, then the predictor variables are

$$Z_{t-1,1}, \ Z_{t,1}, \ Z_{t+1,1}, \ Z_{t-1,2}, \ Z_{t,2}, \ Z_{t+1,2} \tag{1.5}$$

which corresponds to the predictor variables

$$W_{t,1}, \ W_{t,2}, \ \cdots, \ W_{t,6} \tag{1.6}$$

in the generalized predictor matrix (Eq. 1.2).

The orthogonal variables $Z_{t,1}, \ Z_{t,2}, \ \cdots Z_{t,k}$ here, unlike in the previous method, can be interpreted as preferred modes of spatial variation in tree growth. This is a conceptual advantage. Unfortunately however, the lagged predictors that make up the predictor matrix are not mutually orthogonal. Thus one objective of transforming--elimination of the effects of multicolinearity--is sacrificed.

The method also does not allow for variations in persistence structure from site to site. Instead, persistence in large-scale patterns of tree growth is adjusted for by lagged predictor variables such as Z_{t-1}. In addition, the choice of lags is again uncertain, and may lead to the pitfalls discussed earlier.

A modified version of the method just discussed has recently been used by Fritts, Lofgren, and Gordon (1979). The modification is to include in the predictor matrix orthogonal variables that are transformations of "corrected" tree-ring indices. The correction consists in removing autocorrelation from each tree-ring series individually by fitting the tree-ring series to a first-order autoregressive [AR(1)] model. The residuals from the models are the "corrected" tree-ring indices.

The corrected tree-ring indices are then orthogonally transformed as the original tree-ring indices were in the previous method. The orthogonal variables from both the original tree-ring data and the corrected tree-ring data are all included as predictors in the predictor matrix (Eq. 1.2).

The modification is probably an improvement in that it recognizes the site-to-site variations in persistence and attempts to adjust for it. The other problems associated with the previous method, however, are still present. In addition, the set of potential predictors is now larger, increasing the possible number of trial-and-error reconstructions that may be run. The likelihood of a spuriously high R^2 is consequently increased.

The method of correcting the tree-ring indices is also not ideal. The persistence may not follow an AR(1) model, but a more general ARMA (p,q) model (Hipel and McLeod 1978). Moreover, climatic persistence may inadvertently be removed along with nonclimatic persistence in fitting an AR(1) model to the tree-ring index without also considering the autocorrelation of the climate variable over the same period.

In summary, lagging schemes previously used in tree-ring recon-
structions suffer from the following problems.

1. Excessive reliance on trial-and-error reconstructions, or step-
    wise selections from large pools of potential predictors may
    lead to spuriously high calibration statistics. An inappro-
    priate reconstruction model may consequently be selected, and
    the reconstruction may be unreliable.

2. Site-to-site differences in persistence of tree-ring indices are
    largely ignored, especially by methods that link the persistence
    adjustment to large-scale patterns of tree-growth anomalies.

3. Multicolinearity may lead to physically unrealistic regression
    equations and unreliable reconstructions. This is true of
    multiple linear regression models using lagged tree rings, and
    of models using lagged orthogonal variables as predictors.

4. Adjustment of tree rings for persistence by AR(1) modeling
    without regard for the autocorrelation structure of the climatic
    variable to be reconstructed may be misleading.

Each of the lagging schemes discussed in this chapter has its
advantages and disadvantages. The geographical scale of the study, the
amount of autocorrelation in the climatic and tree-ring series, and the
type of information desired from the study help determine the most
appropriate scheme. For some studies, more thorough treatment of per-
sistence than offered by these schemes may not be warranted. Where
detailed treatment is desired, however, modern time-series methods are
available that make the problem tractable.

An adequate choice of lagging schemes and of lags to include in reconstruction models can be made only if the statistical form of the lagged responses of the individual tree-ring series to the climatic variable of interest is understood. The time-series methods described in the next chapter can be used to study the lagged response, and to select appropriate lagging schemes tailored to the individual tree-ring series.

CHAPTER 2

METHODS

Autoregressive-moving-average (ARMA) time series modeling and transfer function modeling are first briefly described. Applications for studying the lagged response of a tree-ring index to a climatic or hydrologic variable are then proposed, and suggestions for selecting lags for reconstruction models are given. Finally, an alternative method to lagging to adjust for nonclimatic persistence in reconstruction models is described.

Several other time series and statistical methods are used in this study; but since they have been previously used in dendroclimatology and widely in other fields, their general descriptions are deferred to the appendices. Aspects particular to this study are elaborated on as the need arises.

Autoregressive-Moving-Average Modeling

An ARMA model is a particular form of time series model for transforming an original time series x_t, whose observations may be correlated, into a series of uncorrelated, identically distributed residuals, or random shocks α_t (Box and Jenkins 1968). The series x_t is assumed to be given as deviations from some mean level $\bar{x}$ in the discussion that follows.

The suite of possible ARMA models includes autoregressive, moving average, and mixed models. In the autoregressive AR(p) model,

16

x_t is linearly dependent on previous values x_{t-1}, x_{t-2}, ..., x_{t-p} and on the residual α_t. Thus

$$x_t = \phi_1 \, x_{t-1} + \alpha_t \qquad\qquad (2.1)$$

and

$$x_t = \phi_1 \, x_{t-1} + \phi_2 \, x_{t-2} + \alpha_t \qquad\qquad (2.2)$$

are AR (1) and AR (2), respectively, where ϕ_1 and ϕ_2 are the parameters of the model.

In the moving average MA (q) model of order q, x_t is linearly dependent on α_t and on one or more previous residuals α_{t-1}, α_{t-2}, ..., α_{t-q}. Thus

$$x_t = \alpha_t - \theta_1 \alpha_{t-1} \qquad\qquad (2.3)$$

$$x_t = \alpha_t - \theta_1 \alpha_{1-1} - \theta_2 \alpha_{t-2} \qquad\qquad (2.4)$$

are MA (1) and MA (2), respectively, and θ_1, θ_2 are the moving-average parameters.

The mixed autoregressive-moving-average ARMA (p,q) model of order (p,q) is a hybrid model in which x_t depends on past values x_{t-1}, x_{t-2}, ..., x_{t-p} and on current and past residuals α_t, α_{t-1}, α_{t-q}. Thus

$$x_t - \phi x_{t-1} - \cdots - \phi_p x_{t-p} = \alpha_t - \theta_1 \alpha_{t-1} - \cdots \theta_q \alpha_{t-q} \qquad\qquad (2.5)$$

is a general ARMA (p,q) model.

The main steps in ARMA modeling are: (1) identification of the model, (2) estimation of the parameters, and (3) diagnostic checking of the fitted model. Identification refers to the selection of the type (AR, MA, or ARMA) and order (p,q) of the model. Models in this study were identified by the Akaike Information Criteria (Akaike 1974),

computed from

$$AIC\ (p,q) = N \log\ (S_\alpha^2) + 2\ (p+q) \tag{2.6}$$

where N is the number of observations (years) in the time series x_t, and S_α^2 is the sample variance of the residuals α_t of the fitted ARMA (p,q) model. According to the criterion, the model with the lowest AIC is the best model.

The identification and estimation steps necessarily overlap in using the AIC, since trial-and-error fitting entails estimation of parameters for each entertained model. Maximum likelihood estimates of the parameters were calculated by a modified steepest descent algorithm (Box and Jenkins 1976, p. 233) with the packaged International and Statistical Libraries, Inc. (IMSL) subroutine FTMAXL.

Diagnostic checking is the evaluation of the adequacy of fit of a model. Various methods are recommended by Box and Jenkins (1976, Ch. 8). Two methods were used in this study: (1) inspection of the sample autocorrelation function of the residuals, and (2) calculation of the "Q" statistic

$$Q = N \sum_{k=1}^{k} r_k^2\ (\alpha) \tag{2.7}$$

which is approximately distributed as χ^2 with N-p-q degrees of freedom (Box and Pierce 1970). In Eq. 2.7, N is the number of years of data used in fitting the ARMA (p,q) model, and $r_k(\alpha)$ is the sample auto-correlation of the residuals α_t at lag k. The summation is carried out over K lags, where the size of K is left to the judgment of the investigator; in this study K = 20.

Large autocorrelations in the residuals are a sign of inadequate fit, and will stand out in inspection of the autocorrelation plots, as well as inflate the statistic Q (Box and Jenkins, 1976, Ch. 8).

Confidence limits on the residuals of the autocorrelations depend on the values of the estimated ARMA parameters (Box and Pierce 1970). Autocorrelations and their two-standard-error confidence limits were computed from equations given in Appendix A.

Transfer-Function Modeling

Box-Jenkins transfer-function modeling is a particular approach for identifying a physically realizable linear system in the time domain, in the presence of noise. This approach was developed largely by Box and Jenkins (1968), and the description here follows their book on time series analysis (Box and Jenkins 1976).

The system is illustrated in Figure 1. The input x_t and output y_t are assumed to be stationary. In the applications to be discussed later, x_t is a climatic variable and y_t a tree-ring index, and both series are assumed to be given as deviations from their mean levels.
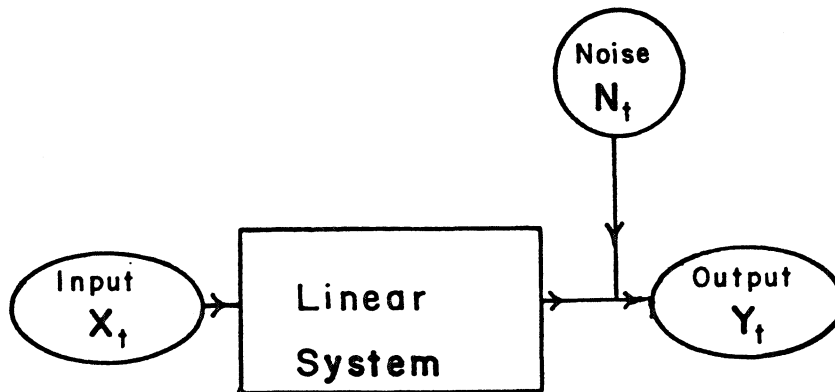
Figure 1. Diagram of Linear System.

The system is represented mathematically by

$$y_t = \sum_{k=0}^{\infty} v_k\, x_{t-k} + N_t, \qquad (2.8)$$

where the weights v_0, v_1, v_2, ... are called the impulse response function, and N_t is the noise term. The impulse response function weights the importance of past and current observations of the input.

The conversion of input deviations to output deviations by an impulse response function is illustrated in Figure 2 for an input and an output that are initially at their mean levels. The output deviation y_t can be regarded as a linear aggregate of a series of super-imposed impulse response functions scaled by the deviations x_t. The input deviations at times $t = 1$, $t = 2$, and $t = 3$ produce impuse response patterns of deviations in the output, which add together to produce the overall output response (Box and Jenkins 1976, p. 339). The impulse response v_k weights the importance of an input deviation at time t to the output deviation at time $t + k$.

The transfer function model of order (r,s,b) is a reformulation of the linear model (Eq. 2.8) into

$$y_t = \delta_1 y_{t-1} + \delta_2 y_{t-2} + \ldots + \delta_r y_{t-r}$$

$$+ \omega_o x_{t-b} - \omega_1 x_{t-b-1} - \ldots - \omega_s x_{t-b-s}$$

$$+ N_t - \delta_1 N_{t-1} - \delta_2 N_{t-2} - \ldots - \delta_1 N_{t-r}, \qquad (2.9)$$

where δ_1, ... δ_r, ω_o, ω_1, ... ω_s are parameters of the model, and the order of the model is defined by:

r = the number of lagged terms on y_t
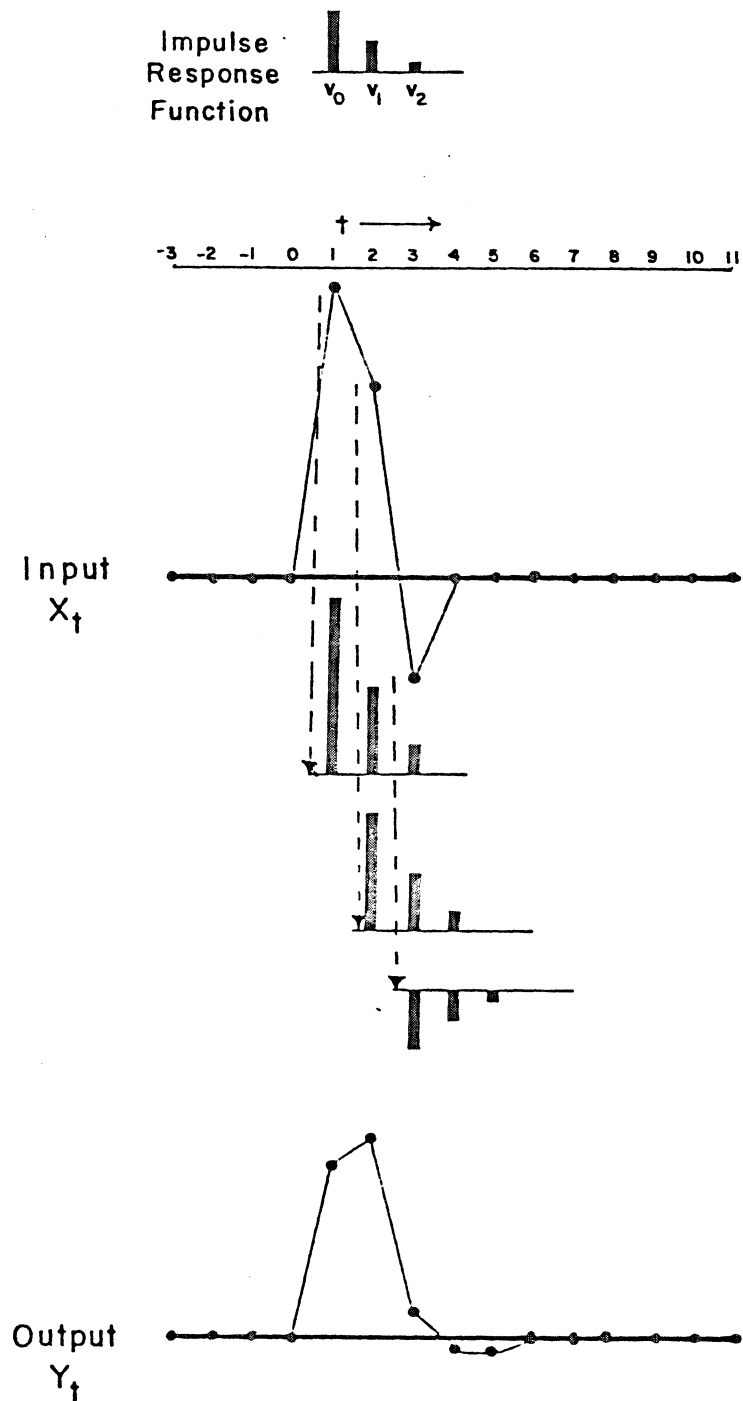
Figure 2.   Linear Transfer by a Response Function -- Linear transfer of
input X to output Y by impulse response function V
(adapted from Box and Jenkins 1976, p. 349).

s = the number of lagged terms on x_t

b = delay time of response.

The model (2.9) reformulates dependence on an indefinite number of past inputs x_{t-1}, x_{t-2}, x_{t-3}, ... into dependence on a specific number of past inputs x_{t-1} ... x_{t-s} and past outputs y_{t-1} ,,, y_{t-r}. The usefulness of this reformulation is evident if x_t is a climatic variable, and y_t a tree-ring index.

Transfer function modeling, like ARMA modeling, can be broken down into the stages of identification, estimation, and diagnostic checking (Box and Jenkins 1976, p. 335). The objectives of this study, however, are satisfied by the identification stage, which yields the numbers r and s of past years' output (tree rings) and input (climate) influencing the current year's output.

Identification is accomplished by plotting the estimated impulse response weights and comparing the decay patterns of the weights to theoretical patterns corresponding to transfer function models of specific orders (r, s, b). The next two sections describe estimation of the impulse response function and identification of the transfer function model.

Estimation of the Impulse
Response Function

The impulse response function v_0, v_1, v_2 ... in (2.8) can be estimated from sample crosscorrelations between prewhitened input and transformed output (Box and Jenkins 1976, p. 379). The procedure is diagrammed in Figure 3 and described in the following paragraphs.
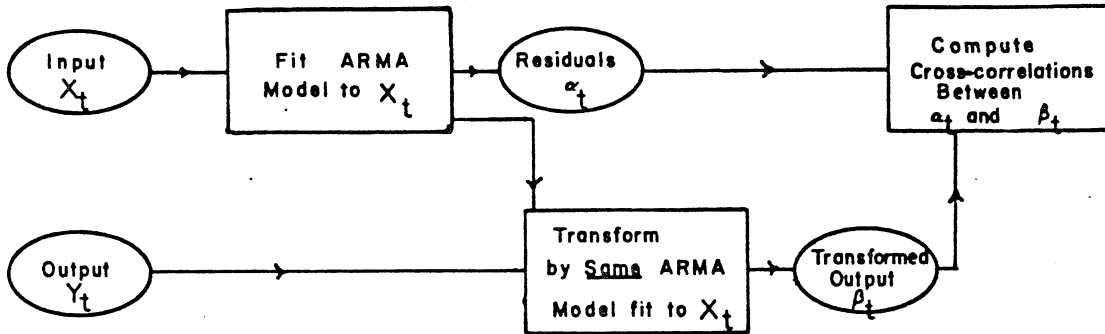
Figure 3. Procedure for Estimating the Impulse Response Function.

Prewhitening of the Input. Prewhitening refers to the removal of autocorrelation from a time series by fitting the series to an ARMA model. The procedure is conveniently shown mathematically by adopting the backward-shift notation of Box and Jenkins (see Appendix B). The general ARMA model (Eq. 2.5) can be written

$$\phi(B) \ x_t \ = \ \theta(B) \ \alpha_t \tag{2.10}$$

where $\phi(B)$ and $\theta(B)$ are polynomials of order p and q, respectively, defined as

$$\phi(B) = 1 - \phi_1 B - \phi_2 B^2 - \ldots - \phi_p B^p \tag{2.11}$$

and

$$\theta(B) = 1 - \theta_1 B - \theta_2 B^2 - \ldots - \theta_q B^q, \tag{2.12}$$

and B is the backward shift operator such that $Bx_t = x_{t-1}$.

An ARMA (p,q) model is first fit to the input x_t. The residuals α_t from the fitted model are related to the original time series (mean removed) x_t by

$$\phi(B) \; \theta^{-1} \; (B) \; x_t = \alpha_t \qquad\qquad (2.13)$$

The series α_t is the prewhitened input, and is ideally made up of random shocks or white noise, although this may not be true if the model is a poor fit. Given the fitted model, the residuals α_t can be generated from x_t by Equation (2.13).

Transformation of the Output. Equation (2.13) gives α_t as a linear transformation of x_t. The transformed output is generated by applying the same linear transformation to y_t. Thus

$$\phi(B) \; \theta^{-1}(B) \; y_t = \beta_t \qquad\qquad (2.14)$$

The series β_t is generally not random, since the transformation $\phi(B) \; \theta^{-1}(B)$ was originally derived to transform x_t to random residuals. Only if x_t and y_t happened to follow exactly the same ARMA model would β_t be random.

Computation of Sample Crosscorrelation Functions. The cross-correlations $r_{\alpha,\beta}(k)$ between α_t and β_t at lag k are directly proportional to the impulse response weights v_0, v_1, v_2, ... in Eq. (2.8). The sample crosscorrelations thus provide estimates of the impulse response weights (Box and Jenkins 1976, p. 380; Chatfield 1975, p. 221). The relationship is

$$v_k = \frac{s_\beta}{s_\alpha} \; r_{\alpha\beta}(k) \qquad\qquad (2.15a)$$

where s_α, s_β are the sample standard deviations of α_t and β_t (Box and Jenkins 1976, p. 380).

The significance of a given v_k can be judged from two-standard error confidence limits for the crosscorrelations $r_{\alpha\ \beta}(k)$. These confidence limits can be computed from

$$2 \text{ SE} = 2/\sqrt{\text{Var}(r_k)} \qquad (2.15b)$$

where $\text{Var}(r_k)$ is the sample variance of $r_{\alpha\beta}(k)$ computed by Eq. (A.11) in Appendix A. Note that $\text{Var}(r_k)$ <u>cannot</u> be computed by Eq. (A.12) because the sample variance of $r_{\alpha\beta}(k)$ is a function of the autocorrelation in α_t and β_t, and while α_t is random, β_t is generally not.

Identification of Transfer-Function Model

Identification of the transfer-function model [Eq. (2.9)] consists of finding the order (r,s,b) or, equivalently, of finding how many previous observations of y_t and x_t are important in determining the current value of y_t.

The main tool for identification is the estimated impulse response function (Box and Jenkins 1976, p. 378). The general linear model [Eq. (2.8)] can be written in backward-shift notation (see Appendix B) as

$$y_t = V(B)\ x_t + N_t \qquad (2.16)$$

where x_t and y_t are input and output deviations, N_t is the noise term, and $V(B) = v_0 + v_1 B + v_2 B^2 + v_3 B^3 + \ldots$ is the impulse response operator (see Appendix B).

The general transfer-function model can similarly be written in backward-shift notation as

$$y_t = \delta^{-1}(B)\ \omega(B)x_t + N_t \qquad (2.17)$$

where $\delta(B) = 1 - \delta_1 B - \delta_2 B^2 - \ldots - \delta_r B^r$ and $\omega(B) = \omega_0 - \omega_1 B - \omega_2 B - \ldots - \omega_s B^{\bar{s}}$ are the output operator and input operators, and other terms are defined as before in Equation (2.9).

Comparison of Equation (2.17) with Equation (2.16) yields the identity

$$V(B) = \delta^{-1}(B)\omega(B) \qquad (2.18)$$

which gives the relationship between the impulse response function v_0, v_1, v_2, $\ldots$ and the transfer function parameters δ_1, δ_2, $\ldots$ δ_r, ω_0, ω_1, $\ldots$ ω_s.

Box and Jenkins (1976, p. 378) show how this relationship allows selection of values for r, s, and b in the transfer function model from inspection of the plotted estimates v_0, v_1, v_2, v_3, $\ldots$ of the impulse response function. Characteristic decay pattern of the impulse response weights are shown to correspond to specific-order (r, s, b) transfer-function models. Identification is accomplished by comparing plotted estimates of the impulse response weights with characteristic decay patterns. Figure 4 shows characteristic decay patterns for some particular transfer function models of various orders r and s. Box and Jenkings (1976, p. 349) also allow for delay in the initial response by including a delay parameter b in the model. In this study, however, $b = 0$, since the initial response to a climate fluctuation is year t occurs in the ring for year t.

Pattern matching by visual inspection is necessarily subjective and becomes more and more difficult as the noise level N_t becomes larger relative to the signal x_t (Box and Jenkins 1976, p. 387). The
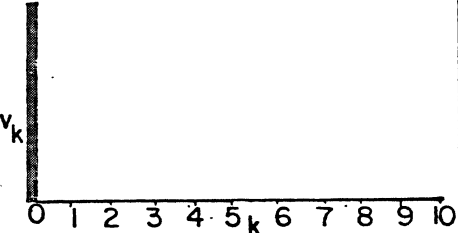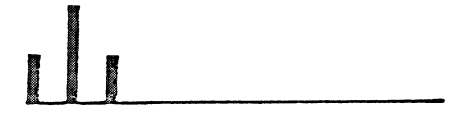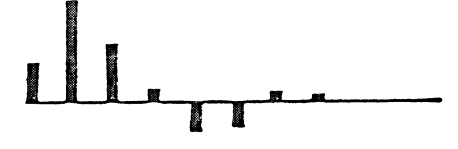
r,s,b	Transfer Function Model	Impulse Response
0,0,0	$y_t = x_t$	
0,2,0	$y = .25 x_t + .50 x_{t-1} + .25 x_{t-2}$	
1,0,0	$y = .50 y_{t-1} + .50 x_t$	
2,1,0	$y = .60 y_{t-1} - .40 y_{t-2} +$ $.40 x_t + .40 x_{t-1}$	
2,2,0	$y = .60 y_{t-1} - .40 y_{t-2} +$ $.20 x_t + .40 x_{t-1} + .20 x_{t-2}$	

Figure 4. Impulse Response Functions for Some Specific Transfer-
Function Models -- Noise term is assumed to be zero.
Adapted from Box and Jenkins (1976, p. 349).

general features of importance in matching are the type of decay pattern (single versus double exponential) and the presence or absence of preliminary values preceding the decay. The pattern-matching steps are shown in a flow chart on Figure 5. Where two or more models seemed equally plausible in this study, the simpler was selected.

The noise term N_t is generated from the impule-response form of the linear model [Eq. (2.8)]. Since the summation in Equation (2.8) is infinite, the impulse response function must arbitrarily be truncated at some lag in generating initial noise estimates. The truncation point was lag $k = 10$ for all models in this study.

N_t is in general not random, but is assumed to follow an ARMA model called the noise model (Box and Jenkins 1976, p. 362). The noise model can be fit by the general ARMA modeling procedure described at the beginning of this chapter.

Analysis of Lagged Response of Tree Rings

Transfer-function modeling and ARMA modeling can be applied to study the lagged response of a tree-ring index to a climatic variable. This section proposes three possible uses.

1. To estimate the number of past years' climate or tree rings that statistically influence the current ring.

2. To determine whether climate in year t affects future ring widths through autocorrelation in the tree rings, or through a more direct pathway.

3. To screen out insensitive tree-ring sites.

Estimated Impulse
Response Function v_j

v_i _____.95 sig. level

_____.95 sig. level v_j

Any Significantly Large Impulse Response Weights?

YES

NO

Noise Level too High. Discard Series

General Shape of Impulse Response Plot?

sharp cutoff

gradual decay

r = 0
s = number of significant weights minus 1

Stop

Simple Exponential Decay ?

no

yes

r = 2

r = 1

n = # of leading weights before start of Decay Pattern.

s = n+r-1

Stop

Figure 5. Flow Chart of Procedure for Identifying Transfer-Function
Models -- Symbols are as defined in Equation (2.9), p. 20 in
text. Sample impulse response plots are also given to
illustrate the types of situations that may be encountered.

Dependence on Past Year's
Climate or Tree Rings

If the climate variable is regarded as the input x_t and a tree-ring index the output y_t in the general linear system [Eq. (2.8)], the estimated impulse response weights indicate the relative importance of past years' climate to the current year's tree-ring index. The identified transfer-function model then reformulates the dependence on past climate into dependence on past years' tree rings.

The model and the reformulation can perhaps be made clearer by a simple example. Consider a transfer function model [Eq. (2.9)] of order ($r = 1$, $s = 0$, $b = 0$),

$$y_t = \delta \, y_{t-1} + \omega_0 x_t + N_t - \delta \, N_{t-1}, \tag{2.19}$$

giving the tree-ring index y_t in year t in terms of climate x_t in year t and tree-ring index in year t-1. The term y_{t-1} in Equation (2.19) can be substituted for by

$$y_{t-1} = \delta \, y_{t-2} + \omega_0 x_{t-1} + N_{t-1} - \delta \, N_{t-2} \tag{2.20}$$

to get

$$y_t = \omega_0 x_t + \omega_0 \, \delta x_{t-1} + \delta^2 y_{t-2} \tag{2.21}$$

$$+ N_t + \delta N_{t-1} + \delta^2 N_{t-2}$$

Successive substitutions of this kind eventually yield

$$y_t = \omega_0 (x_t + \delta x_{t-1} + \delta^2 x_{t-2} + \ldots + \delta^i x_{t-i})$$

$$+ \delta^i y_{t-i} + \text{noise terms} \tag{2.22}$$

Equation (2.22) gives the tree-ring index in year t in terms of weighted past years' climate, some remote past year's tree-ring index, plus noise. To satisfy requirements of stability, $|\delta|$ must be smaller than 1.0 (Box and Jenkins 1976, p. 346). Equations (2.22) and (2.19) therefore show that statistical dependence on one prior ring and current year's climate is equivalent to exponentially decreasing dependence on many past years' climate.

Comparison of Equation (2.22) with the general linear model [Eq. (2.8)] suggests an impulse response function of the shape shown below:
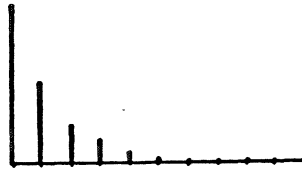
Note that this shape is the characteristic decay pattern (see Figure 4) for a (1,0,0)-order transfer function, which is the initial model given by Equation (2.19).

In practice little is known about the form of the lagged response at the start of analysis. The first step is to estimate the impulse response weights v_0, v_1, v_2, v_3, ... and to plot them along with their confidence limits. The next step is to identify the transfer function model from visual inspection of the impulse response plot, following the guidelines outlined in Figure 5.

If, as in the previous example, the estimated impulse response function decays exponentially, identification leads to a (1,0,0) transfer-function model. Such a result implies that the tree-ring index in year t depends on several past years' climate, but that this

dependence can be adequately summarized statistically as dependence on only one previous year's ring.

Lagged Response Minus Effects of
Autocorrelation

The lag in a tree's response to climate as indicated by the impulse response function can arise from two distinct pathways: inertia in the biological system, or direct influence of climate in year t on one or more subsequent rings. The first pathway is passive, the second active. The distinction is illustrated in Figure 6, which shows a hypothetical response of a tree-ring series to a climate variation in year t. The straight solid lines labeled a and b designate possible pathways of direct influence of climate on ring width. The curved solid lines c and d designate possible independent pathways of persistence-- independent in that autocorrelation in one series need not be driven by autocorrelation in the other series. The dotted lines designate rele- vant pairings for sample autocorrelations $r_{xx}(k)$ and $r_{yy}(k)$, and sample crosscorrelation estimates $r_{xy}(k)$.

Assume that the following notation applies:

$i \neq 0$ direct influence by pathway i

$i = 0$ no direct influence by pathway i

where i may represent pathways a, b, c, or d.

Sample crosscorrelations could indicate statistically signifi- cant lag in response $(r_{xy}(1) \neq 0)$ for any of the following reasons:

1. $b \neq o$: climate in year t directly influences the tree-ring
    index in year $t+1$. A stochastic representation is that the
    tree-ring index is a moving average of several years' climate.
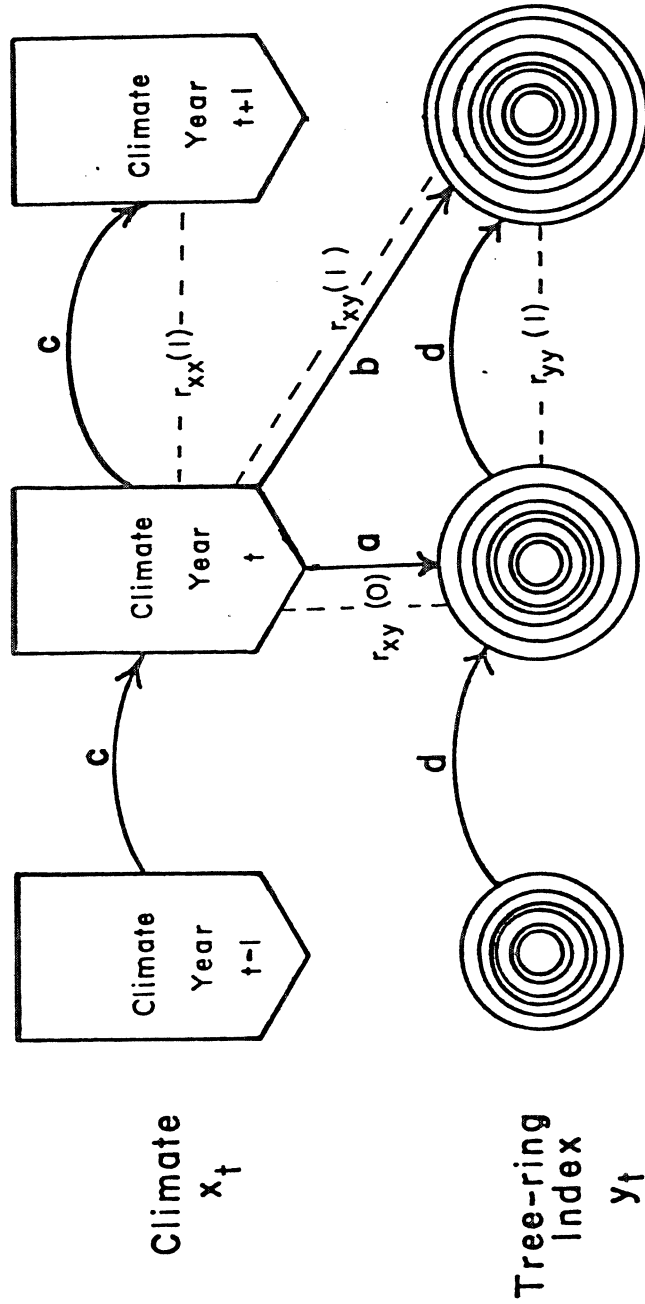
Figure 6. Schematic Diagram of Lagged Response of Tree-Rings to Climate -- Solid lines a, b, c, and d represent possible direct pathways of influence between series and between successive observations within series. Relevant autocorrelations are given by $r_{xx}(k)$ and $r_{yy}(k)$, where k is the lag; relevant crosscorrelations are given by $r_{xy}(k)$.

2. $a \neq 0$, $b = 0$, $c = 0$, and $d \neq 0$: climate in year t causes a
    growth response in year t and the inertia in the biological
    system of the tree leads to a related deviation from normal in
    ring width in year t+1. A stochastic representation is that the
    tree ring depends on the previous year's tree-ring index and the
    current year's climate. Here the system is autoregressive.

3. $a \neq 0$, $b = 0$, $c \neq 0$, $d = 0$: climate in year t causes a growth
    response in year t, and autocorrelation in the climatic variable
    indirectly leads to a spuriously significant non-zero cross-
    correlation $r_{xy}(1)$ through similar autocorrelation induced in
    the tree-ring series.

The only direct pathway for a lag in response is number 1: the
other two pathways may lead to a spuriously high $r_{xy}(1)$ solely because
of autocorrelation in the individual series. ARMA modeling can be used
to distinguish direct lag from spurious lag. The spurious effects of
autocorrelation can be eliminated by removing the autocorrelation from
(prewhitening) the time series before computing their sample cross-
correlation functions (Jenkins and Watts 1968, p. 340). A statistically
significant crosscorrelation between the prewhitened series at lak k
indicates a direct lag in response. The required steps in the procedure
are summarized below.

1. Fit the climatic series and the tree-ring index series for a
    common time period to separate ARMA models. This can be accom-
    plished by the modeling procedures described earlier in this
    chapter. The ARMA residuals are the prewhitened series.

2. Compute the sample crosscorrelation function between the pre-
   whitened series and test the significance of the crosscorrela-
   tion estimates by computing the two-standard-error confidence
   limits by Equation (2.15b). Note that since both series are
   random, the sample variance in Equation (2.15b) can be computed
   by

$$\text{Var } (r(k)) = 1/N \tag{2.23}$$

   where N is the sample size (Jenkins and Watts 1968, p. 340; and
   Equation A.11 in Appendix A).

Screening Out of Insensitive
Tree-Ring Series

The sample crosscorrelation between two time series may be
spuriously large because of autocorrelation in the individual series
(Jenkins and Watts 1968, p. 338). A better estimate of the degree of
relationship between the series can be found by the procedures just dis-
cussed: ARMA modeling and subsequent crosscorrelation analysis of ARMA
residuals. If none of the sample crosscorrelations are significant, it
may be concluded that the series are not significantly related to one
another (Jenkins and Watts 1968, p. 340). The procedure just discussed
can therefore be used to screen out climatically insensitive tree-ring
series.

Selection of Lags for Reconstruction Models

The information on the lagged response given by the transfer-
function modeling and the crosscorrelation analysis between prewhitened
series can be used to select lags for reconstruction models. The

general problem, as discussed in Chapter 1, is which lags, ... t-2, t-1, t, t+1, t+2, ... of the tree-ring indices to include in a regression model to predict climate in year t.

The order (r,s,b) of the identified transfer-function model provides useful information on the required negative lags. The transfer function model [Eq. (2.9)] indicates that the tree-ring index in year t depends on the climate back through year t-s and on r previous years' tree-ring indices. The larger of r and s therefore marks the upper limit on the number of past years that need to be considered in adjusting the tree-ring index for persistence. Appropriate negative lags for the reconstruction model are accordingly lags through t-τ, where τ is the larger of r and s in the identified transfer function model.

The selection of positive lags for the reconstruction model is more complicated than the selection of negative lags. Positive lag k is included to take advantage of any information on climate in year t in the ring for year t+k. The size of the estimated impulse-response weight v_k [Eq. (2.8)] measures the relative importance of climate in year t to the tree-ring index in year t+k. One possible approach, therefore, is to include positive lags t+k in the reconstruction model, where k is any lag with a significantly large estimated impulse-response weight v_k.

This adv ice must be tempered by the additional consideration, however, that the lag in the response may be a spurious result of autocorrelation, as described earlier in reference to Figure 6. The purpose of including positive lags in reconstruction models is to gain additional information on climate in year t not already found in ring t

adjusted for prior growth. The crosscorrelation analysis on prewhitened variables may therefore be a more appropriate tool than the impulse weights for selecting positive lags. The positive lags to include would accordingly be those with significantly large crosscorrelations.

The importance of the decision on positive lags to the final reconstructions is discussed further in referring to the trial applications in Chapter 3. First, however, a possible alternative reconstruction technique that makes use of prewhitening of regression variables is described.

An Alternative Reconstruction Model

If the crosscorrelations between prewhitened climate and pre-whitened tree-ring index are insignificant except at lag zero, the ring in year t adjusted for past conditions provides all of the available information on climate in year t. The prewhitened variables--ARMA residuals--in such a system conceptually represent random shocks of climate and tree growth. The single significant spike in the sample crosscorrelation at lag zero indicates that random shocks of climate are related to random shocks of tree growth, with no lag in the response. A consistent reconstruction model is to reconstruct shocks of climate in year t from the random shock of tree growth in year t. The random shocks of tree growth required as predictors are residuals from fit of the tree-ring series to an ARMA model.

For example, consider the simple system illustrated in Figure 7, with climate deviations y_t, tree-ring index deviations x_t, and an impulse response function v_k. For convenience, noise is assumed to be
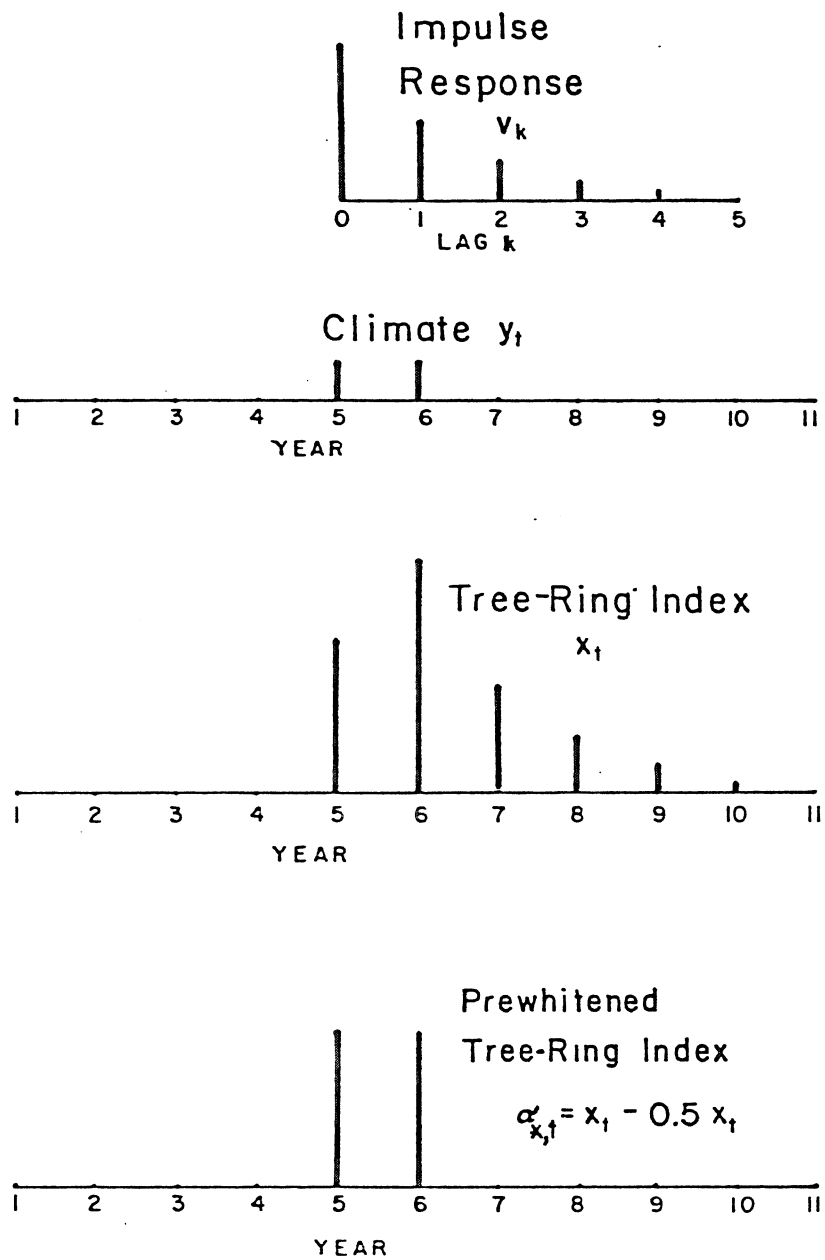
Figure 7. Diagram Illustrating Use of Prewhitening to Filter the
Climatic Signal from a Tree-Ring Series -- The lengths of
the bars are proportional to deviations of the series from
their mean levels.

zero, and tree rings and climate are assumed to be at the mean levels in the years immediately preceding the two wet years $t = 5$ and $t = 6$. The climate deviations for those years are transferred to output deviations (tree-ring index) according to the impulse response [Eq. (2.8) and Figure 2].

Cursory inspection of the climate and tree-ring index plots in Figure 7 suggests that perhaps rings t+1, t+2, and t+3 should be included as predictors of climate in year t in a reconstruction model. This suggestion may be misleading, however, because the information on climate in years 5 and 6 from subsequent rings may be redundant. More appropriate representation if the random shock concept holds true is a one-to-one correspondence between random shocks, as can be seen from the tree-ring series prewhitened by the model $\alpha_{x,t} = x_t - 0.5\, x_{t-1}$. The appropriate reconstruction model therefore is to prewhiten the tree-ring index, and scale the resulting ARMA residuals by a constant. For a system including noise, the constant might represent a regression coefficient that would allow some per cent of the variance of the y_t to be predicted by the shocks $\alpha_{x,t}$.

A reconstruction model consistent with the random-shock concept is proposed here for more general conditions. The main steps are to (1) remove the autocorreleation from (prewhiten) the tree-ring series and climate series individually by fitting ARMA models to them, (2) regress the prewhitened climatic variable against the prewhitened tree-ring indices, (3) generate a reconstructed series of the prewhitened climate variable using the estimated regression equation, and (4) build back the autocorrelation into the reconstructed prewhitened climatic variable.

The procedure is summarized in flow chart form in Figure 8, and is discussed in detail in the following sections.

Mathematical Procedure

Prewhitening. The tree-ring index x_t and climate variable y_t are fit to ARMA (p,q) models

$$\phi_x(B) \ x_t = \theta_x(B) \ \alpha_{x,t} \qquad (2.24)$$

and

$$\phi_y(B) \ y_y = \theta_y(B) \ \alpha_{y,t} \qquad (2.25)$$

where $\phi_x(B)$, $\theta_x(B)$, $\phi_y(B)$, and $\theta_y(B)$ are backward shift operators analogous to those described in the section on transfer-function modeling [Eqs. (2.11) and (2.12)]. The notation is explained in Appendix B. The residuals $\alpha_{y,t}$ and $\alpha_{x,t}$ are the prewhitened variables. Ideally, $\alpha_{y,t}$ and $\alpha_{x,t}$ are white noise, although they may not be if the ARMA model is poorly fit. A common period is used for fitting both models.

Crosscorrelation Functions. Sample crosscorrelation estimates $r_{\alpha_x \alpha_y}(k)$ between $\alpha_{x,t}$ and $\alpha_{y,t}$ at lag k are computed [Eqs. (A.9) and (A.10) in Appendix A] for the same period used to fit the ARMA models.

The sample crosscorrelations are plotted and tested for significance. Assuming the filtered series are random, the standard error of the crosscorrelation estimates is

$$SE = \sqrt{1/N} \qquad (2,26)$$

where N is the number of years in the series (Jenkins and Watts 1968, p. 340).
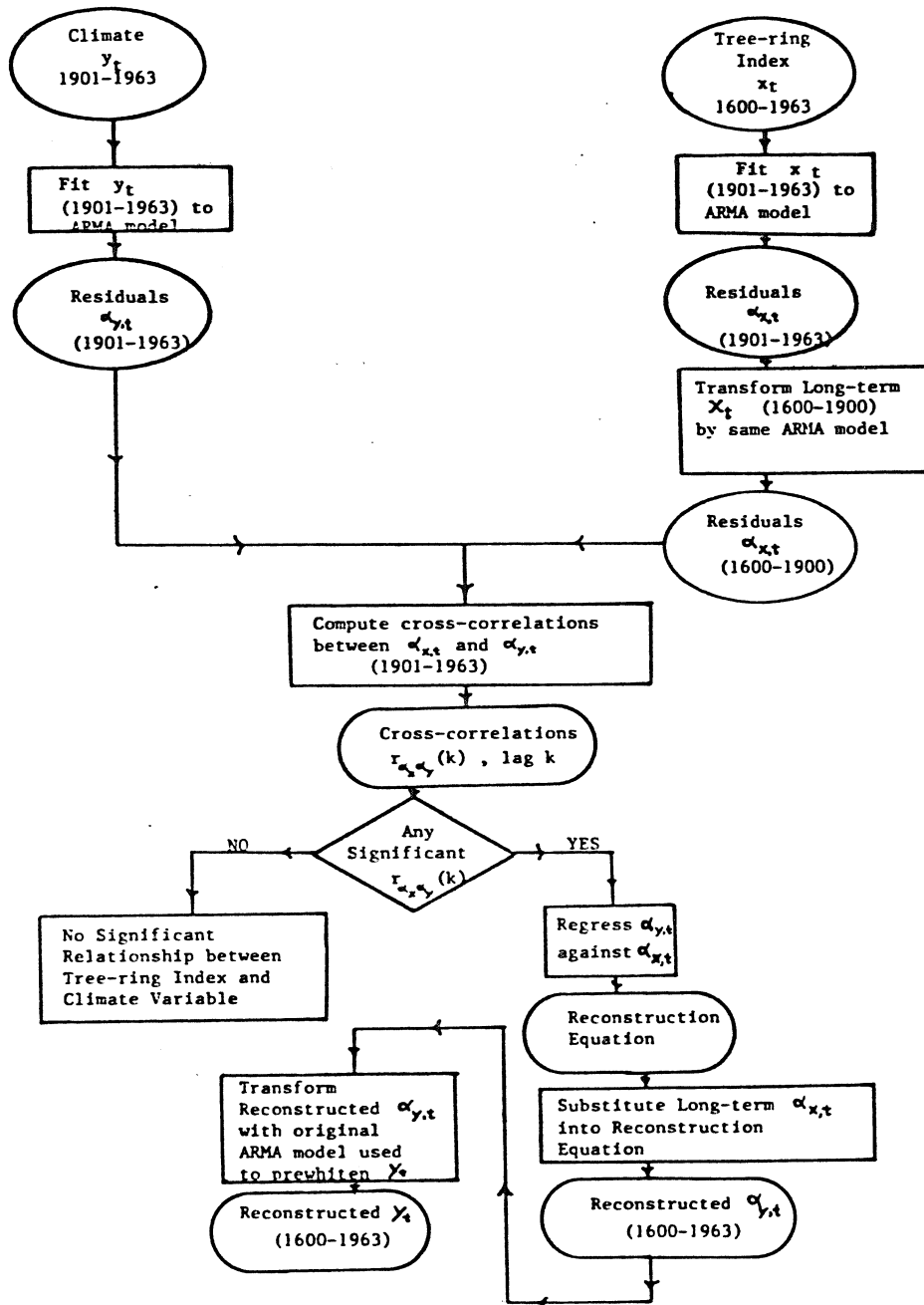
Figure 8. Procedure for Reconstructing a Climate Series from a Tree-Ring Series Using Prewhitened Variables -- Climate data are assumed to cover the period 1901-1963, and tree rings to cover 1600-1963.

Regression. The prediction equation is derived by simple linear regression (Draper and Smith 1966) of prewhitened climate $\alpha_{y,t}$ on prewhitened tree-ring index $\alpha_{x,t}$. The resulting equation is of the form

$$\hat{\alpha}_{y,t} = \hat{b}_0 + \hat{b}_1 \alpha_{x,t} \qquad (2.27)$$

where $\hat{b}_0$ and $\hat{b}_1$ are the constant and regression coefficient and the hat ($\hat{}$) denotes predicted or estimated values.

Transformation of Long-Term Tree-Ring Series. The regression equation (2.27) provides estimates of the prewhitened climate variable $\alpha_{y,t}$ from the prewhitened tree-ring index $\alpha_{x,t}$. The long-term tree-ring record must therefore be converted from x_t into $\alpha_{x,t}$ before substituting in Equation (2.27). The conversion is made by applying the original ARMA prewhitening model for x_t to the long-term tree-ring index:

$$\alpha_{x,t} = \theta_x^{-1}(B) \; \phi_x(B) \; x_t \qquad (2.30)$$

where the terms are defined as in Equation (2.24). The long-term series $\alpha_{x,t}$ is not necessarily white noise, even if $\alpha_{x,t}$ in the calibration period is, because the prewhitening model [Eq. (2.24)] was estimated from data in the calibration period only.

Reconstruction of Prewhitened Climate. The series $\alpha_{x,t}$ generated in the previous step is substituted into the regression equation (2.27) to generate long-term estimates $\hat{\alpha}_{y,t}$ of the prewhitened climate variable:

$$\hat{\alpha}_{y,t} = \hat{b}_0 + \hat{b}_1 \alpha_{x,t} \qquad (2.31)$$

Building Autocorrelation Back Into the Reconstructed Series.

The long-term reconstruction $\hat{\alpha}_{y,t}$ is transformed by

$$\hat{y}_t = \phi_y^{-1} (B) \; \theta_y(B) \; \hat{\alpha}_{y,t} \qquad (2.32)$$

where the operators $\phi_y(B)$ and $\theta_y(B)$ are the same as in the original pre-whitening model [Eq. (2.25)] and $\hat{y}_t$ is the desired long-term recon-struction in terms of the original climate variable.

Discussion of the Method

Hypothetical Examples. The operations in the reconstruction procedure and the logic behind them can perhaps be made clearer by con-sidering some simple hypothetical examples. Consider first the simple system with the following properties: (1) climate y_t follows a simple AR(1) model

$$y_t - 0.5 \; y_{t-1} = \alpha_{y,t} \qquad (2.33)$$

(2) the trees build in no additional autocorrelation (pathway a = 0 in Figure 6) and the tree-ring index series follows the same AR(1) model as the climate:

$$x_t - 0.5 \; x_{t-1} = \alpha_{x,t} \qquad (2.34)$$

Analogous to the situation described in Jenkins and Watts (1968, p. 338), direct estimates of the crosscorrelations between x_t and y_t might wrongly indicate a lag in the relationship between x_t and y_t, manifested by large crosscorrelations at lags other than zero.

Prewhitening produces series

$$\alpha_{y,t} = y_t - 0.5 \; y_{t-1} \qquad (2.35)$$

and

$$\alpha_{x,t} = x_t - 0.5 \, x_{t-1}, \qquad (2.36)$$

which are white noise correlated significantly only at lag zero. The regression equation [Eq. (2.27)] is

$$\hat{\alpha}_{y,t} = \hat{b}_0 + \hat{b}_1 \, \alpha_{x,t}. \qquad (2.37)$$

The long-term tree-ring indices are transformed by

$$\alpha_{x,t} = x_t - 0.5 \, x_{t-1} \qquad (2.38)$$

and substituted into Equation (2.37) to get a reconstruction of $\alpha_{y,t}$, which is subsequently transformed back into the original climate variable by the equation

$$\hat{y}_t = 0.5\hat{y}_{t-1} + \hat{\alpha}_{y,t} \qquad (2.39)$$

This first example is trivial in the sense that no lags are needed for reconstruction: a satisfactory reconstruction would simply be the tree-ring index scaled by some regression constant. The proposed reconstruction method accomplishes the same thing as simple scaling, though in a roundabout way. A certain amount of autocorrelation is removed at the prewhitening stage, and the same amount is built back in when the reconstructed prewhitened climate variable is transfored by Equation (2.39) back into the original climate variable.

Consider next an example in which the tree-ring index series is appreciably autocorrelated, but the climate variable is not. Assume that the climate variable y_t is random, and that the tree-ring index x_t follows the ARMA model

$$x_t - 0.5 \, x_{t-1} = \alpha_{x,t} \qquad (2.40)$$

The regression equation is

$$\hat{\alpha}_{y,t} = b_0 + b_1 \alpha_{x,t} \qquad (2.41)$$

Since the climate variable is assumed to be white noise, $y_t = \alpha_{y,t}$, and the reconstruction equation is

$$\hat{y}_t = b_0 + b_1 \alpha_{x,t} \qquad (2.42)$$

In this example, a prewhitened tree-ring index serves as the predictor for the climate variable. A similar procedure, discussed in Chapter 1, has been used in tree-ring reconstruction by Fritts et al. (1979). There are some important differences, however. Fritts et al. (1979) assumed that the ARMA model for the tree-ring index was ARMA(1,0), fit the model to the long-term tree-ring index series, and did not model the climate variable. The method proposed here fits a general ARMA (p,q) model to the tree-ring data from the same period covered by the climatic series, and also fits an ARMA model to the climate series. This method reduces to that of Fritts only if the following conditions are satisfied: (1) the climate series in the calibration period is random; and (2) the tree-ring series follows an AR(1) model in the calibration period, and the same AR(1) model in the long term.

As a final example, assume that the tree-ring index and climate variable are autocorrelated, but not equally, so that the climate follows the AR(1) model

$$y_t - 0.2 y_{t-1} = \alpha_{y,t} \qquad (2.43)$$

and the tree-ring index follows the different AR(1) model

$$x_t - 0.5 x_{t-1} = \alpha_{x,t} \qquad (2.44)$$

The regression model is

$$\hat{\alpha}_{y,t} = \hat{b}_0 + \hat{b}_1 \alpha_{x,t} \tag{2.45}$$

Persistence is removed from the tree-ring index and climate variable by Equations (2.43) and (2.44). The regression equation (2.45) is then used to reconstruct $\alpha_{y,t}$; and finally, persistence is built back into the reconstruction by the transformation

$$\hat{y}_t = 0.2 \, \hat{y}_{t-1} + \hat{\alpha}_{y,t} \tag{2.46}$$

This example is a hybrid of the previous two examples: auto-correlation in the tree-ring index arises partially from autocorrelation in the climatic variable, and partially from inertia in the trees' response to climate. Prewhitening of the tree-ring index series removes both climatic and nonclimatic persistence. The prewhitened tree-ring index series is therefore best related not to the original climatic variable, but to the adjusted climatic variable given by Equation (2.43). Conceptually, the prewhitened variable $\alpha_{y,t}$ represents the random shocks of climate that induce corresponding random shocks of tree growth.

Limitations. An important shortcoming of the method proposed above is that all information on climate in year t is assumed to come from current and past rings x_t, x_{t-1}, x_{t-2}, ... Future rings x_{t+1}, x_{t+2}. ... do not enter into the reconstruction for year t. For example, the model given by Equation (2.46) can be rearranged and expanded into

$$\hat{y}_t = 0.2 \, \hat{y}_{t-1} + \hat{b}_0 + \hat{b}_1 \, (x_t - 0.5 \, x_{t-1}) \tag{2.47}$$

A long-term reconstruction of y_t can be generated from (2.47) by assuming a starting value for y_{t-1}, and substituting in tree rings x_t. A reconstruction for year t therefore requires (1) previous year's reconstruction, $\hat{y}_{t-1}$, (2) tree-ring indices for years x_t and x_{t-1}.

In reality, however, the ring in year x_{t+1} and rings in subsequent years can possibly hold independent information on climate in year t not found in the ring for year t adjusted for the past rings x_{t-1}, x_{t-2}, ... This possibility was discussed earlier regarding Figure 6.

The physical system could easily give rise to such a lag in response. For example, assume that the ring in year t has essentially finished growing in early summer, and that heavy rains throughout the summer and fall provide favorable moisture conditions for high net photosynthesis and food storage through July, August, and September. These high food reserves may help lead to a wide ring in year t+1. If the climate variable is water-year (October-September) total precipitation, climate in year t has affected ring growth in year t+1; and the ring in t+1 holds information on climate in year t not found in the ring for year t. The converse situation would apply of severe drought occurred in summer and fall, with low net photosynthesis, root dieback, and foliage damage helping to contribute to a narrow ring in year t+1.

Another possible limitation of the method is that the ARMA models may fit the data poorly. The ARMA residuals may consequently be autocorrelated, and the formula for confidence limits on the cross-correlation [Eq. (2.23)] of prewhitened variables may not apply.

A related problem is the possibility that more than one sample crosscorrelation estimate $r_{\alpha_x \alpha_y}(k)$ may be significant by the

two-standard-error criterion. The regression model [Eq. (2.27)] relating $\alpha_{y,t}$ to $\alpha_{x,t}$ may then be inappropriate, since $\alpha_{y,t}$ is significantly correlated with $\alpha_{x,t}$ at some lag k other than k = 0. One possible solution is to compromise the random shock model and alter the regression equation to allow for lagged $\alpha_{x,t}$ as predictors of $\alpha_{y,t}$. For example, if $r_{\alpha_x \alpha_y}(k)$ is significant at lags k = 0 and k = 2, the altered regression model is

$$\hat{\alpha}_{y,t} = \hat{b}_0 + \hat{b}_1 \alpha_{x,t} + \hat{b}_2 \alpha_{x,t+2} \qquad (2.48)$$

where terms are as defined in Equation (2.31).

Model (2.48) implicitly allows the tree-ring index in years t + 1 and t + 2 to help determine the predicted climate in year t; this may be an advantage over (2.27), considering the physical system. The random shock concept no longer applies in (2.48) however, since a moving average of random shocks can not logically be interpreted as a random series itself. This last point makes the altered form statistically inconsistent, and for this reason, only the unlagged form of the prewhitened model [Eq. (2.27)] has been considered in the trial applications in the next chapter.

CHAPTER 3

APPLICATION OF THE BOX-JENKINS APPROACH TO
DATA FROM TWO TEST REGIONS

The methods discussed in Chapter 2 have been applied to test

data from two regionsin the western United States. The first section of

this chapter describes the data. Subsequent sections describe the

results of applying transfer functions and ARMA modeling to study the

lagged responses of individual tree-ring series to climate. Finally,

climate is reconstructed by the prewhitened-variable method, and the

reconstructions are compared with reconstructions from regression models

using lagged tree-ring indices.

Data

The two geographical areas selected for application of the Box-

Jenkins techniques are shown on the maps in Figures 9 and 10. In the

analyses that follow, they are referred to as the North region and the

South region. The South region was selected because of the abundance of

climatically sensitive tree-ring data on file from there, and the

author's previous work with the data (Meko, Stockton, and Boggess 1980).

The North region, not nearly as well represented by high quality tree-

ring collections as the South, was selected to test the application of

the proposed methods where the climatic signal/noise ratio in the tree

rings is relatively small. A reconstruction for the North was also of

interest because of the great importance of that area to water supply
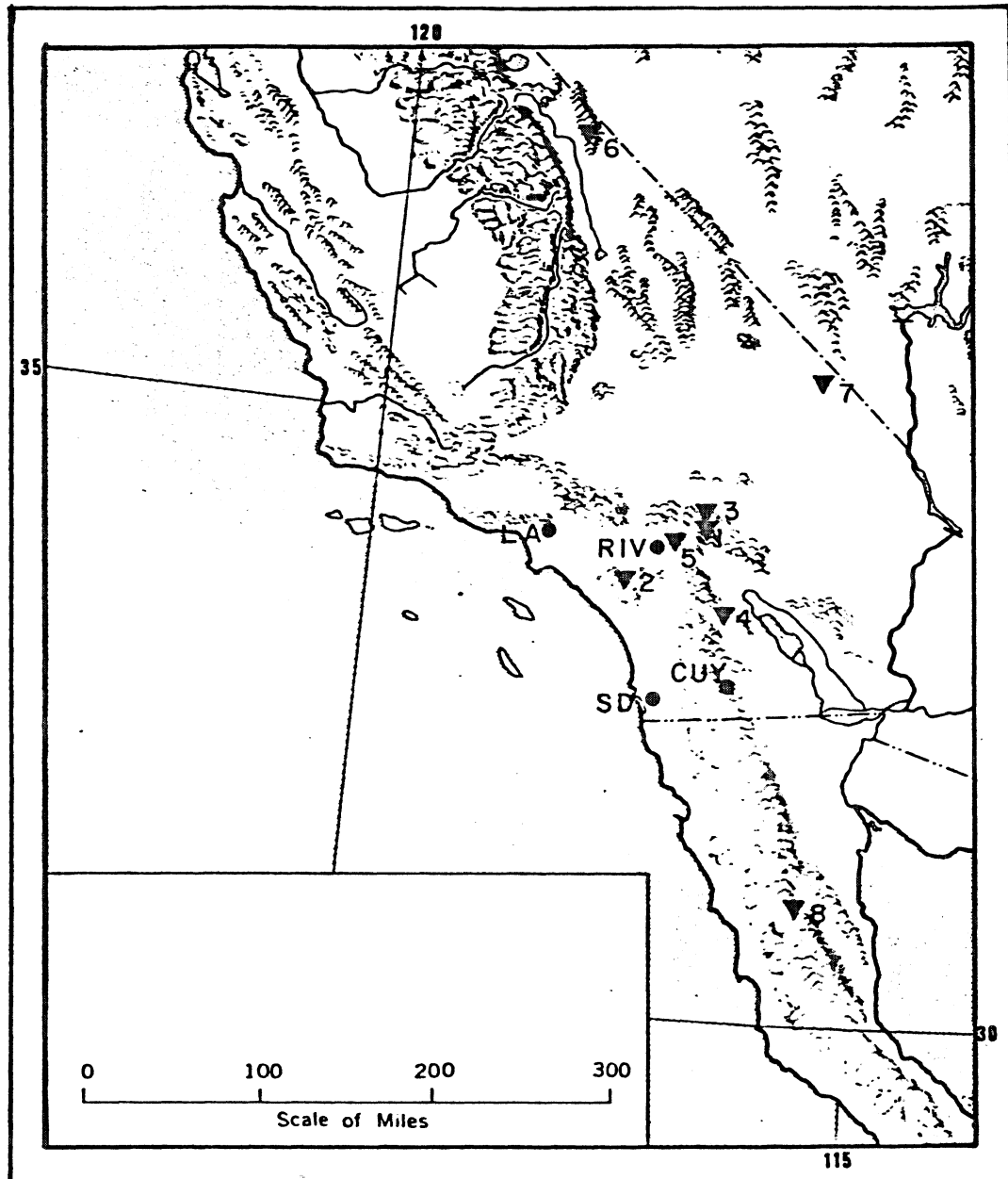
Figure 9. Map Showing Locations of Tree-Ring Sites and Climatic
Stations in the South Region — Tree-ring sites are marked
by triangles and are numbered as in Table 1. Climatic
stations, marked by dots, are Los Angeles (Civic center
station), Riverside (Fire Station #3), San Diego, and
Cuyamaca.
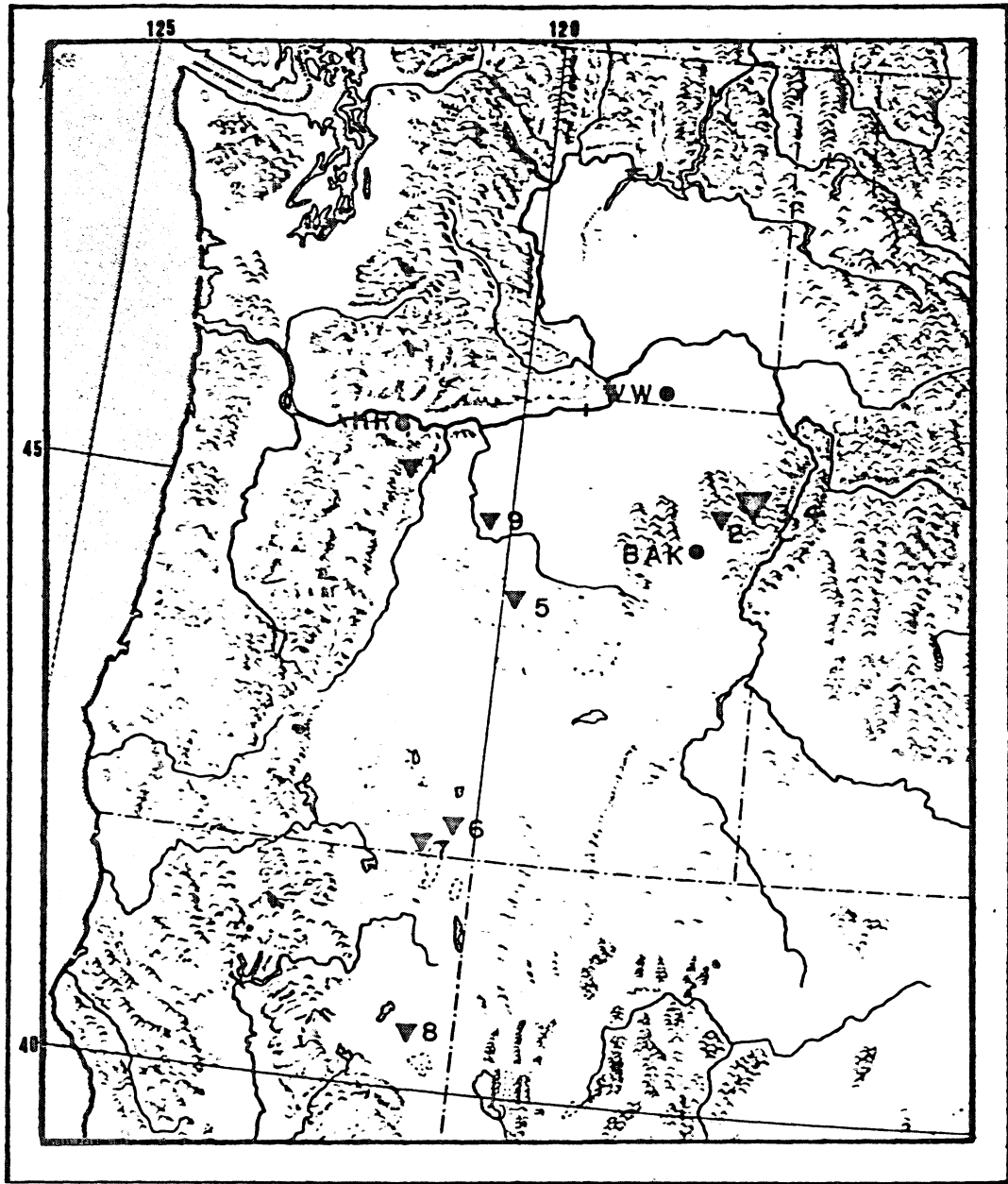
Figure 10. Map Showing Locations of Tree-Ring Sites and Climatic
Stations in the North Region -- Tree-ring sites are marked
by triangles and are numbered as in Table 1. Climatic
stations, marked by dots, are Hood River (Experiment
Station), Walla Walla, and Baker.

in the western United States. In addition, reconstructions for both regions would make possible a study of north-south coherence of dry and wet periods.

Climatic Data

Conceptually, the methods proposed in Chapter 2 can be applied to study the relationship between tree-ring series and any climatic or hydrologic variable, although trees generally respond to more than one climatic variable. The variable selected for the trial applications of the Box-Jenkins technique was a regional precipitation index representing rainfall grouped over a year corresponding roughly to the growth year of the tree. Precipitation indices were computed for the North and South regions by the following procedure.

1. September through August precipitation was totaled for individual weather stations.

2. Each annual precipitation series was standardized, or converted to "Z-scores" by subtracting the mean and dividing by the standard deviation.

3. The individual station Z-scores were averaged.

Four stations (Figure 9) were averaged to form the South precipitation index, and three stations (Figure 10) to form the North index.

The station precipitation records were taken from annual summaries of Local Climatological Data (U. S. Weather Bureau, ESSA and NOAA) and were checked for homogeneity by double-mass analysis (Bruce and Clark 1966, p. 160). Means and standard deviations for 1901-1963 in the South and 1897-1961 in the North were used for standardization.

In the following discussion, these years are referred to as the calibration period in the two regions.

Precipitation Climatology of the South Region. Most of the precipitation in the South region falls in the winter months, with a February peak in the long-term monthly medians (Figure 11). Precipitation is usually high from November through April, and low in the late spring, summer, and early fall. This pattern is typical of the entire area that includes the tree-ring sites and climatic stations (Pike 1972, p. 113). Cool-season precipitation in the region is associated with extratropical Pacific cyclones that become more frequent with southward displacement of the polar jet stream from early fall through late winter (Pike 1972, p. 18). Summer rainfall usually comes from convective showers in moist, unstable, tropical air that occasionally flows into the region from warm oceans to the south. The summer rainfall is large enough in some parts, especially away from the coast, to give a small secondary maximum in the monthly distribution of precipitation in July or August (Pike 1972, p. 113).

The precipitation index time series of the South is plotted in Figure 12 along with the standardized single-station precipitation for Cuyamaca. Broad swings above and below the mean characterize the years after the mid-1930's: rainfall was generally high from the mid-1930's to the mid-40's, and low from the late 1940's through the early 1960's. The 1970's were also dry until the extremely wet year 1978. The years 1941 and 1961 were the extremes in single-year wetness and dryness. The spatial variability of annual precipitation is illustrated by the
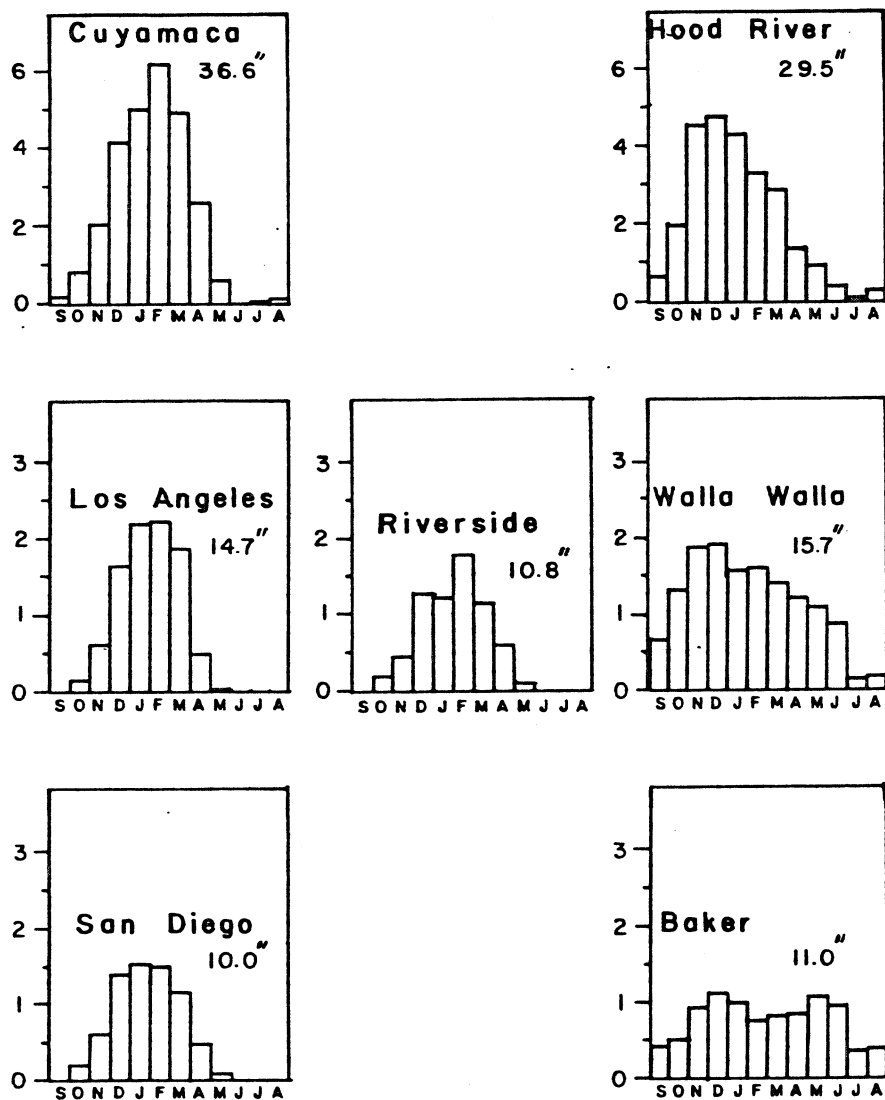
Figure 11. Monthly Distribution of Rainfall at Climatic Stations --
Graphs show median monthly precipitation for period 1901-
1978 in inches. Mean annual precipitation is also given.
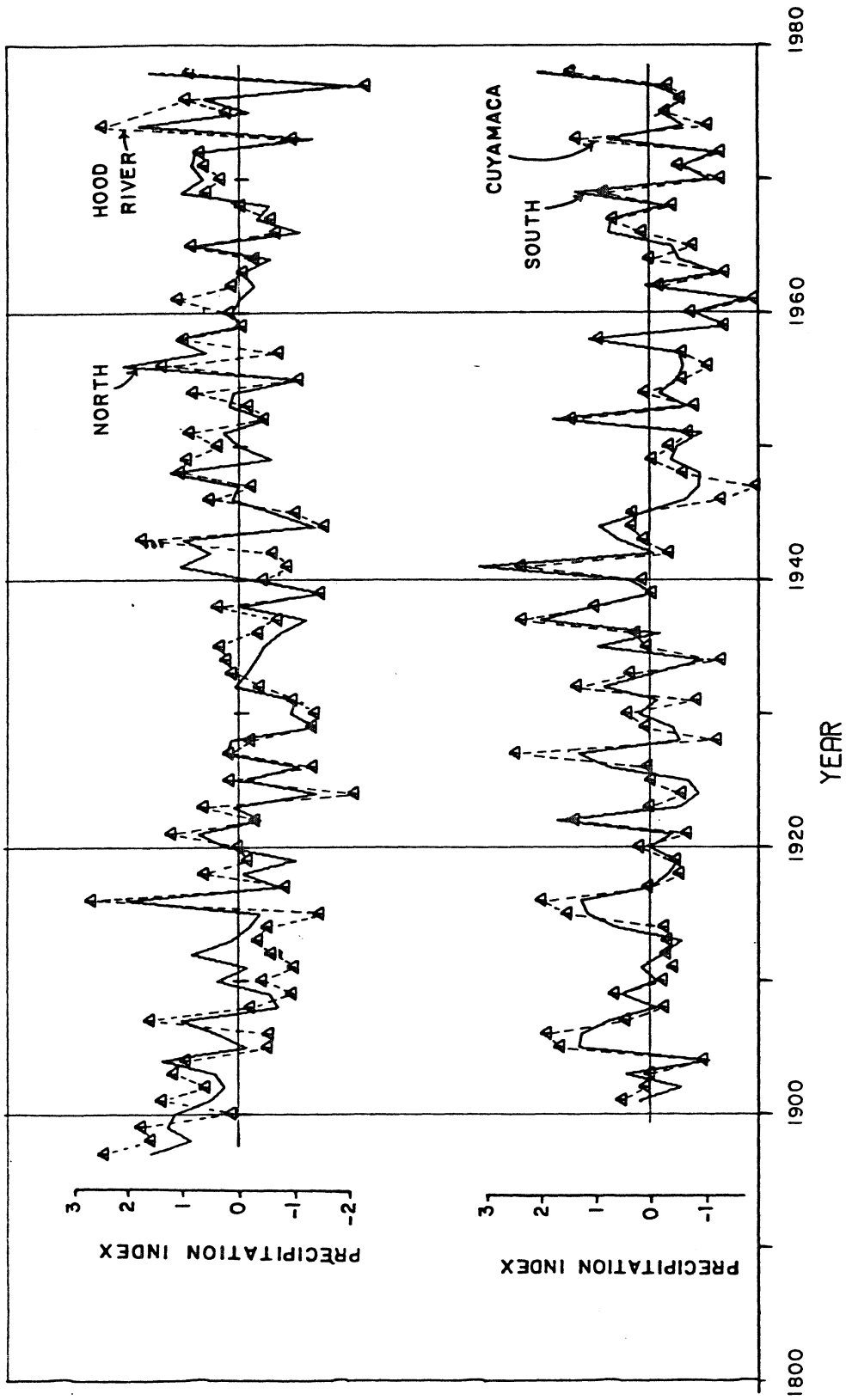
Figure 12. North and South Precipitation Indices and Single-Station Precipitation Indices for Cuyamaca, California and Hood River, Oregon -- See page 53 in text for description of indices.

occasionally large deviations of the single station record for Cuyamaca
from the regional index. For example, 1947 was the driest year by far
at Cuyamaca, but was only moderately dry by the regional index.

Precipitation Climatology of the North Region. The winter
months do not dominate the monthly distribution of precipitation in the
North as much as in the South. Cool-season precipitation in the North
is again largely governed by the gradual southward displacement of the
polar jet stream from early fall through late winter (Pike 1972, p. 18).
The month of peak average precipitation in winter varies from November
to January, depending on geographical location within the region, and on
topography (Pike 1972, p. 78).

Convective precipitation is increasingly important from west to
east over the region; at the eastern end of the region, the month of
peak precipitation is shifted to late spring. Pike's (1972, pp. 113-
114) maps of precipitation-regime boundaries indicate that the climatic
stations and tree-ring sites in Figure 10 may be grouped in the fol-
lowing way.

1. At Hood River and tree-ring sites 1, 6, 7, and 8, winter rain-
    fall dominates with a January peak in the monthly distribution.

2. At Walla Walla and tree-ring sites 5 and 9, the peak month in
    winter precipitation is shifted to November, and late spring
    convective showers become increasingly important in the annual
    total precipitation.

3. At Baker and tree-ring sites 2, 3, and 4, convective precipita-
    tion is heavy enough to make June the peak rainfall month;

winter rains give a secondary maximum in November, December, or
January.

Evidently, the North precipitation index is more complex in
makeup than the South. A given year's value of the index in the North
may reflect precipitation anomalies that occurred at various times of
the year, ranging from early fall through late spring, while the South
index more clearly reflects winter anomalies in rainfall. This in-
homogeneity in climate over the area regarded here as a region must be
considered a possible source of error in attempting to reconstruct the
regional climate.

The time-series plots of the North regional precipitation index
and the Hood River index (Figure 12) show gradually declining precipita-
tion from the beginning of the record in 1897 through the late 1930's,
increasing precipitation from the late 1930's until the late 1950's, and
relatively little low frequency variation thereafter. Prominent wet
years were 1915 and 1941; by far the most prominent dry year was 1977,
both according to the regional index and the Hood River record.

Tree-Ring Data

The tree-ring data used were in the form of indices, which are
annual ring widths adjusted for an underlying trend of decreasing ring
width with increasing tree age. The age trend is removed by fitting a
mathematical curve (exponential or polynomial) or straight line to the
ring widths, and dividing each ring width by the corresponding year's
value of the fitted curve (Stokes and Smiley 1968, Fritts 1976). Tree-
ring indices from several cores are averaged to form the tree-ring index

for a site. Typically, ten or more trees, each represented by at least
two cores, are included in the average (Fritts 1976).

All sites had been previously collected by other researchers,
and the data were on file at the Laboratory of Tree-Ring Research at The
University of Arizona. Consequently, the data probably are not the most
ideal for reconstructing climatic variation; but the main objective here
is to demonstrate the use of the Box-Jenkins technique. The locations
of sites are shown on the maps in Figures 9 and 10, and additional in-
formation on location, species, and sample record length is given in
Table 1. Many of the series extend well back beyond the 1500's; but to
ensure an adequate sample size for climatic inferences, only the data
from 1600 on were used in this study. The year of collection marks the
latest date of the period available for calibration with climatic data.
With a few exceptions, the South series were collected in the mid- to
late-1960's, and the North series in the early 1960's.

Time series plots of the tree-ring indices (Figure 13) show
general site-to-site coherence in major periods of low and high growth
within regions, but considerable variation in details. The standard
deviation differs by almost a factor of two between the most variable
and least variable series in the South, and by more than a factor of two
in the North. These differences are significant at the .05 confidence
level based on an F-test on the ratios of variances (Walpole and Myers
1972, p. 242), even when the effective sample size is adjusted for per-
sistence as recommended by Dawdy and Matalas (1964, pp. 8-86). The long-
term means are constrained to equal 1.0 by the method of converting
ring widths to indices; the means in Tables 2 and 3 differ from 1.0 only

Table 1. List of Tree-Ring Sites -- Sites are numbered as in Figures 9 and 10.

No.	Site	Lat	Long	Elev(m)	Species[a]	Period[b]
1S	San Gorgonio	34°07!	116°49'	3280	LP	42BC-1970
2S	Santa Ana	33 34	117 33	1210	BCS	1611-1972
3S	Baldwin Lake	34 16	116 49	2280	PP	1513-1966
4S	Santa Rosa	33 32	116 28	2190	CIC	1684-1972
5S	Southern California	34 03	117 05	1400	BCS	1415-1966
6S	White Mountains	37 25	118 10	3110	BCP	800-1963
7S	Clark Mountain	35 32	115 35	2190	WF	1596-1968
8S	San Pedro Martir Low	31 00	115 25	1980	PP	1449-1971
1N	Dufer	45°16'	121°08'	580	PP	1600-1964
2N	Union	45 09	117 37	1430	PP	1565-1964
3N	Chief Joseph	45 17	117 17	2560	WBP	1538-1964
4N	Slickrock Creek	45 17	117 19	1980	LP	1160-1965
5N	Paulina	44 16	119 53	1310	PP	1600-1965
6N	Abert Rim Lookout	42 23	120 14	2130	PP	1511-1964
7N	Lakeview	42 06	120 34	1830	PP	1421-1964
8N	Susanville	40 29	120 33	1830	PP	1485-1963
9N	Peacock Canyon	44 55	120 15	1900	DF	1670-1978

[a]LP   limber pine (Pinus flexilus; James)
 BCS   bigcone spruce (Pseudotsuga macrocarpa; Mayr.)
 PP   ponderosa pine (Pinus Ponderosa; Laws)
 CIC   California incense cedar (Libocedrus decurrens; Torr.)
 BCP   bristlecone pine (Pinus aristata; Engelm.)
 WF   white fir (Abies concolor; Gord and Glend.)
 WBP   whitebark pine (Pinus albicaulis; Engelm.)
 DF   Douglas fir (Pseudotsuga menziesii; Franco)

[b]Data are available for this period, but this study does not use data from earlier than 1600 because of inadequate sample size.
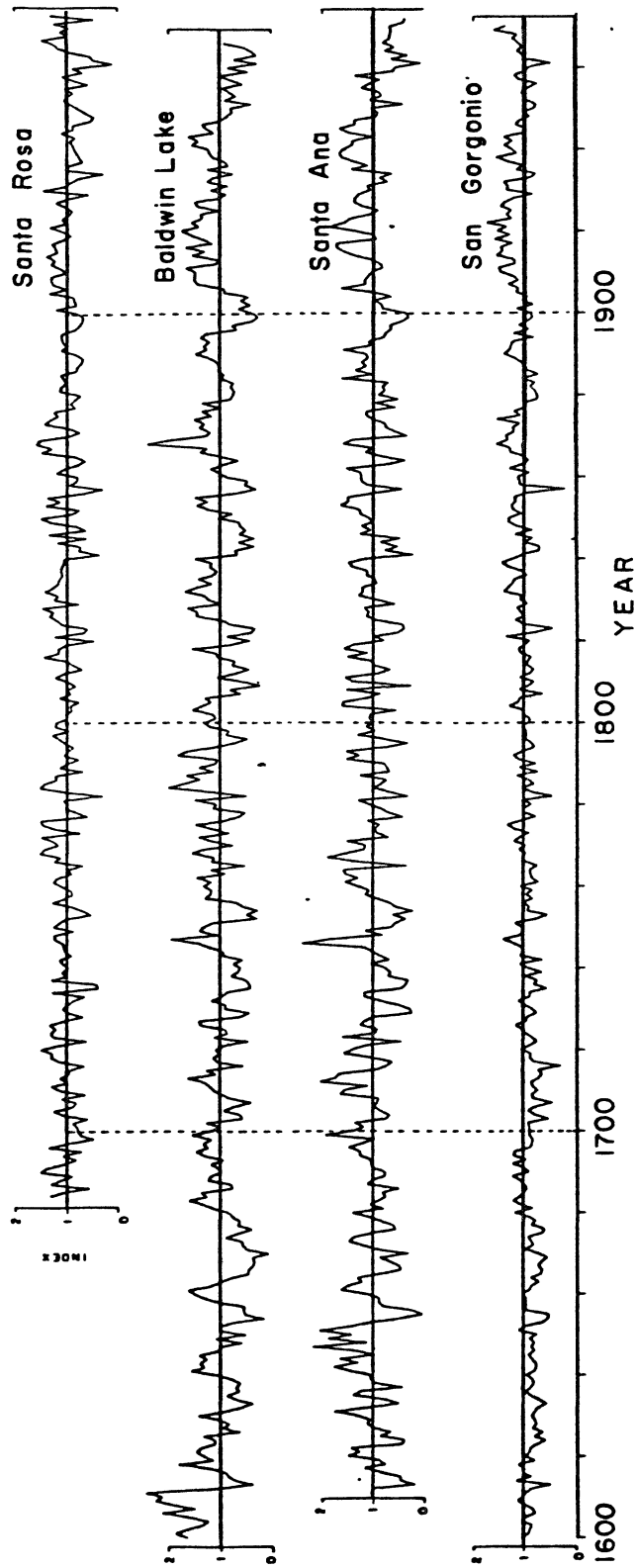
Figure 13. Time Series Plots of Tree-Ring Indices -- See Table 1 for additional information.
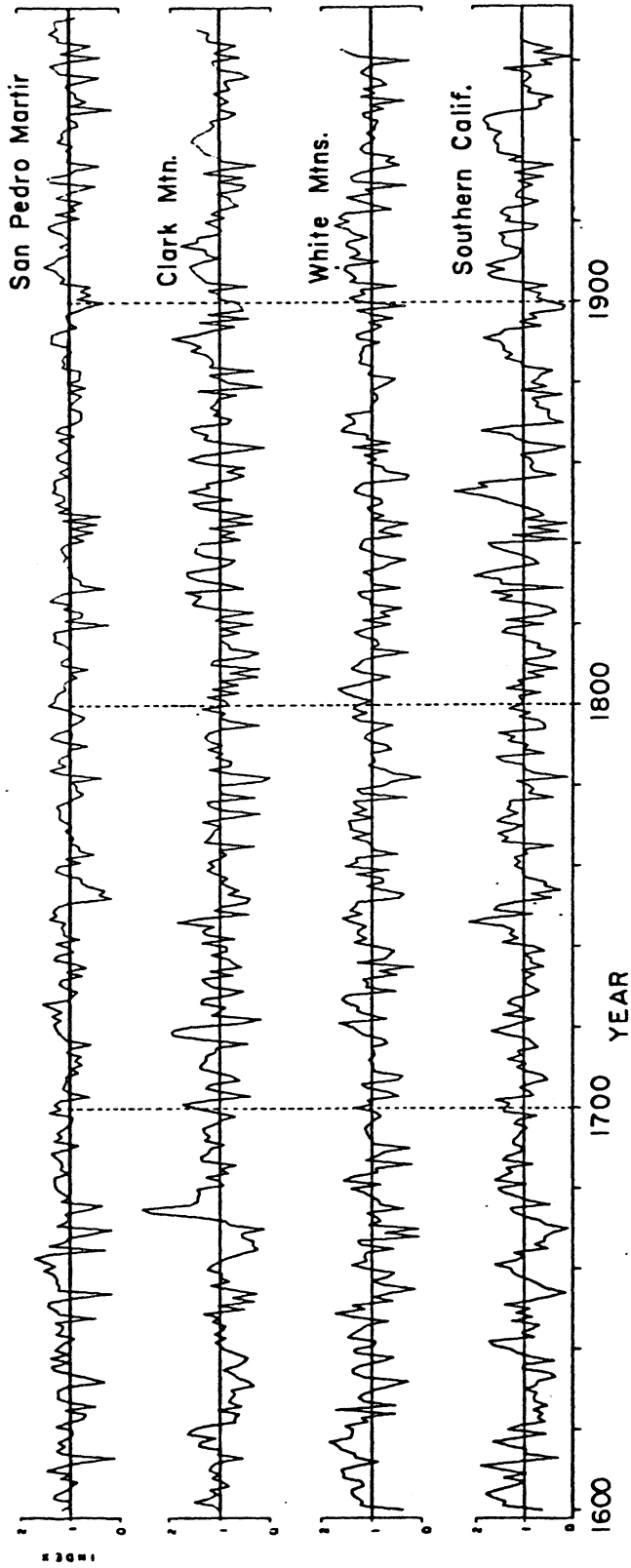
Figure 13.--Continued Time Series Plots of Tree-Ring Indices.
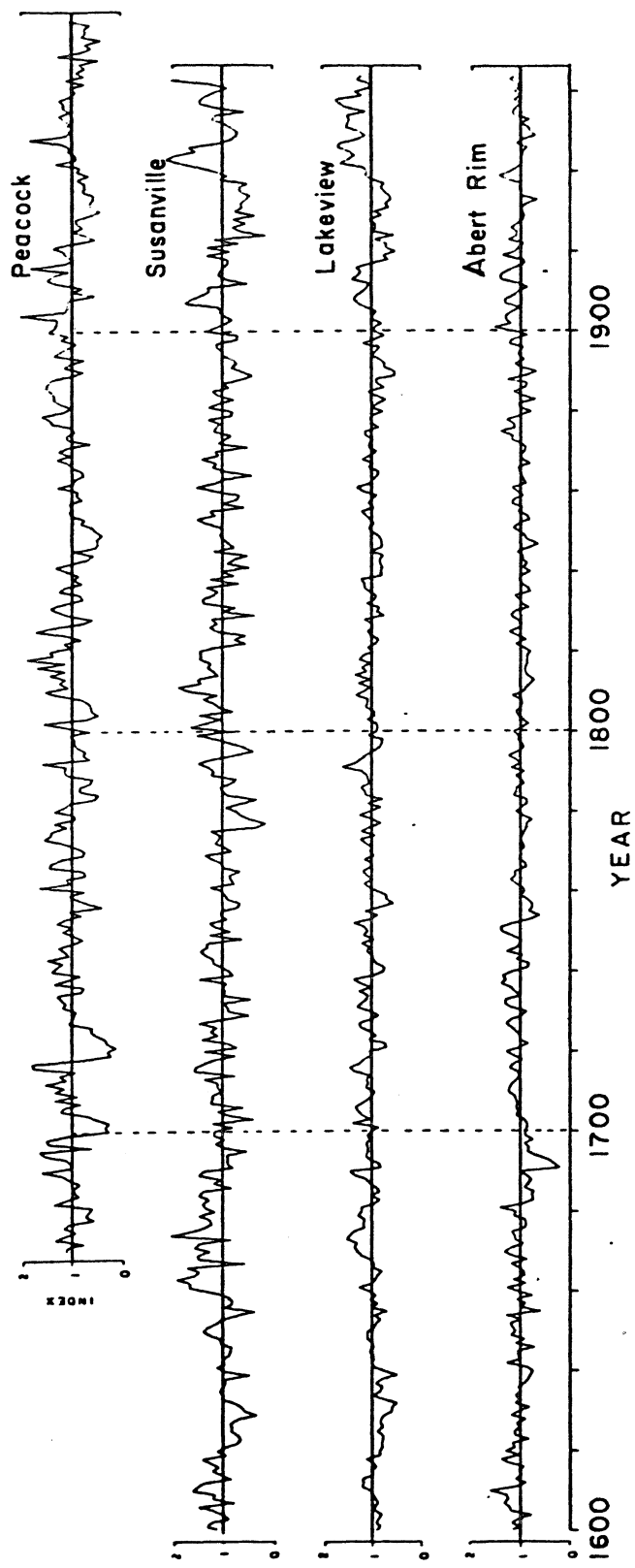
Figure 13.--Continued Time Series Plots of Tree-Ring Indices.
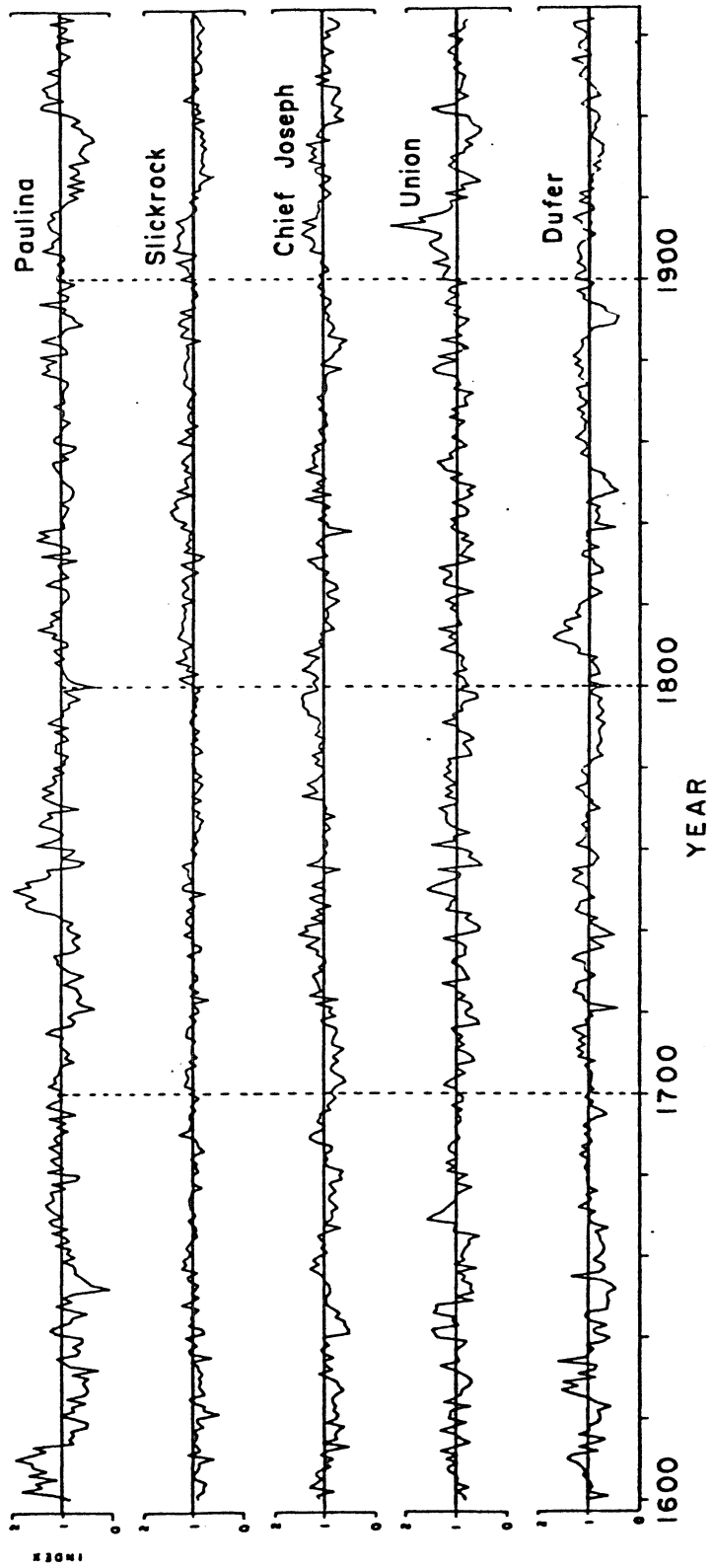
Figure 13.--Continued Time Series Plots of Tree-Ring Indices.

Table 2. Long-Term Statistics of Tree-Ring Indices in South Region —
Period for computations was 1684-1963 for Santa Rosa and
1610-1963 for all other sites.

Site	Mean	Median	St. Dev.	Skew
San Gorgonio	.99	.98	.23	.13
Santa Ana	1.00	1.01	.40	.09
Baldwin Lake	.99	1.01	.40	.19
Santa Rosa	1.00	1.01	.27	-.32
S. California	.99	1.00	.41	.06
White Mountains	1.02	1.01	.35	-.47
Clark Mountain	.99	1.01	.39	.08
Martir	1.01	1.05	.28	-1.00

Table 3. Long-Term Statistics of Tree-Ring Indices in North Region —
Period for computations was 1673-1961.

Site	Mean	Median	St. Dev.	Skew
Dufer	1.00	1.02	.20	-.17
Union	1.00	1.00	.24	.87
Chief Joseph	1.00	1.00	.19	.10
Slickrock	1.02	1.02	.15	.25
Paulina	1.01	1.00	.25	.31
Abert Rim	1.00	.99	.18	-.29
Lakeview	1.04	1.03	.22	.33
Susanville	1.03	1.04	.34	.08
Peacock	1.00	1.02	.33	.06

because they are not computed on the entire record length. The close-ness of the means and medians attests to the representativeness of the mean as a measure of central tendency. Comparison of the tabled skew coefficients with Monte-Carlo derived distribution graphs of Wallis, Matalas, and Slack (1974, p. 17) indicated that except possibly for the Martir and Union sites, skews are not significantly different from zero.

A key property regarding the lagged response is the persistence structure of the individual time series. The difference in persistence among tree-ring series and between tree-ring series and the precipita-tion indices shows clearly in the sample autocorrelation plots in Figures 14 and 15. The South tree-ring series are in general less persistent than the North series, as measured by the size of the first order auto-correlation and the number of autocorrelations significant at the 95% confidence level. There are exceptions to the rule, however (e.g., San Gorgonio, Susanville, Abert). The number of significant autocorrela-tions varies from none (San Pedro Martir, White Mts.) to five (Slick-rock).

The precipitation indices, in contrast, are much more nearly random. The only significant autocorrelation in either series is at lag 5 in the North series, and then only barely so at the 95% confidence level. The persistence in the tree-ring series is therefore not related to a corresponding persistence in precipitation.

Transfer Function Modeling

The transfer-function methods described in Chapter 2 were applied to the regional precipitation indices and the tree-ring indices.
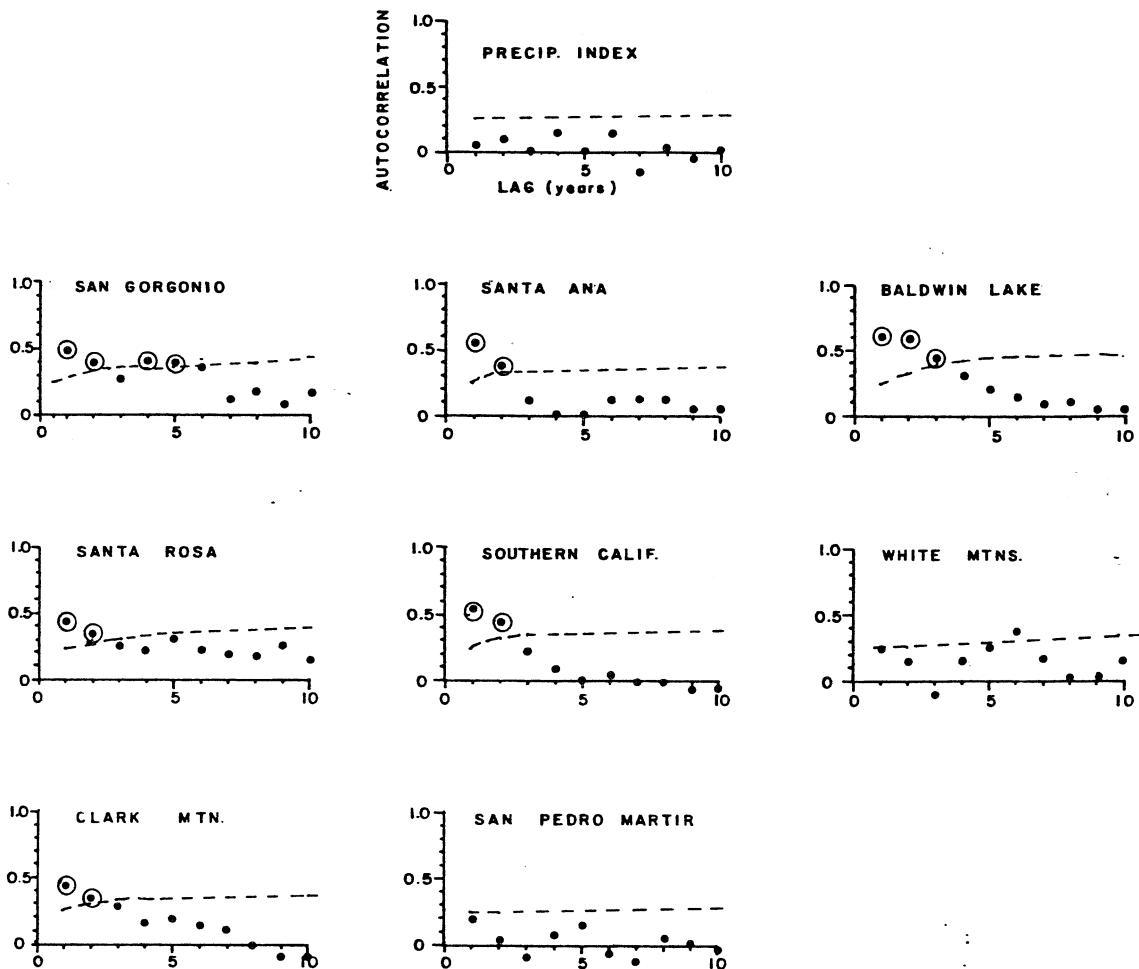
Figure 14. Sample Autocorrelation Functions of Precipitation Index and Tree-Ring Indices in the South Region — Autocorrelations significant at the two-standard-error level (dashed line) (see Appendix A) are circled. Period for computations was 1901-1963.
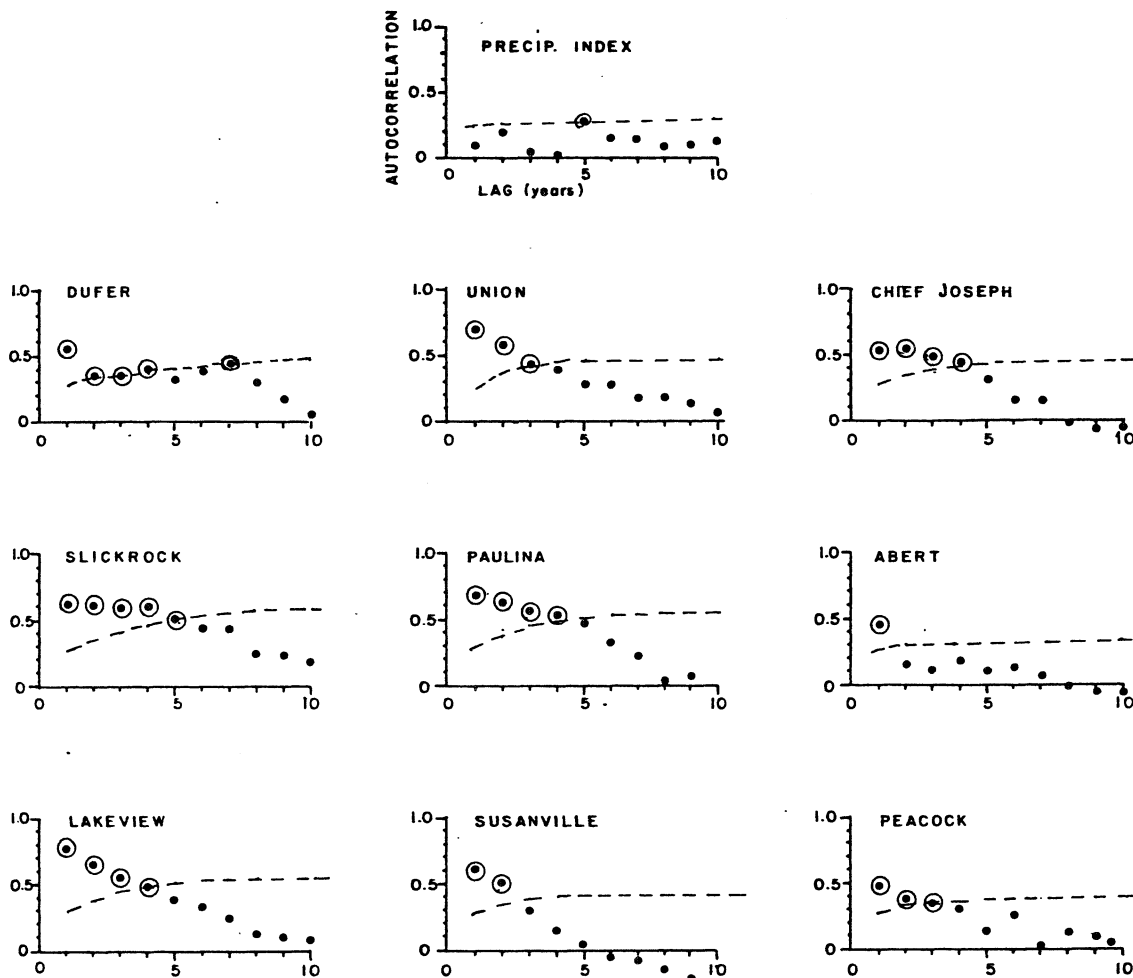
Figure 15. Sample Autocorrelation Functions of Precipitation Index and
Tree-Ring Indices in the North Region -- Period for
computations was 1897-1961. Remainder of legend is as in
Figure 14.

A separate transfer-function analysis was run for each tree-ring series, with the regional precipitation index as input and tree-ring index as output. The years for derivation of the transfer function were 1901–1963 in the South and 1897–1961 in the North.

Relevant equations were given in Chapter 2, and are not repeated here except occasionally for clarity. Where equations are used, mathematical symbols follow the notation of Chapter 2.

Impulse Response Functions

The regional precipitation indices were prewhitened using the "best fit" ARMA model. The Akaike Information Criteria [Eq. (2.6)] was used to determine the best fit model, which was the AR(1) model

$$x_t = 0.0674 = \alpha_t \qquad (3.1)$$

for the South precipitation index, and the AR(2) model

$$x_t - 0.0605\ x_{t-1} - 0.1977\ x_{t-2} = \alpha_t \qquad (3.2)$$

for the North, where x_t is the precipitation index (mean subtracted) and α_t are the ARMA residuals, which are referred to as the prewhitened input. The small coefficients in these models reflect the low auto-correlation in the precipitation indices (see Figure 14). Accordingly, prewhitening removes very little of the variance from the original series. The variance of α_t is 99% of the variance of x_t in the South and 87% in the North.

Each tree-ring series was then transformed by the same ARMA model that had been fit to the regional precipitation indices. Tree-ring indices in the South were transformed by

$$y_t - 0.0674 \ y_{t-1} = \beta_t \qquad\qquad (3.3)$$

and those in the North were transformed by

$$y_t - 0.0605 \ y_{t-1} - 0.1977 \ y_{t-2} = \beta_t \qquad\qquad (3.4)$$

where y_t is the tree-ring index (mean subtracted) and β_t is the trans-
formed output.

Sample crosscorrelations between prewhitened input and trans-
formed output were calculated, along with 95% confidence limits from
formulas given in Appendix A. These crosscorrelations are proportional
to the impulse response weights. The sample crosscorrelations and their
confidence limits are plotted in Figure 16. The individual plots are
discussed below.

South. The only series with no significantly large weights was
White Mountains: this series was consequently omitted from further
analysis for lack of sufficient relationship to the precipitation index.

The remaining plots varied greatly, but were similar in some
important aspects. First, the lag-zero weight was largest at all sites,
indicating that current year's rainfall was more important than past
years' rainfall. Second, the lag-1 weight was large relative to other
lags at four of the sites. The resulting pattern resembled a rapid
exponential decay at Santa Ana, Santa Rosa, and Clark Mountain, indi-
cating a rapid die-off in importance of past years' climate, with sig-
nificant influence limited to lags at years t and t-1.

Third, significant climatic input at higher-order lags than t-1
was indicated for Baldwin Lake and Southern California. The marked
difference between these two plots and those which decay rapidly
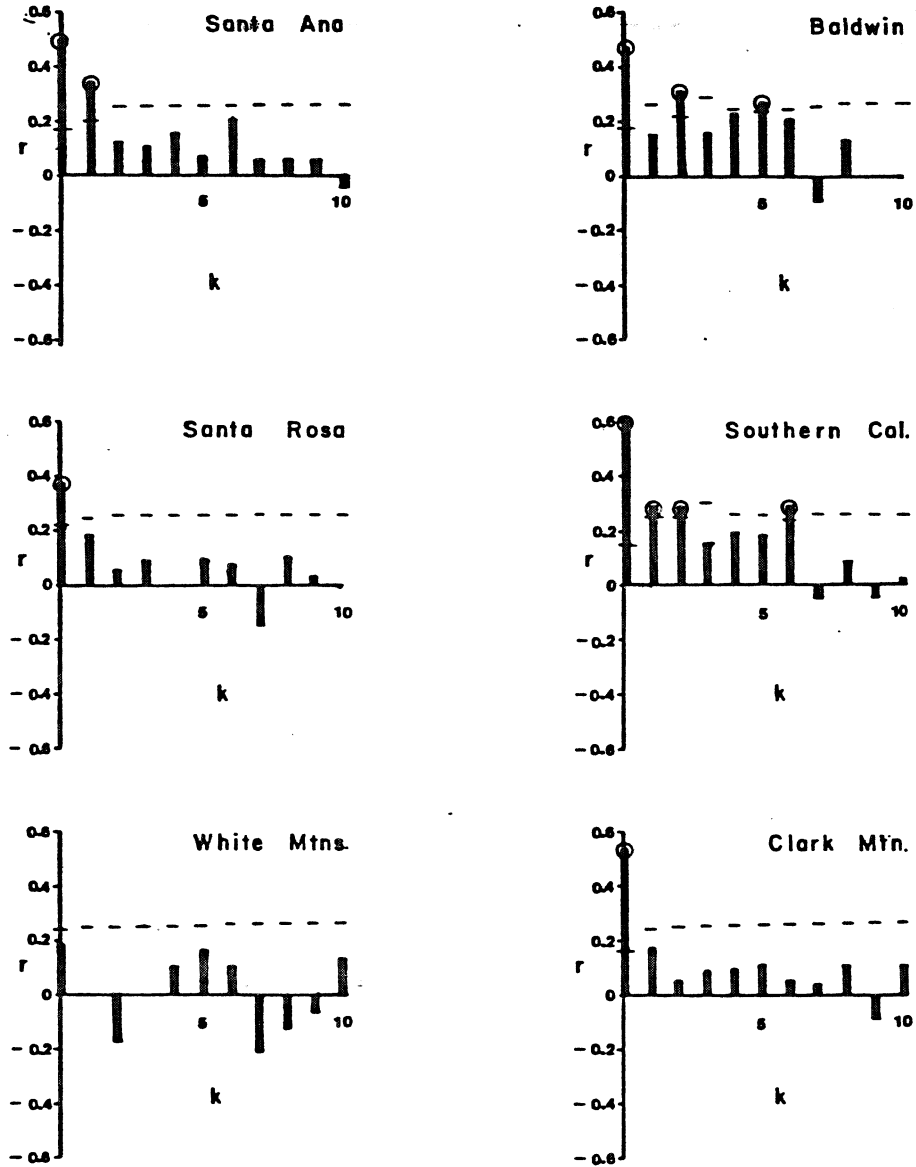
Figure 16. Estimated Impulse Response Weights -- First eight plots are
for South sites; last nine are for North sites. Plotted
values are the crosscorrelations given by Equation (2.15)
on page 24. Two-standard-error level of significance is
indicated by a dashed line [see Equation (A.12) in
Appendix A). Significant weights are circled.
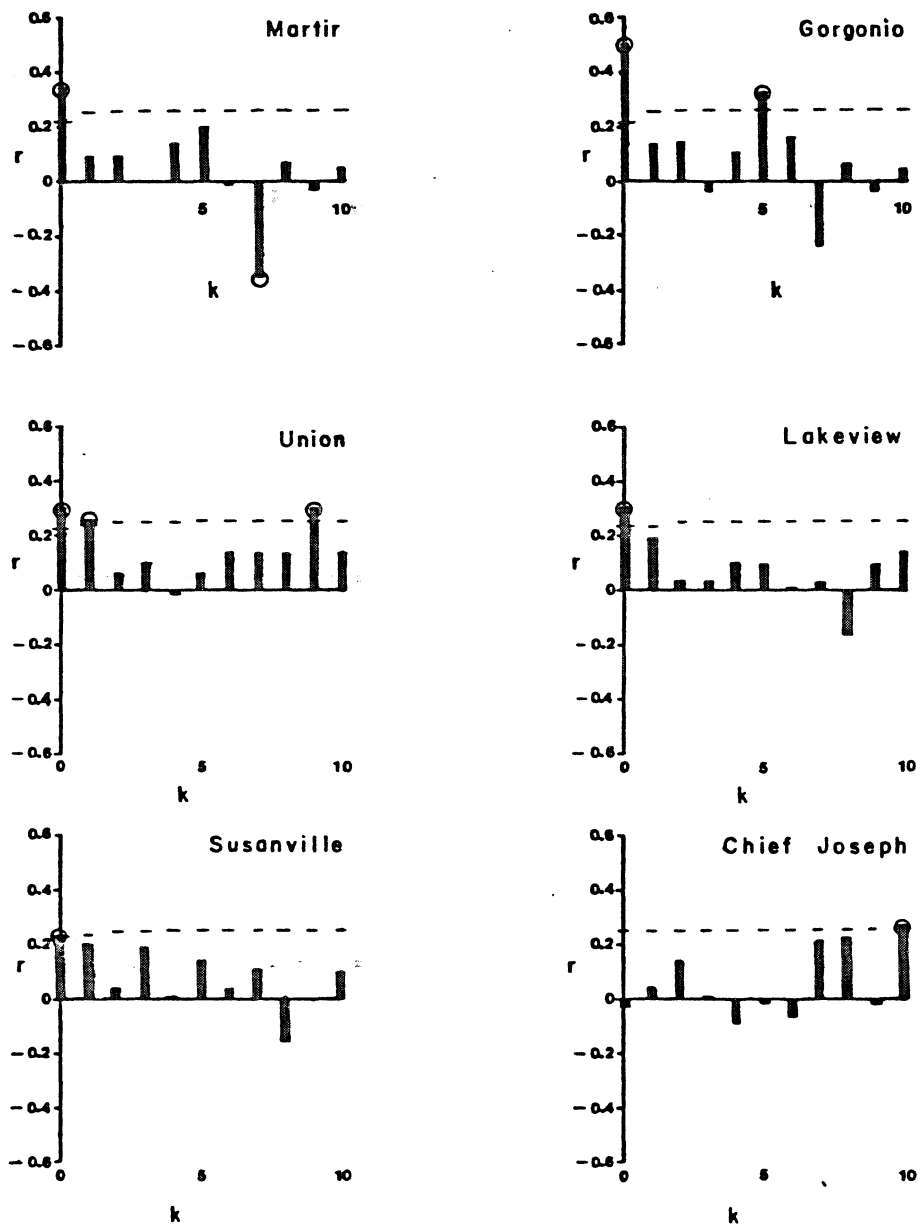
Figure 16.—Continued Estimated Impulse Response Weights.
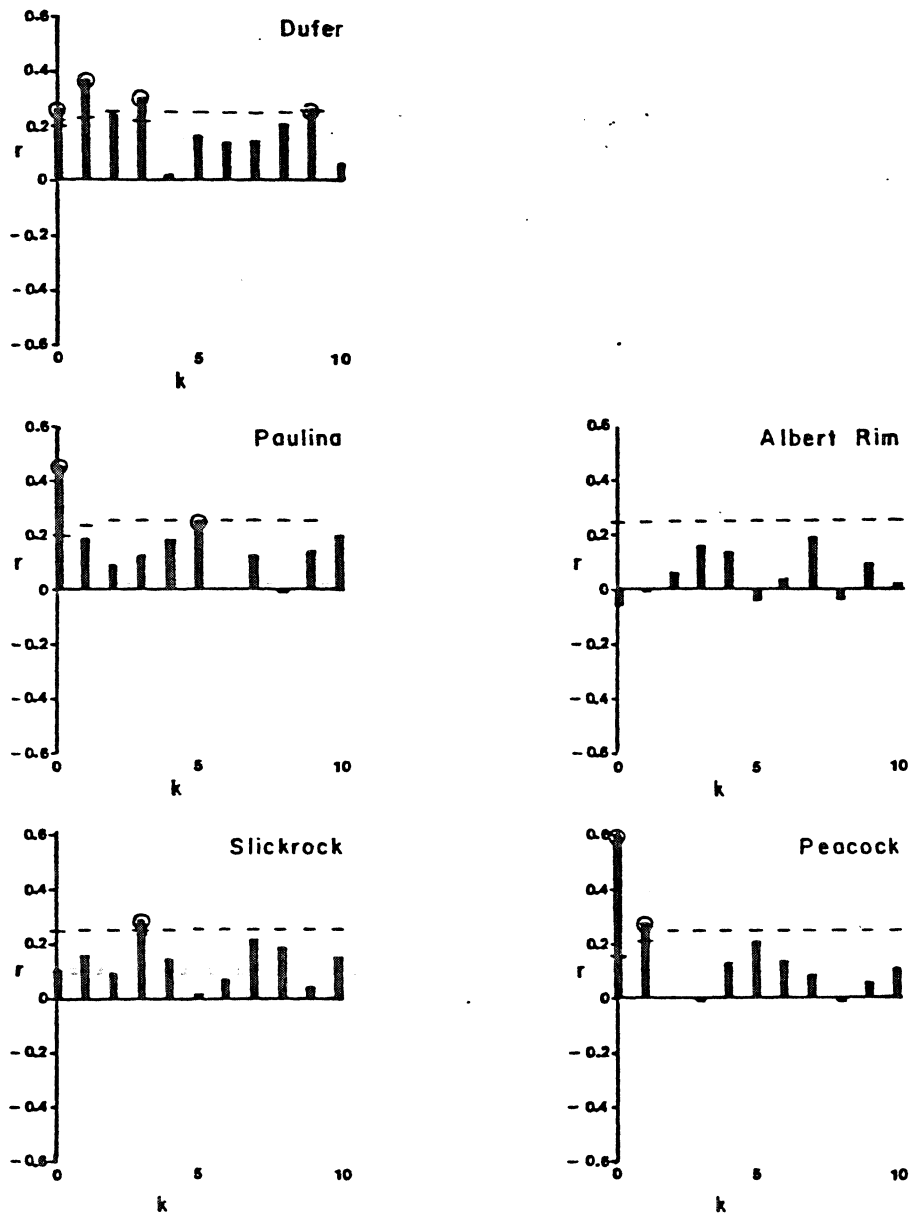
Figure 16.—Continued Estimated Impulse Response Weights.

Dufer is an exception, however, with a lag-1 maximum, and Union is a
borderline case in which the lag-0 weight is only slightly larger than
the lag-1 weight. Like Baldwin Lake and Southern California in the
South, Dufer shows significant climate input at lags higher than 1.

General. The estimated impulse response functions indicate that
the lagged response of tree-rings to annual rainfall varies greatly from
site to site, both in the number of past years' rainfall that are im-
portant, and in the relative importance of each year. The number
appears to vary between 1 and 3, assuming that the higher-order sig-
nificant spikes occasionally found on the plots in Figure 16 are
due to noise. The most important year is generally the current year, t,
although year t-1 may approach year t in importance, and may even
dominate (as in Dufer).

A recurring pattern in lagged response is a rapid die-off in
importance of past years' climate that resembles an exponential decay,
with weights becoming small after lag 1. On the other hand, some
impulse patterns decay more slowly, or in a form resembling a damped
sine wave, with significantly larger weights at lags higher than 1.
These latter sites can be interpreted as having relatively long
"memory" of climate.

Transfer Functions

The estimated impulse response functions weight the importance
of current and past years' climate to the current year's ring. As
described in Chapter 2, the transfer function reformulates this rela-
tionship in terms of dependence on past years' rings and past and

current years' climate. The impulse response form [Eq. (2.8)] was

$$y_t = v_0 x_t + v_1 x_{t-1} + v_2 x_{t-2} + \ldots + \text{noise term} \qquad (3.5)$$

where y_t is the tree-ring index, x_t is the precipitation index, and v_0, v_1, v_2, ... are the impulse response weights. The transfer-function [Eq. (2.9)] reformulates Equation (3.5) into

$$y_t = \delta_1 y_{t-1} + \delta_2 y_{t-2} + \ldots + \delta_r y_{t-r}$$

$$+ \omega_0 x_t - \omega_1 x_{t-1} - \ldots - \omega_r x_{t-s} - \text{noise term} \qquad (3.6)$$

where r is the number of past years' tree-ring index, and s is the number of past years' rainfall index upon which the tree-ring index y_t is dependent.

Models were identified by the procedures described in Chapter 2. The identified models are listed in Tables 4 and 5. The noise term N_t was generated from the impulse weights by the linear Equation (2.8), with k truncated at 10:

$$N_t = y_t - \sum_{k=0}^{10} v_k x_{t-k}, \qquad (3.7)$$

where y_t is the observed tree-ring index (mean subtracted), x_t is the rainfall index (mean subtracted), and v_k is the impulse response weight at lag k.

Identified Models. Identification for some of the models was conjectural, as the variance of the noise term was nearly as large as the variance of the output signal given by the summation in (3.7). Nevertheless, the decay patterns in the estimated impulse response weights (Figure 16) suggested at least two distinct orders of

Table 4. Identified Transfer-Function Models in South Region.

Site	$(r,s,b)^a$	Model Equation^a	S/N^b	Noise^c Model
Gorgonio	(2,1.0)	$y_t = \delta_1 y_{t-1} + \delta_2 y_{t-2} + \omega_0 x_t + \omega_1 x_{t-1}$	1.84	(1,0,0)
Santa Ana	(1,0,0)	$y_t = \delta_1 y_{t-1} + \omega_0 x_t$	2.09	(1,0,0)
Baldwin Lk.	(2,1,0)	$y_t = \delta_1 y_{t-1} + \delta_2 y_{t-2} + \omega_0 x_t + \omega_1 x_{t-1}$	2.45	(1,0,1)
Santa Rosa	(1,0,0)	$y_t = \delta_1 y_{t-1} + \omega_0 x_t$	1.28	(1,0,2)
S. California	(1,0,0)	$y_t = \delta_1 y_{t-1} + \omega_0 x_t$	3.63	random^d
Clark Mtn.	(1,0,0)	$y_t = \delta_1 y_{t-1} + \omega_0 x_t$	1.67	(1,0,0)
Martir	(2,1,0)	$y_t = \delta_1 y_{t-1} + \delta_2 y_{t-2} + \omega_o x_t + \omega_1 x_{t-1}$	1.42	random
White Mtns.^{e}	(1,0,1)		1.24	(1,0,1)

^{a}Terms as defined in Equation (2.9).

^{b}Signal to Nosie Ratio: ratio of variance of output y_t to variance of noise N_t in Equation (3.7), where N_t was computed assuming impulse weights negligible for k > 10.

^{c}Order of model selected by AIC criterion [Equation (2.6), page 18].

^{d}No significant autocorrelations of N_t.

^{e}No significant impulse weights.

Table 5. Identified Transfer-Function Models in North Region.

Site	$(r,s,b)^a$	Model Equation[a]	S/N^b	Noise[c] Model
Dufer	(2,2,0)	$y_t = \delta_1 y_{t-1} + \delta_2 y_{t-2} + \omega_0 x_t + \omega_1 x_{t-1} + \omega_2 x_{t-2}$	2.38	(1,0,0)
Union	(2,1,0)	$y_t = \delta_1 y_{t-1} + \delta_2 y_{t-2} + \omega_0 x_t + \omega_1 x_{t-1}$	1.72	(1,0,0)
Paulina	(1,0,0)	$y_t = \delta_1 y_{t-1} + \omega_0 x_t$	1.82	(2,0,0)
Lakeview	(1,0,0)	$y_t = \delta_1 y_{t-1} + \omega_0 x_t$	1.38	(1,0,0)
Peacock	(1,0,0)	$y_t = \delta_1 y_{t-1} + \omega_0 x_t$	1.73	random[d]
Ch. Joseph[e]			1.38	(2,0,0)
Slickrock[f]			1.55	(2,0,0)
Abert Rim[e]			1.12	(1,0,0)
Susanville[e]			1.35	(1,0,0)

a,b,c,d,e As in Table 4.

[f] Erratic impulse response function.

transfer-function models. The most common was (r = 1, s = 0, b = 0), inferred from an impulse response function judged to decay as a simple exponential. This pattern occurred in 4 of the 8 South series and 3 of the 9 North series. The second major decay type was judged to be more complex than simple exponential, and is represented by the impulse plots for Baldwin Lake and Dufer. This type of decay suggests either a (2,1,0) or (2,2,0) transfer-function model (see Figure 4).

The noise term N_t generated by Equation (3.7) varied greatly from site to site, both in magnitude as given by variance, and in persistence structure, as given by the best fit ARMA model by the AIC criterion [Eq. (2.6)]. The noise was generally not random. Considering some of the possible sources of noise (e.g., growth curve errors, growth surges caused by fires or insect manifestations), this result probably should be expected.

Implied Lagged Response. The identified transfer-function models are generally consistent with a physical system in which the tree-ring index in year t depends statistically on input from the rainfall in year t and possibly in years t-1 and t-2, plus input from the tree-ring index in year t-1 and possibly t-2.

The simplest form (r = 1, s = 0, b = 0) implies important input from only the rainfall in year t and the previous year's ring width. The most complicated form (r = 2, s = 2, b = 0) implies important input from the past two years' climate and the past two years' tree-ring index.

Selection of Lags for
Reconstruction Models

A simple reconstruction model was assumed in which the regional
rainfall index y_t was to be predicted from a single lagged tree-ring
index series x_t. The question was then how many lags on x_t to include
in the regression model to (1) adjust for the priming of the ring growth
in year t by previous years' climate and (2) take into account the
possible information on climate in year t residing in rings for years
after year t. Following the procedures in Chapter 2, the orders of the
identified transfer function model were used to select negative lags and
the estimated impulse-response weights were used to select positive lags.
Lags for single-site reconstruction models are listed in Table 6.

The simplest lag model has as predictors tree rings lagged only
t and t-1; this model is implied by a $(r = 1, s = 0, b = 0)$ transfer-
function model with an impulse weight on lag 1 insignificant at the two-
standard error level. The next simplest model is t-1, t, t+1, implied
again by a (1,0,0) transfer function model, but with a significant
impulse weight on lag 1.

The decision on negative lags was between one lag (t-1) or two
lags (t-1, t-2); the noise level in the climate-tree ring system was
probably too large to justify using higher lagged models (see Box and
Jenkins 1976, p. 387). The decision on positive lags was sometimes very
ill-defined, especially when several lagged impulse weights were large
and it was desired to keep the total number of predictors small. A
rational approach was adopted in which the lowest-order positive lags
were preferred. The logic here is that climate in year t probably

Table 6. Implied Lags for Regression Models.

Site	TFM[a]	Significant[b] Impulse Weights	t-2	t-1	t	t+1	t+2	t+3
South Region:								
Gorgonio	(2,1,0)	0,5	x	x	x			
Santa Ana	(1,0,0)	0,1		x	x	x		
Baldwin L.	(2,1,0)	0,2	x	x	x		x	
Santa Rosa	(1,0,0)	0		x	x			
S. Calif.	(1,0,0)	0,1,2,6		x	x	x		
Clark	(1,0,0)	0		x	x			
Martir	(1,0,0)	0		x	x			
North Region:								
Dufer[c]	(2,1,0)	0,1,3		x	x	x	x	x
Union	(2,1,0)	0,1,0	x	x	x	x		
Paulina	(1,0,0)	0,5		x	x			
Lakeview	(1,0,0)	0		x	x			
Peacock	(1,0,0)	0,1		x	x	x		

[a] Order of transfer-function model rewritten from Tables 4 and 5.

[b] Lags of impulse response weights significant at two-standard error level.

[c] Impulse response weight at lag t+2 for Dufer was not significant at two-standard-error level, but was nearly so. Lag on t-2 was not included to keep total number of predictors under six.

influences the ring in year t+1 more strongly than the ring in years

t+2, t+3, ... The selected positive lags in Table 6 are thus partly

a result of subjective judgment. The number of positive lags ranges

from zero to three.

ARMA Modeling and Crosscorrelations of
Prewhitened Series

The impulse response function does not distinguish between

lagged response arising fro direct influence of climate y_t on tree rings

in subsequent years, and indirect influences from inertia in the tree-

ring response in year t. The crosscorrelations between prewhitened

climatic and tree-ring series were proposed in Chapter 2 as a tool for

studying the lagged-response unmasked from the effects of autocorrela-

tion. The ARMA models for prewhitening the regional precipitation

indices were necessary in the transfer-function modeling, and have

already been discussed. In that analysis, the tree-ring indices were

not prewhitened themselves, but only transformed by the ARMA models fit

to the precipitation indices. In this analysis, the precipitation

indices and the tree-ring indices are separately fit to ARMA models.

Prewhitening Models

The prewhitening models and their estimated parameters are listed

in Table 7 and the plots of prewhitened series are shown in Figures 17

and 18. The site-to-site variation in persistence of tree-ring series

(Figures 14 and 15) is reflected in the wide range of variance ratios

in Table 7. Prewhitening removed only about 9% of the variance of the

White Mountains series, but more than 50% of the variance of other

Table 7. Prewhitening Models -- Models for first 9 series (South) were fit to 1901-1963 data. Models for last 10 series (North Region) were fit to 1897-1961 data.

Series	Order[a] (p,d,q)	Parameters				Variance[b] Ratio	Sig_Q[c]	n_r[d]
		ϕ_1	ϕ_2	ϕ_3	θ_1			
South Index[e]	(1,0,0)	.067				.98	.49	0
Gorgonio	(1,0,1)	.920			.637	.67	.05	0
Santa Ana	(1,0,0)	.591				.66	.99	0
Baldwin L.	(2,0,0)	.354	.443			.45	.78	1
Santa Rosa	(1,0,0)	.454				.77	.50	0
S. California	(1,0,0)	.576				.66	.99	1
White Mtns.	(1,0,0)	.253				.91	.55	1
Clark Mtn.	(1,0,0)	.457				.78	.85	0
Martir	(1,0,0)	.202				.94	.90	0
North Index[e]	(2,0,0)	.061	.197			.87	.68	1
Dufer	(1,0,0)	.572				.63	.71	0
Union	(2,0,0)	.559	.197			.50	.88	1
Ch. Joseph	(2,0,0)	.339	.371			.60	.44	0
Slickrock	(3,0,0)	.293	.319	.223		.47	.58	0
Paulina	(2,0,0)	.490	.295			.46	.26	1
Abert	(1,0,0)	.460				.76	.81	0
Lakeview	(1,0,0)	.770				.40	.99	0
Susanville	(1,0,0)	.625				.60	.90	0
Peacock	(1,0,0)	.487				.75	.26	1

[a]See Equation (2.5), p. 17.

[b]Ratio of variance of residuals to variance of original series.

[c]Significance level of "Q" statistic, defined by Equation (2.7), p. 18.

[d]Number of significant autocorrelations of residuals at two-standard-error level from Equation (A.3) in Appendix A.

[e]Regional precipitation index.
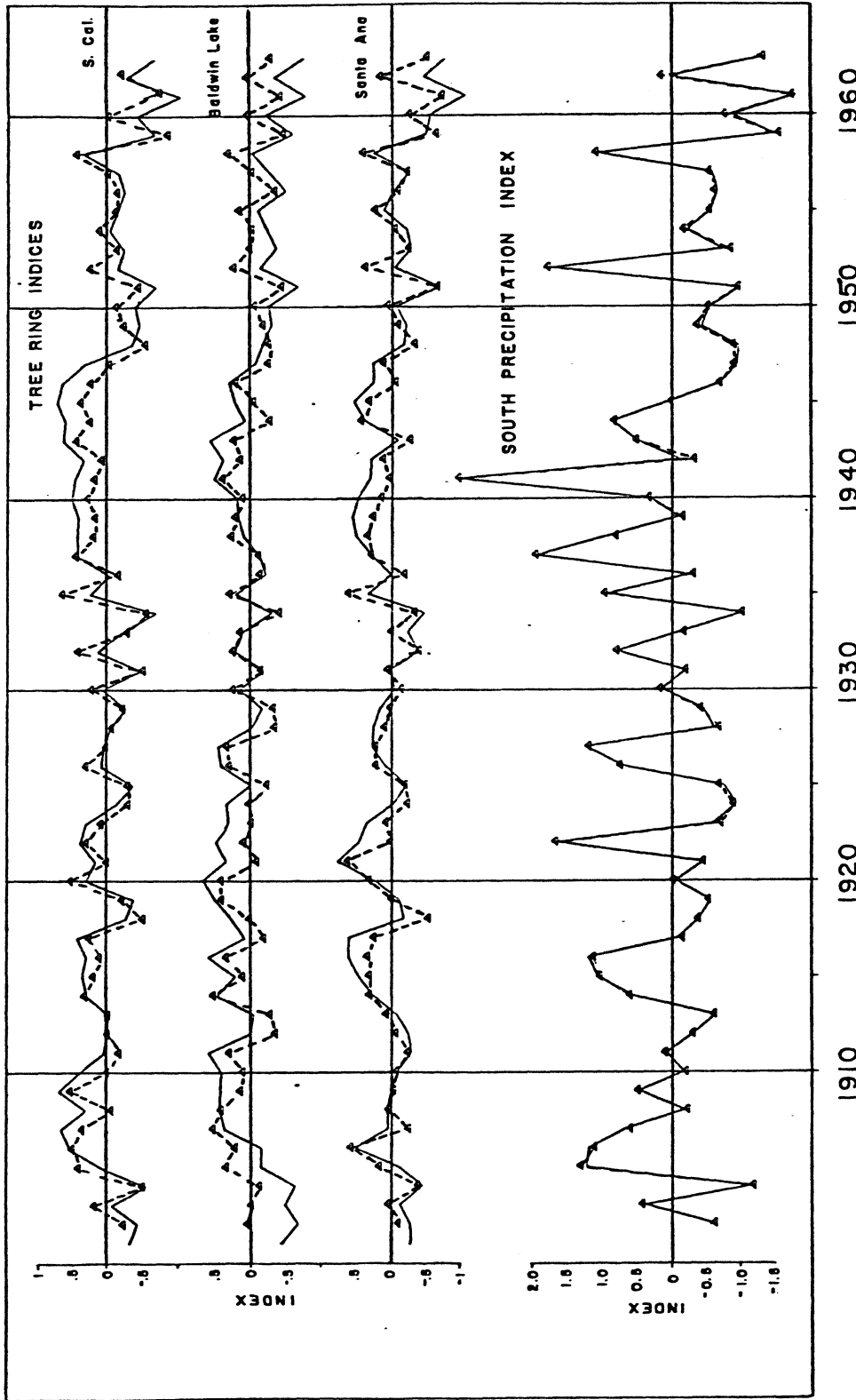
Figure 17. Time Series Plots of Prewhitened Tree-Ring Indices and Precipitation Index in the
South Region -- The original series are given by the solid line, and the ARMA
residuals from models in Table 7 are given by the dashed line.
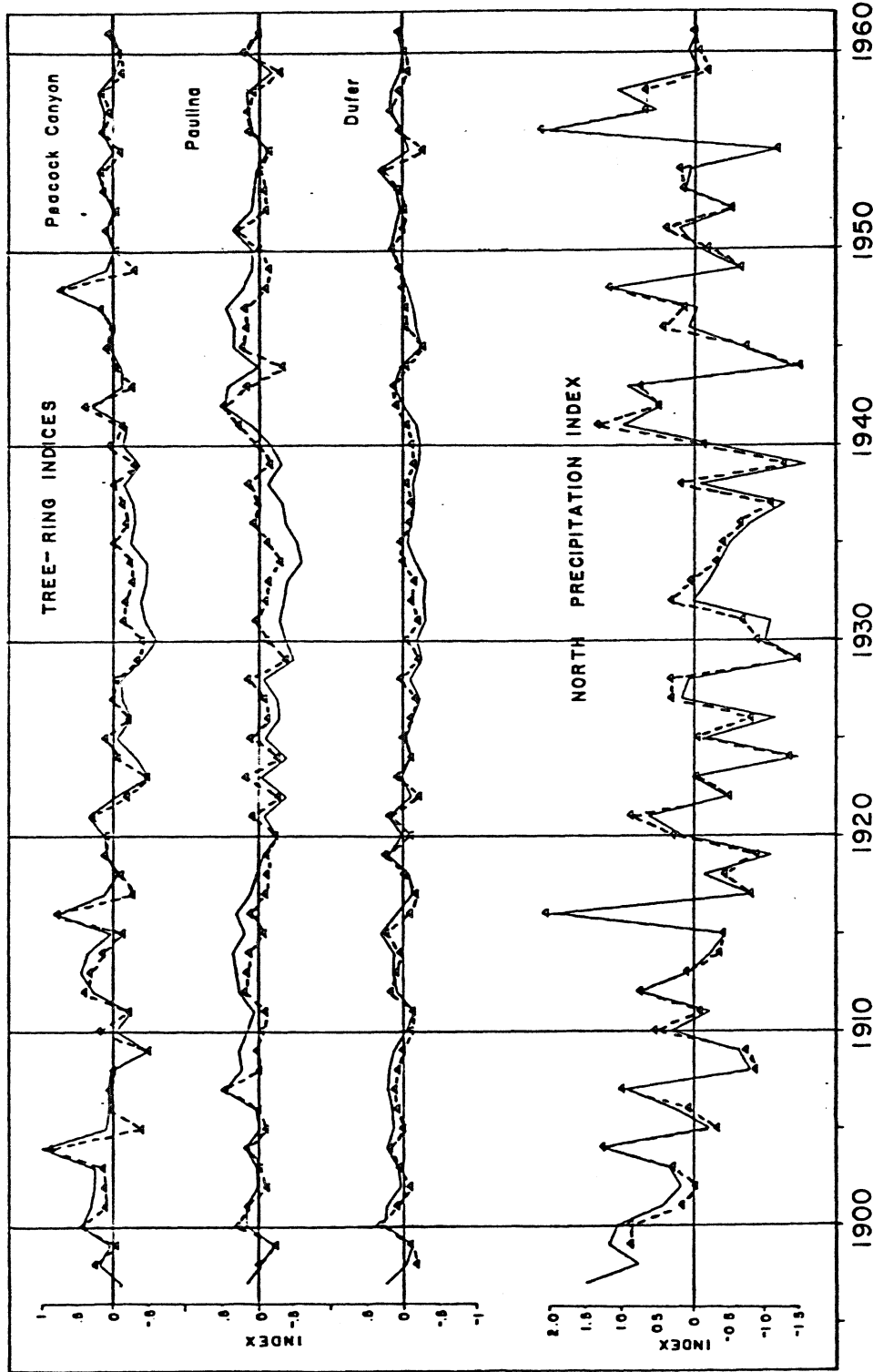
Figure 18. Time Series Plots of Prewhitened Tree-Ring Indices and Precipitation Index in the North Region -- The original series are given by the solid line, and the ARMA residuals from models listed in Table 7 are given by the dashed line.

series. The "Q" statistic [Eq. (2.7)] indicated adequate removal of autocorrelation for all series except possibly San Gorgonio. A value of .05 under the SigQ column indicates the chance is only 5% that the value of Q could have arisen from a random series. The most common form of model selected by the AIC criterion [Eq. (2.6)] was ARMA (1,0,0) followed by ARMA (2,0,0).

The preponderance of autoregressive (AR) tree-ring models with nearly random climatic series suggests that the tree-ring index generally is aptly viewed as an autoregressive process rather than a moving average of several years' climate. The distinction is important. For example, assume that two very dry years occur back to back in 1847 and 1848. In a moving average system the climate in both 1847 and 1848 would be necessary to predict the ring-width deviation in 1848. This information could not be adequately gleaned from the ring in 1847 and the climate in 1848. In an AR system, on the other hand, the effects of the 1847 drought and previous years' climate are condensed into the ring deviation of 1847. The 1847 ring and the 1848 climate are therefore suffi- cient to predict the ring in 1848. The practical importance of this result is that reconstruction models that included negatively lagged tree-ring indices to adjust for persistence are appropriate only under the AR systems. The fitted models therefore lend support to the use of negative lags in reconstruction models.

Crosscorrelations

The sample crosscorrelations between prewhitened and rainfall indices and prewhitened tree-ring indices are plotted in Figure 19

Original   Prewhitened

CROSSCORRELATION

LAG (years)   LAG (years)
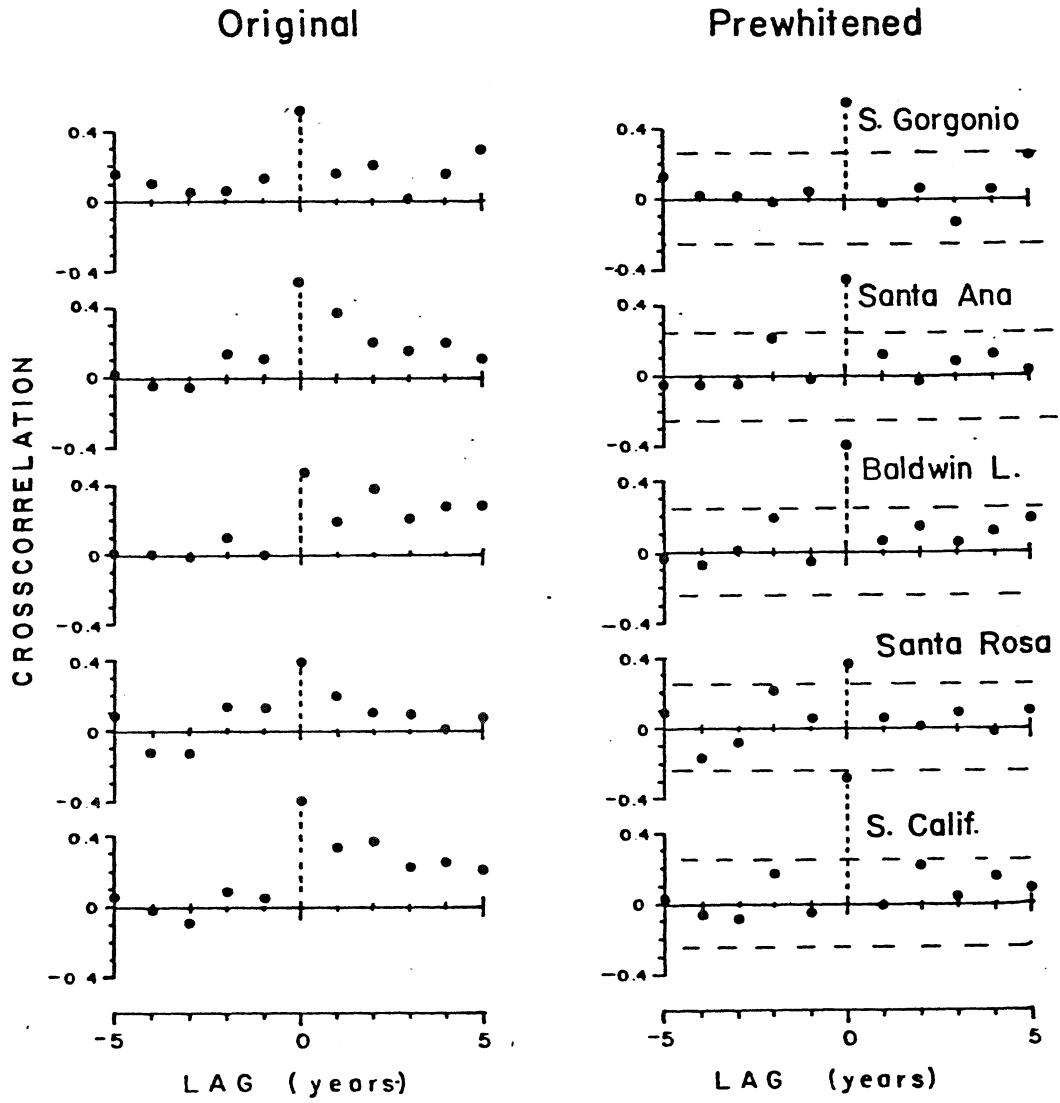
Figure 19. Sample Crosscorrelations Between Prewhitened Tree-Ring
            Indices and Prewhitened Regional Precipitation Indices —
            Crosscorrelations between the original variables (before
            prewhitening) are shown at left for comparison. The two-
            standard-error significance level from Equation (2.15b),
            page 25, is shown by the dashed line. Periods for
            computation were 1901-1963 for the first 8 series (South),
            and 1897-1961 for the last 9 series (North).
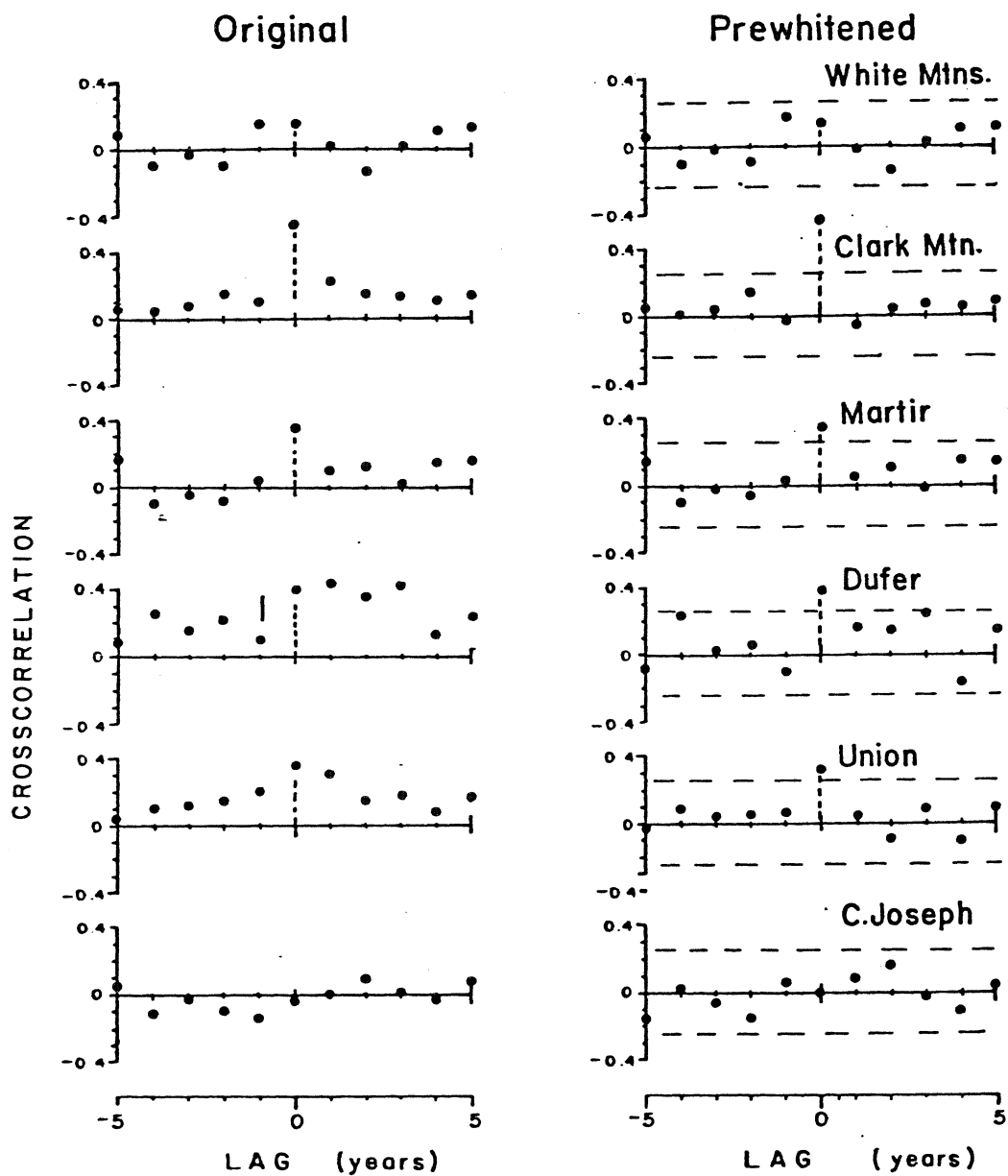
Figure 19.--Continued Sample Crosscorrelations Between Prewhitened
Tree-Ring Indices and Prewhitened Regional Precipitation
Indices.
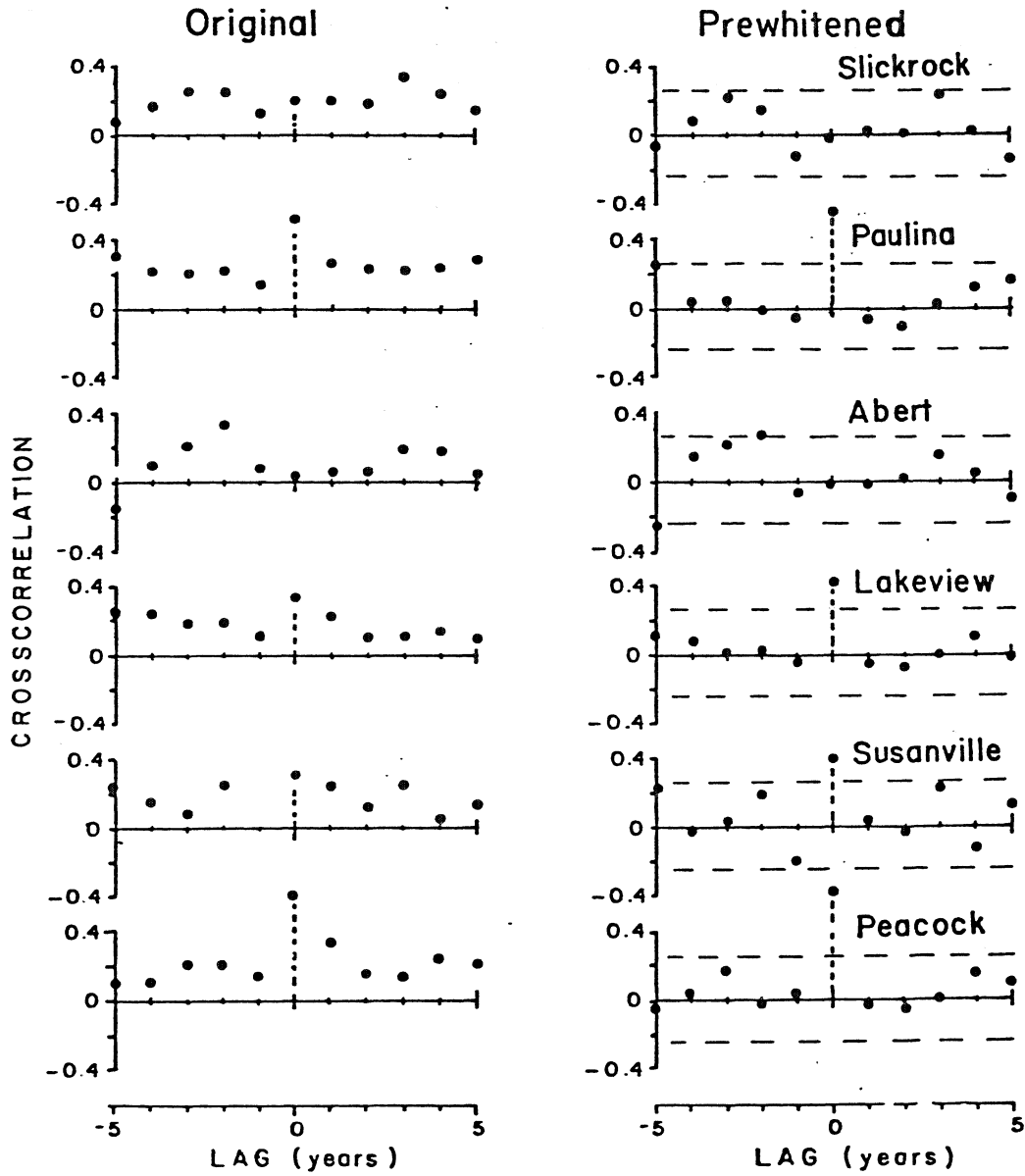
Figure 19.—Continued   Sample Crosscorrelations Between Prewhitened
Tree-Ring Indices and Prewhitened Regional Precipitation
Indices.

along with crosscorrelations between the original variables. Pre-whitening noticeably increased the size of the lag-zero correlations relative to correlations at other lags (e.g., Santa Ana, Southern California, Dufer, and Union). The only significant crosscorrelations for the prewhitened series by the two-standard-error criterion [Eq. (2.23)] were at lag zero.

This result implies that the rainfall index in year t affects future years' tree-ring index only through autocorrelation in the tree-ring series. In terms of the lagged-response diagram (Figure 6) no direct influence occurs by pathway b. The random shock concept described in Chapter 2 is therefore plausible, and the proposed reconstruction model using prewhitened variables may be appropriate.

Reconstruction using prewhitened variables was shown in Chapter 2 to differ fundamentally from reconstruction using positively lagged tree rings as predictors. According to the random shock model, tree rings in year t+1, t+2, ... offer no new information on climate in year t not available from the tree-ring index in year t adjusted for prior growth. To test the importance of positive lags, the regional precipitation indices were reconstructed by regression with prewhitened variables, and by regression with lagged tree-ring models that included positive lags, and the results were compared.

Regression Analyses

Reconstructions of regional precipitation indices were generated separately from three tree-ring series in each region. The reconstruction equations were estimated by multiple linear regression.

Single-site reconstructions were generated by two methods: regression with prewhitened variables (PWV model) and regression on lagged tree rings (LTR model). The procedures for the PWV model were discussed in Chapter 2 and summarized in Figure 8. The LTR method consisted of regressing the regional precipitation index on the lagged tree-ring index, where the lags for each tree-ring series were selected from the results of the transfer-function modeling (Table 6).

The regression equation for the PWV model was given in Equation (2.27) and is rewritten below, where the terms are defined as before:

$$\hat{\alpha}_{y,t} = \hat{b}_0 + \hat{b}_1 \alpha_{x,t} \tag{3.8}$$

The regression equation for the LTR model is

$$\hat{Y}_t = \hat{b}_0 + \sum_{i=1}^{I} \hat{b}_i X_{t-\ell_i} \tag{3.9}$$

where

Y_t is the predicted regional precipitation index in year t,

X_t is the tree-ring index in year t,

$\hat{b}_0$ is the estimated regression constant,

$\hat{b}_1$, $\hat{b}_2$, ... $\hat{b}_I$ are regression coefficients,

I is the total number of lagged terms on the tree-ring index X_t included as predictors, and

ℓ_1, ℓ_2, ... ℓ_I are the particular lags in the model (e.g., $I = 3$, $\ell_1 = -1$, $\ell_2 = 0$, $\ell_3 = +1$).

Regression equations were estimated with the SPSS (Statistical Package for the Social Sciences) computer package (Nie et al. 1975). Computational formulas for summary regression statistics reported here

can be found in most elementary statistical texts, and are included in
Appendix C.

General Results of Single-Site
Regression Analyses

The estimated regression models are summarized in Tables 8 and
9. Accuracy of prediction as measured by per cent variance explained,
R^2, differed little between the PWV and LTR predictions for four of the
six sites. For Baldwin Lake and Dufer, however, the LTR prediction was
more accurate than the PWV prediction. Not surprisingly, the LTR re-
gression equations for those sites had relatively large weights on
positive lags. The PWV prediction can be expected to differ appreciably
from the LTR prediction in this situation since the prediction of rain-
fall index in year t by the PWV model uses information from the current
and past tree rings only. The R^2 results for Dufer and Baldwin Lake
suggest that for those sites, contrary to the random shock concept,
useful information on rainfall in year t does reside in subsequent years'
rings.

The plots of actual and reconstructed precipitation indices
(Figures 20 and 21) show that the LTR model generally reconstructed
amplitudes of peaks and troughs better than the PWV model: the droughts
centered about 1930 in the North and 1961 in the South are striking
examples. The severity of drought in extremely dry years was also more
accurately reconstructed by the LTR model (e.g., 1959 and 1961 from
Baldwin Lake; and 1929, 1937, 1939, and 1944 for Dufer). The resulting
higher R^2 of the LTR predictions was offset, however, by a lack of skill
in in tracking certain high frequency variations in the precipitation

92

Table 8. Estimated Regression Equations in the South Region -- Summary of regression equations for three selected tree-ring sites in Southern Region. The first equation is for regression of the regional precipitation index against tree ring indices. The second equation is for a regression using the corresponding prewhitened (PW) series as predictand and predictors. The calibration period is given below the site name. R^2 is the multiple correlation coefficient squared. F is the overall F level for the equation (see Appendix C). R_1^2 is the R^2 adjusted for loss of degrees of freedom. R_2^2 is the square of the correlation coefficient between actual and predicted precipitation index for the years 1901-1963. The number of standard errors by which a coefficient differs from zero is given in parentheses below the coefficient. Refer to Equations (3.8) and (3.9), page 90, for form of regression equation.

| Site/Years | Const. | | | Coefficients | | | | R^2 | F | R_1^2 | R_2^2 |
		t-2	t-1	t	t+1	t+2	t+3				
Santa Ana (1901-1966)	-1.198		-.795 (2.6)	1.492 (4.4)	.433 (1.4)			.36	11.6	.33	.37
S. Ana PW (1903-1963)				1.699 (5.3)				.32	28.0	.31	.34
Baldwin L. (1901-1964)	-.885	-.387 (1.1)	-1.199 (3.5)	1.813 (4.7)		.612 (1.9)		.44	11.5	.40	.44
Baldwin L PW (1903-1963)	.001			2.139 (5.8)				.36	33.9	.35	.37
S. Calif. (1901-1964)	-1.212		-.947 (3.9)	1.738 (6.4)	.128 (0.5)			.53	16.6	.50	.53
S. Calif PW (1903-1963)	-.001			1.913 (8.0)				.52	64.4	.51	.52

Table 9. Estimated Regression Equations in the North Region -- Summary of regression equation for three selected tree-ring sites in Northern Region. Remainder of legend as in Table 8, except that R^2_2 is computed for period 1899-1961.

Site/Years	Const.	t-2	t-1	t	t+1	t+2	t+3	R^2	F	R^2_1	R^2_2
				Coefficients							
Dufer (1897-1961)	-2.969		-1.654 (2.5)	1.640 (2.2)	.915 (1.2)	-.119 (0.2)	2.142 (3.3)	.36	6.7	.31	.36
Dufer PW (1899-1961)	-.035			2.218 (3.1)				.14	9.8	.12	.17
Paulina	-1.067		-1.052 (2.2)	2.243 (4.5)				.28	8.4	.25	.30
Paulina PW (1899-1961)	-.036			2.320 (4.9)				.28	23.6	.27	.24
Peacock (1897-1963)	-1.537		-.468 (1.5)	1.638 (5.1)	.342 (1.1)			.38	12.7	.35	.38
Peacock PW (1899-1961)	-.032			1.796 (6.1)				.38	37.4	.37	.36
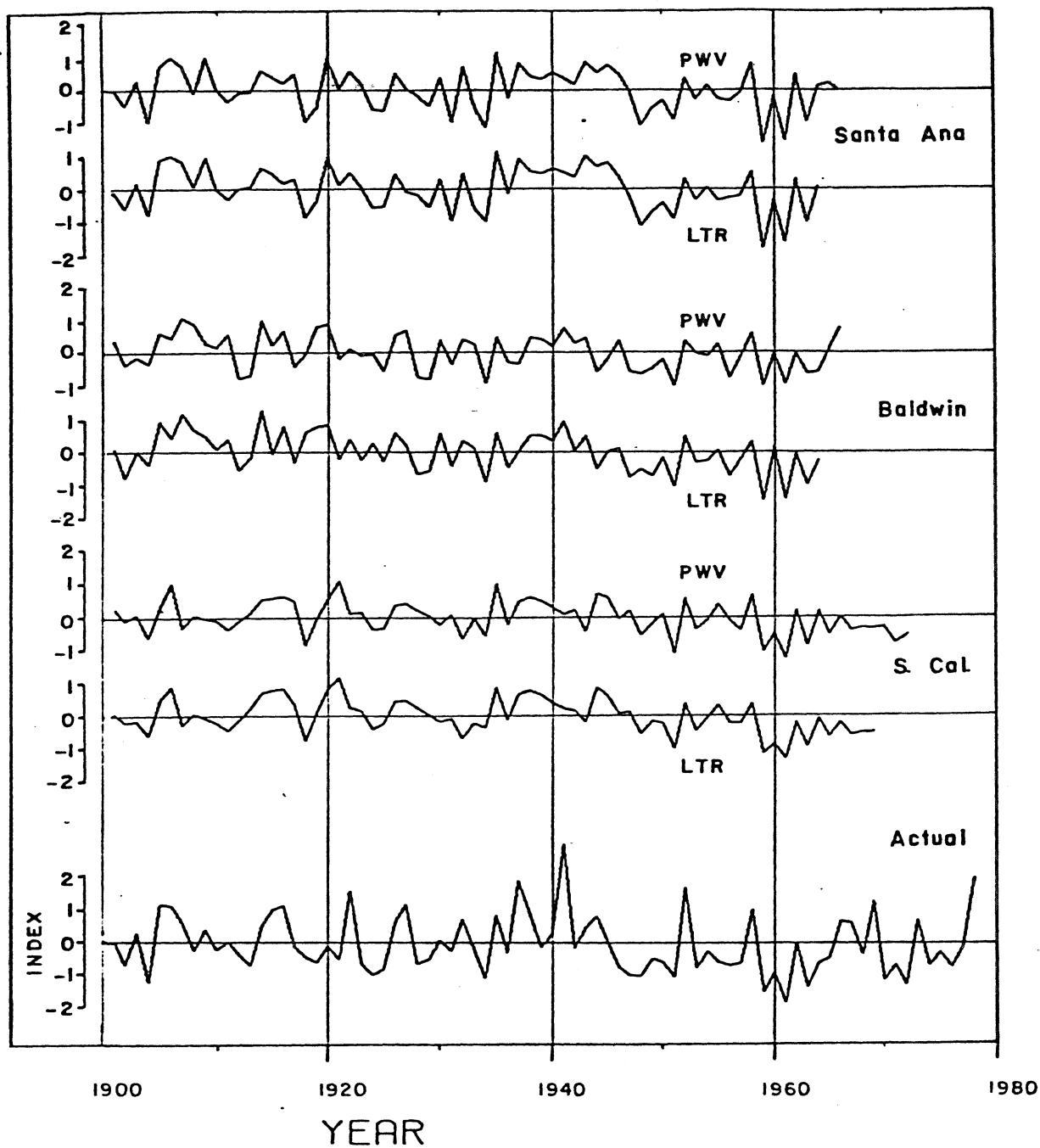
Figure 20. Single-Site Reconstructions of the South Precipitation
Index ‑‑ Reconstructions from 3 tree-ring sites by the
lagged-tree-ring (LTR) and prewhitened variables (PWV)
models are shown, along with the actual South precipitation
index.
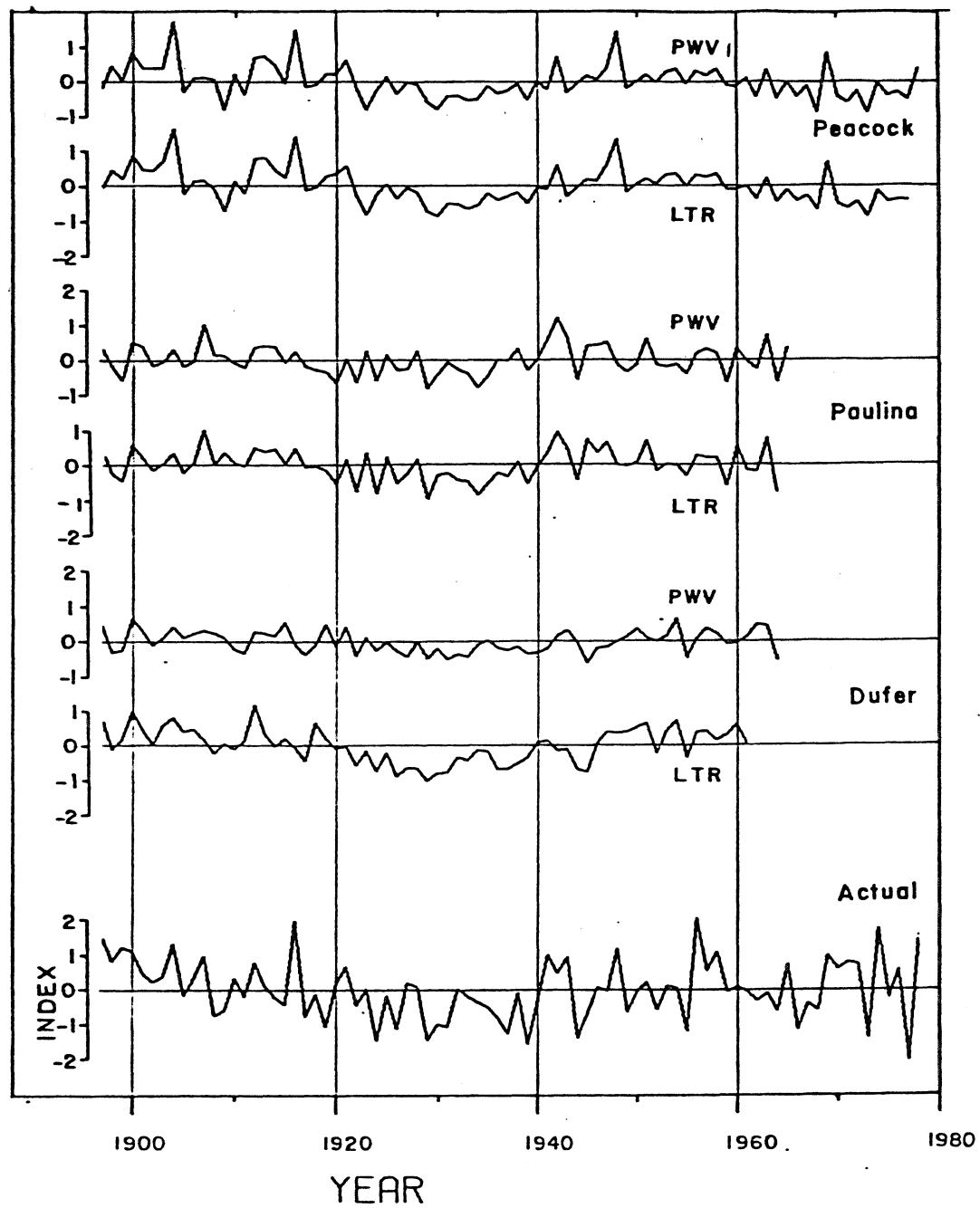
Figure 21. Single-Site Reconstructions of the North Precipitation
Index — Remainder of legend is as in Figure 20.

index. For example, the Dufer LTR model failed to predict the 1927, 1928, and 1938 breaks in the North drought, while the PWV model did predict rainfall index above the mean for those years (see Figure 21).

The large LTR prediction errors in some years may be partially due to the use of positive lags. This can be seen by considering the Dufer LTR regression equation (Table 10), and the sequence of years 1928-1931. The Dufer equation, which has large positive coefficients on lags t+1 and t+3, would be unlikely to correctly predict a wet year that immediately preceded an extended severe drought. The North precipitation index was above normal in 1928, but 1929, 1930, and 1931 were all among the 10 driest years in the 1897-1961 record. Consequently, although the Dufer tree-ring index was near average in 1928, that year was predicted in drought (see Figure 21) because of the weighting on 1929 and 1931 by the regression equation.

The Baldwin Lake plot (Figure 20) illustrates another possible problem with positive lags. Note that the LTR regression equation for Baldwin (Table 8) has a relatively large weight on t+2, and also that a major feature of the actual South precipitation index is the sequence of very dry years 1959, 1961, and 1963. The large regression weight on lag t+2 may have come about partially because the time series of drought in the region had a prominent sequence of severe drought in alternate years. The regression model therefore may have been largely determined by the sequence of drought in the calibration period. The long-term climate, however, need not contain similar sequences, and accuracy as measured by R^2 in the calibration period may consequently be a poor indicator of accuracy in the long-term reconstructions.

There appears to be a tradeoff in using positive lags. On the one hand, positive lags may substantially increase the R^2 on the prediction equation because the effects of a rainfall anomaly may indeed be distributed over two or more rings. On the other hand, reconstructions for particular years may be thrown off the mark more or less depending on the sequence of wet and dry years at the site. Thus when positive lags are included in the model, and when their regression coefficients are relatively large, care should be taken in drawing inferences about drought conditions in particular years from the reconstruction.

Frequency Response

The relationships between the predicted and actual series in Figures 20 and 21 were studied in more detail with cross-spectral analysis. The procedures used follow Jenkins and Watts (1968), and the relevant equations and particular details of application in this study are given in Appendix D. Three functions—the gain $G(\omega)$, phase $F(\omega)$, and squared coherency $C^2(\omega)$—were used to study the frequency response properties of the system diagrammed below:

ACTUAL	Frequency Response	RECONSTRUCTED
x_t → Regional Precipitation Index		Regional Precipitation Index → y_t
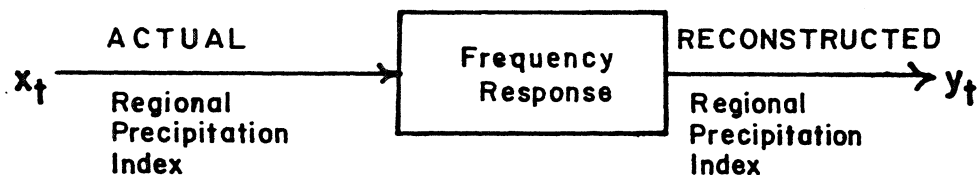
Emphasis was placed on comparing results from regression on prewhitened

variables (PWV models) with those from regression on lagged tree rings

(LTR models).

The gain is analogous to a linear regression coefficient of y_t

on x_t defined at each frequency ω (Chatfield 1975, p. 178). The squared

coherency measures the linear correlation between y_t and x_t at each

frequency ω, and is analogous to the square of the correlation coeffi-

cient (Chatfield 1975, p. 177). The phase measures the length of time

that variations at frequency ω in y_t either lag behind or lead varia-

tions at the same frequency in x_t (Chatfield 1975, p. 177).

A perfect reconstruction (i.e., $y_t \equiv x_t$ in the diagram above)

would be characterized by a gain of one, squared coherency of one, and a

phase of zero at all frequencies. As variations at frequency ω in the

reconstruction differ in magnitude from the variations at frequency ω

in the actual precipitation index, the gain will deviate from one; as

such variations at the same frequency in the two series are imperfectly

correlated, the squared coherency will be lower than one; and as such

variations do not match up in time, the phase will vary from zero. The

flatness of the plots of these three functions indicates the evenness of

the response as a function of frequency. Flat gain and coherency

functions are therefore desirable if inferences about frequency proper-

ties of the climatic variable are to be drawn from the long-term recon-

structions.

Plots of the estimated gain, phase, and squared coherency

functions are shown in Figures 22 and 23. The LTR model was better than

the PWV model at all sites in reconstructing low frequency variations,
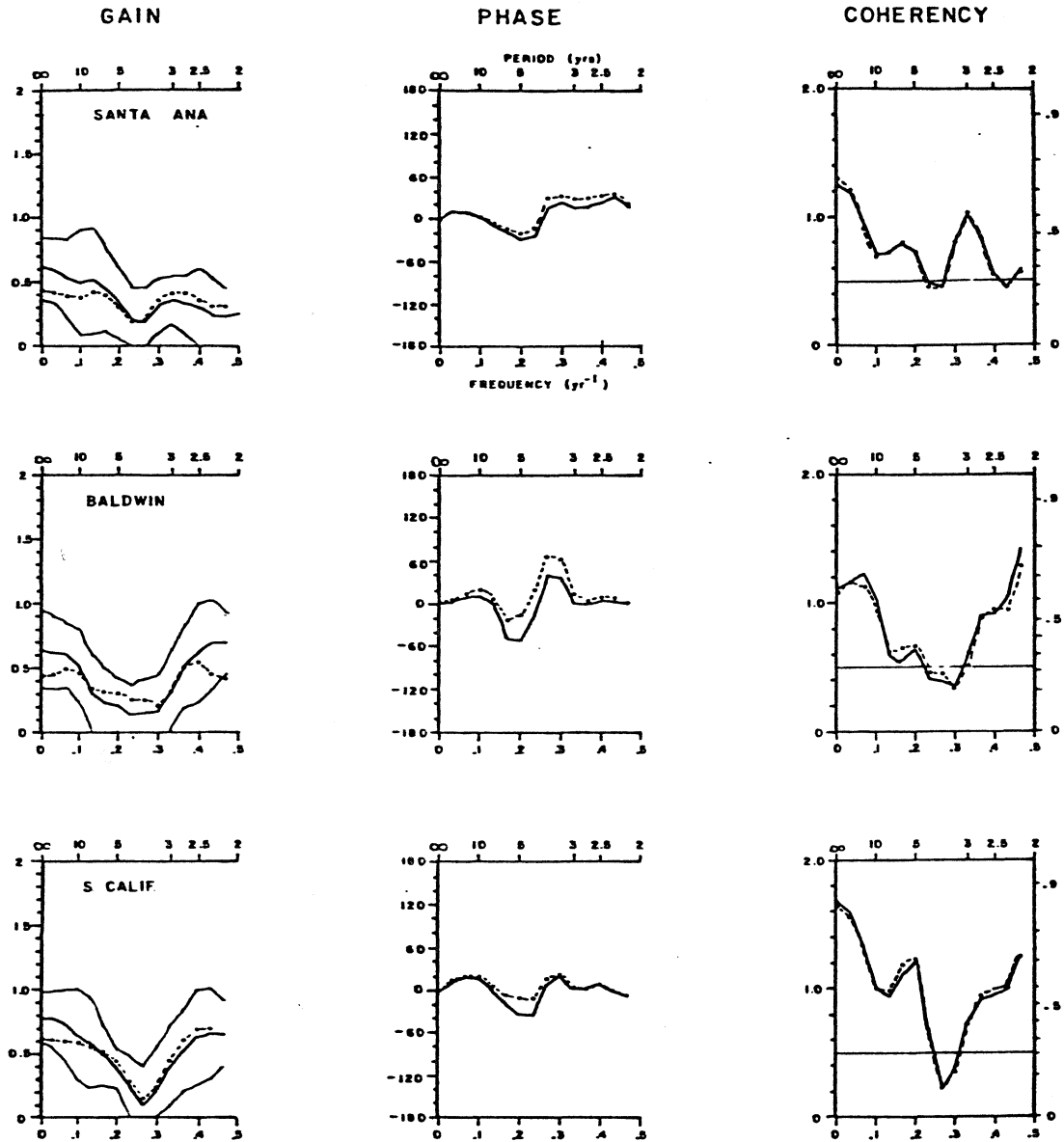
Figure 22. Estimated Gain, Phase, and Squared-Coherency Functions for
Single-Site Reconstructions in the South Region — Heavy
solid line is for the lagged-tree-ring (LTR model. Dashed
line is for the prewhitened-variables (PWV) model. Light
solid line gives the 90% confidence interval on the gain,
and the 95% significance level on the squared coherency.
Units on phase are degrees. Squared coherency is given in
transformed scale (Jenkins and Watts, 1968, p. 379) on
left axis.
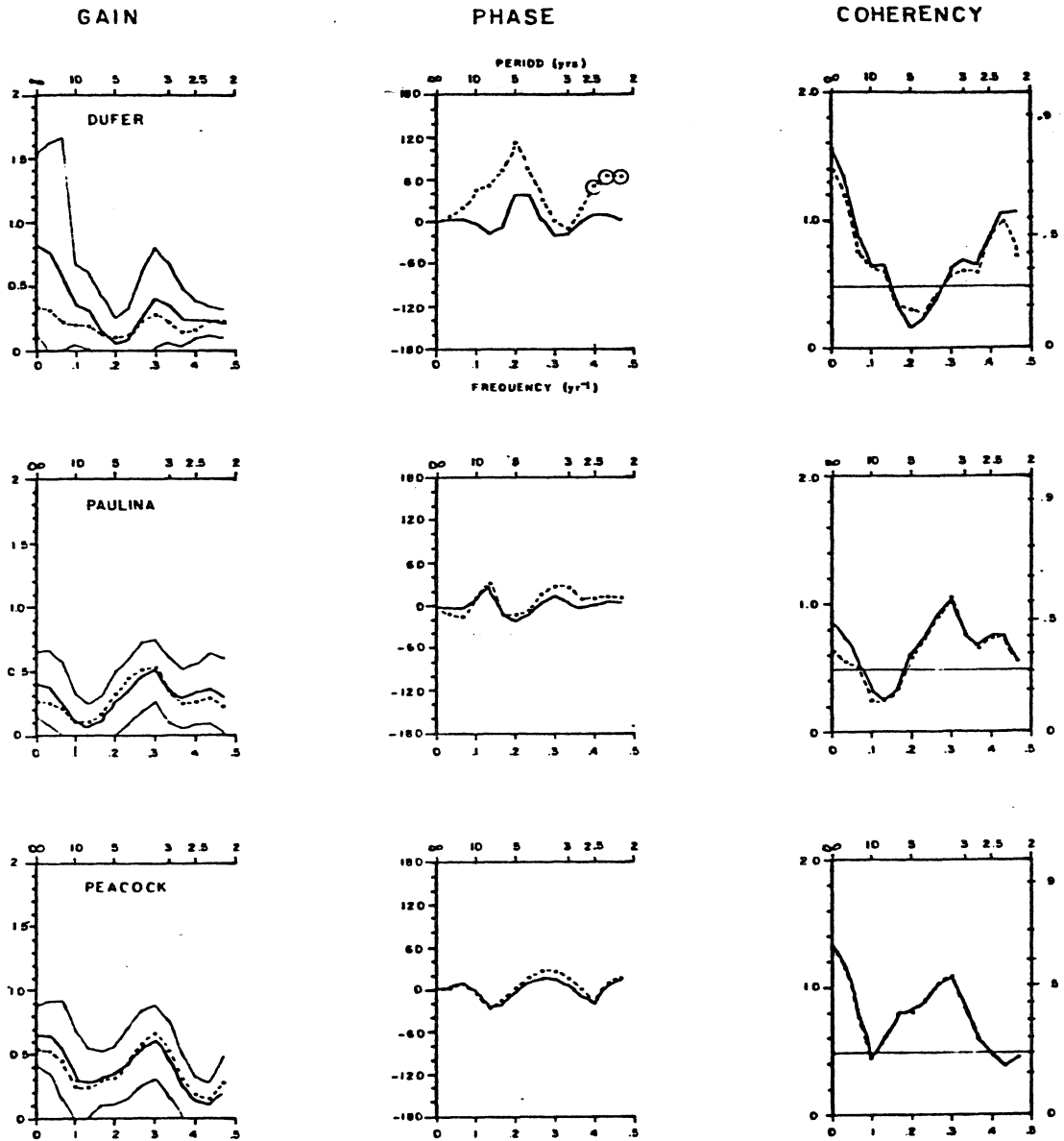
Figure 23. Estimated Gain, Phase, and Squared-Coherency Functions for
Single-Site Reconstructions in the North Region — Phase
estimates significant at the 90% confidence level are
circled. Remainder of legend is as in Figure 22.

as shown by the relative high values for the gain function at low

frequencies. The LTR reconstructions had higher gain and generally

higher squared coherency than the PWV reconstructions at periods longer

than about 10 years. This result agrees with the earlier observation

that the LTR predictions seemed to reflect the amplitudes of broad

swings above and below the mean more accurately than the PWV predictions

(Figures 20 and 21). Largely because of this difference in gain at low

frequencies, the PWV models gave flatter frequency responses than the

LTR models.

At high frequencies, the difference between LTR and PWV re-

sponses was much less pronounced and less consistent from site to site.

For some sites the LTR model gave a slightly better (higher gain,

squared coherency) response, for others the PWV gave better response.

The largest differences at high frequencies were for Dufer and Baldwin

Lake, where the LTR coherencies were higher than the PWV coherencies.

In addition, the LTR gain was considerably higher than the PWV gain at

high frequences for Baldwin Lake. The only three significant (at the

90% level) phase estimates were also found at high frequencies in the

Dufer plot.

The Dufer and Baldwin Lake results at high frequencies probably

reflect the superiority of the LTR model in reconstructing years of

extreme drought or wetness. This tendency was pointed out earlier re-

garding 1959 and 1961 in Baldwin Lake's reconstruction (see Figure 20).

The positive lags may give the LTR model an advantage in extremely dry

years, when effects such as defoliation and root dieback are likely to

be most pronounced.

For the Southern California and Peacock Canyon sites, the model choice made little difference to the frequency response. The LTR and PWV squared-coherency plots were virtually indistinguishable from one another, and the PWV gain plots were only slightly flatter than the LTR gain plots. The relative insensitivity of these sites to model choice may be explained by the estimated impulse response weights (Figure 16). These sites had the largest lag-zero weights—considerably higher than the weights on any non-zero lags. The lag structure is likely to be relatively unimportant in reconstructions for such sites because the bulk of the information on climate in year t is in the ring for year t.

In summary, the frequency response analysis indicates that the PWV model gives a flatter frequency response than the LTR model, but that the LTR model more accurately reconstructs low frequencies and very dry years. The question in selecting one method over another is whether it is preferable to have a reconstruction which accurately reflects the spectral properties of the actual data, but which has a larger noise component, or a reconstruction which emphasizes some frequencies more than others, but which has a smaller noise component. For some series, the choice of reconstruction method makes an appreciable difference to the resulting predictions. A diagnostic analysis of the lagged responses of individual tree-ring series by transfer-function modeling and ARMA modeling can aid in identifying series for which the model choice will make an appreciable difference.

The comparison of the LTR and PWV models has so far been restricted to analyses of accuracy in the calibration method. Such

comparisons may mistakenly favor the LTR model because of the possible problem of calibrating the regression model to the particular <u>sequence</u> of drought in that period. In other words, a large weight on, say, year t+2 is favored by two circumstances: (1) climate in year t affects ring width in year t+2, and (2) climate in year t is correlated with climate in year t+2. The second circumstance acts to obscure the time lag in response. Verification on data outside the calibration period is therefore desirable. Before carrying out this analysis, however, the single-site reconstructions were averaged together to form mean regional LTR and PWV reconstructions.

Mean Reconstructions

The precipitation index was reconstructed separately from individual tree-ring sites in this study to stress the temporal-filtering aspect of the reconstruction equation. This approach would not generally be appropriate when the objective is the most accurate possible reconstruction, because no use is made of the covariance of the tree-ring data in space. A single-site reconstruction is thus likely to unnecessarily contain small-scale noise, while a reconstruction using tree-ring data from several sites is likely to better emphasize the general regional climatic signal. Several different methods of spatial weighting in reconstruction equations were mentioned in Chapter 1. Before evaluating the long-term reconstructions, an attempt was made to reduce the localized noise by simple averaging of the single-site reconstructions into regional mean reconstructions. The procedure consisted of the following steps.

1. The 3 single-site reconstructions were averaged together.

2. The correlation coefficient was computed between the resulting averaged series and the actual regional precipitation index.

3. The variance in the averaged series was re-scaled by multiplying the averaged series by the quantity $r\dfrac{s_1}{s_2}$, where r is the correlation coefficient between the average reconstruction and the actual series, s_1 is the standard deviation of the actual precipitation index, and s_2 is the standard deviation of the averaged series.

A mean PWV reconstruction and LTR reconstruction were generated for each region. The rescaling factors for the mean series are listed in Table 10.

Table 10. Rescaling Factors for Mean Regional Reconstructions -- Terms are defined as above.

Region	Model[a]	r	s_1	s_2	Rescaling Factor
South	LTR	.766	.915	.531	1.32
South	PWV	.753		.490	1.41
North	LTR	.718	.826	.393	1.51
North	PWV	.699		.313	1.76

[a]Lagged tree-ring (LTR) or prewhitened-variable (PWV) reconstruction.

Accuracy of Mean Reconstructions

Calibration Period. The mean regional reconstructions for the periods covered by precipitation records at one or more of the weather stations used in this study are shown in Figures 24 and 25. The actual regional precipitation indices for the calibration period, and precipitation indices from available data for earlier years are also shown. The accuracy of prediction increased from the single-site reconstructions to the mean reconstructions (Table 11). By the R^2 criterion, the South reconstructions were more accurate than the North, and the lagged tree ring (LTR) reconstructions were more accurate than the prewhitened variables (PWV) reconstructions, although the difference between models for the South was very small.

The time series plots in Figures 24 and 25 show that extremely wet years were not reconstructed well. A contingency table summary of accuracy of predicting in various precipitation classes in the South especially supports this observation (Figure 26). Only 3 of the 12 wettest years in the South were correctly predicted by the LTR and PWV reconstructions; in contrast, 7 of the 12 driest years were correctly predicted by the LTR model, and 8 by the PWV model. A similar asymmetry, though much less striking, is found in the North. The lower accuracy in very wet years may reflect a tailing off in the trees' response to additional moisture under very wet conditions.

The inability to reconstruct very wet years caused the coefficients of skew of the reconstructed and actual data to differ appreciably in the South, as shown below.
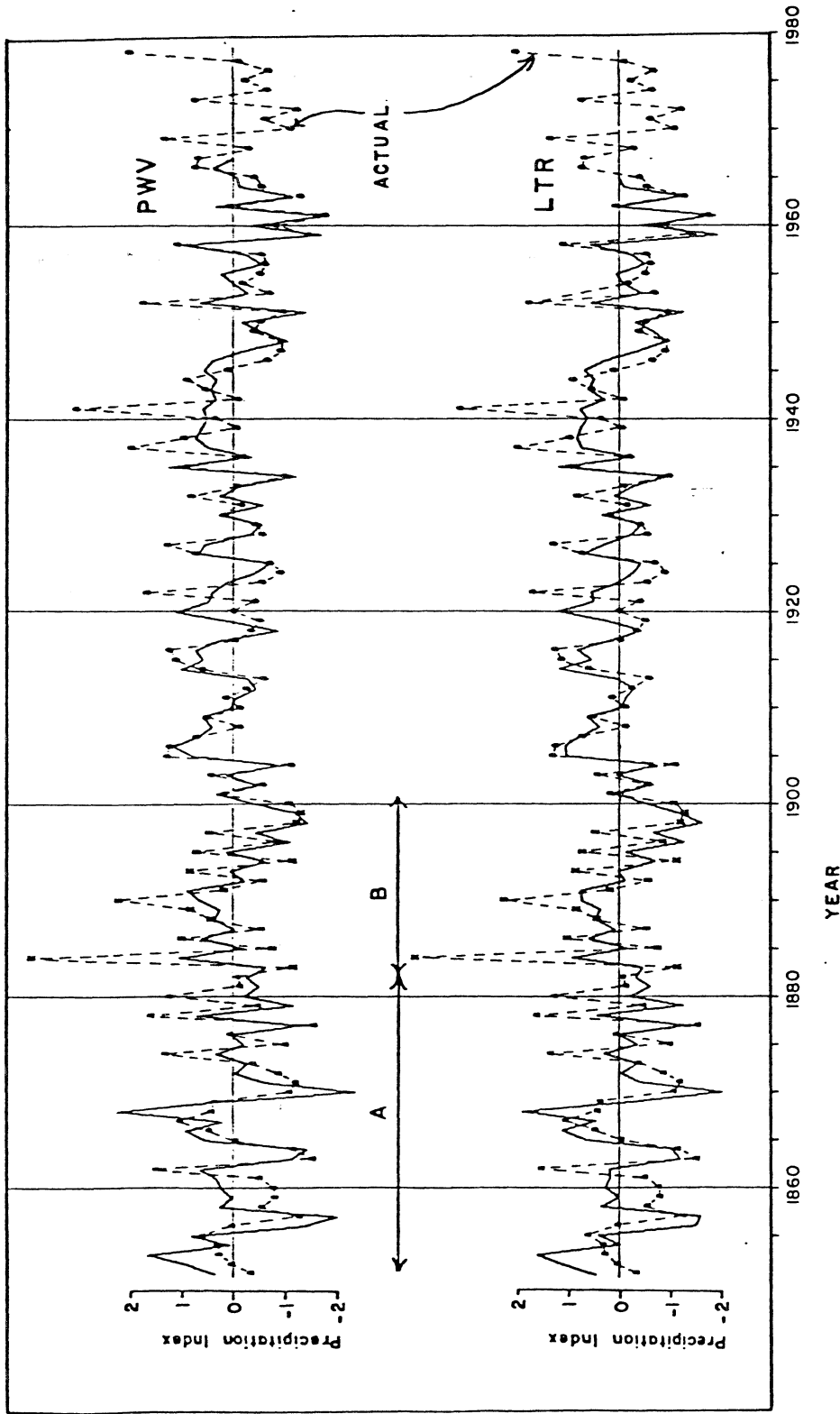
Figure 24. Time Series of Reconstructed and Actual Mean Regional Precipitation Index in the
South Region -- Solid lines are reconstructions by the lagged-tree-ring model (LTR)
and the prewhitened-variables model (PWV); dashed lines are actual data. Actual
index for period A is for San Diego precipitation record. Actual index for period B
is a 3-station index from Los Angeles, Riverside, and San Diego.
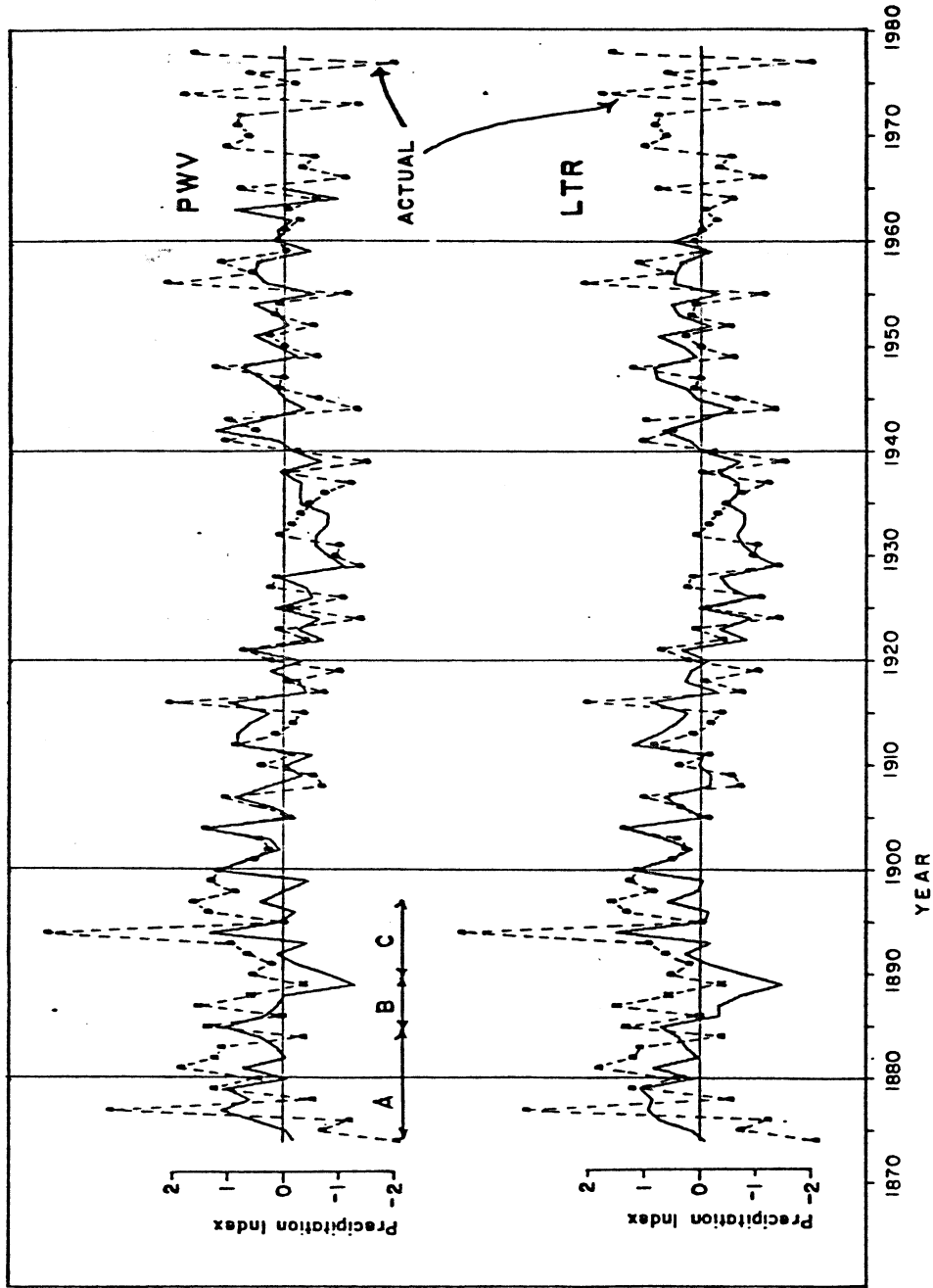
Figure 25. Time Series of Reconstructed and Actual Mean Regional Precipitation Index in the North Region — Solid lines and dashed lines are defined as in Figure 25. Actual index for period A was computed from Walla Walla, Wash. record. Actual index for B is a 2-station index for Walla Walla, and Hood River. Actual index for period C is an earlier extension of the 3-station mean index used in calibration.

Table 11. Decimel Fraction of Variance Explained (R^2) by Single-Site
Reconstructions and Mean Regional Reconstructions -- R is
the correlation coefficient between the actual Regional
Precipitation Index and the reconstructions. Computation
periods are 1901-1963 in the South (top 4 series) and 1897-
1961 in the North (bottom four series).

Site	R		R^2	
	LTR[a]	PWV[b]	LTR	PWV
Santa Ana	.61	.58	.37	.34
Baldwin Lake	.66	.61	.44	.37
S. California	.73	.72	.53	.52
Mean South	.77	.75	.59	.57
Dufer	.60	.41	.36	.17
Paulina	.55	.49	.30	.24
Peacock	.61	.60	.38	.36
Mean North	.72	.67	.51	.45

[a] Lagged tree-rings models.

[b] Prewhitened-variables models.

SOUTH   NORTH
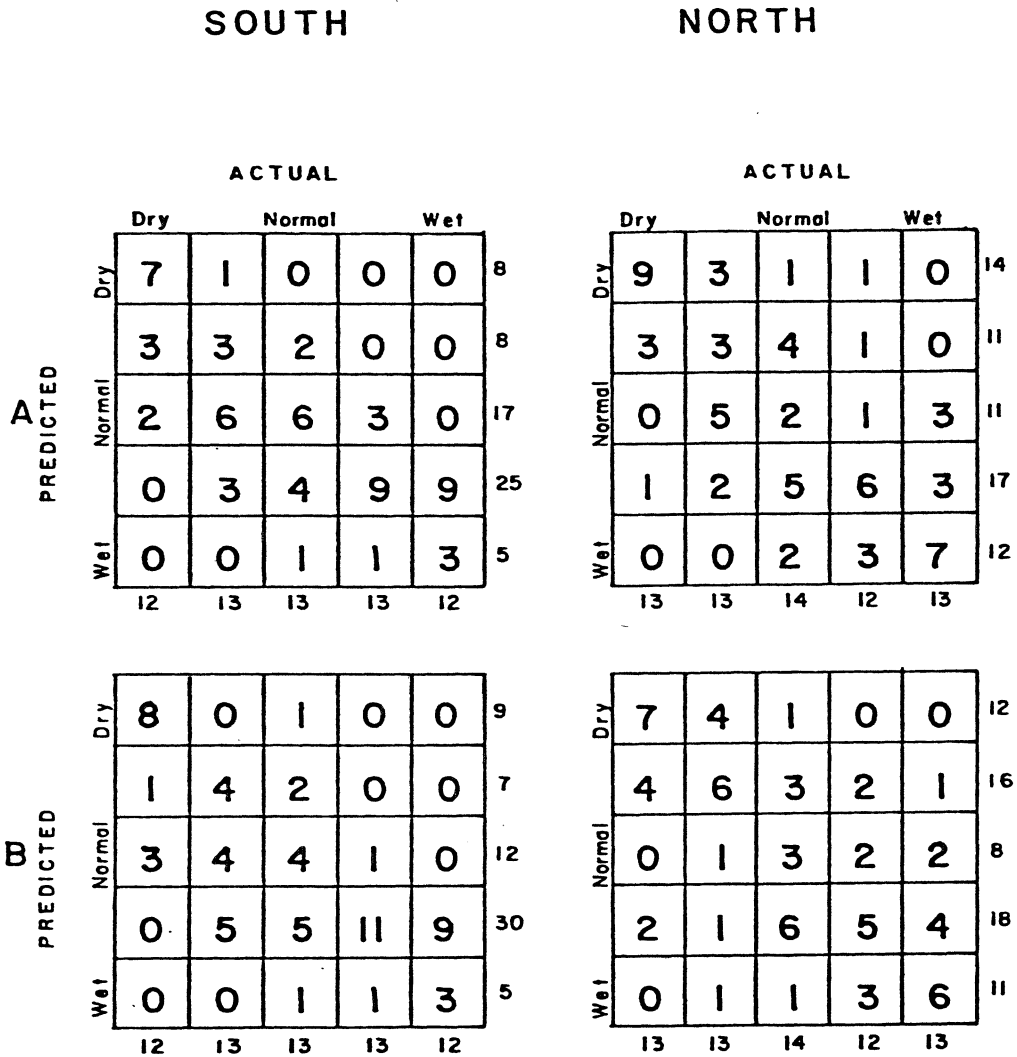
Figure 26. Contingency Table Summary of Accuracy of Reconstructions in Various Precipitation Classes — Series analyzed were regional mean precipitation indices in the South and North regions reconstructed by the lagged-tree-ring model (A), and the prewhitened-variables model (B). Classes were selected to contain roughly equal numbers of years based on the actual regional precipitation index. Periods for analysis were 1901-1963 in the South and 1897-1961 in the North.

	Actual	Reconstructed LTR	PWV
South 1901–1961	.81	−.69	−.65
North 1901–1961	.38	−.03	.30

One possible way of reducing this problem is to calibrate on precipitation series that are less skewed, perhaps from higher elevation weather stations. Another is to transform the precipitation series with a log transform before calibrating with tree rings. This last approach has the offsetting drawbacks of providing a least-squares prediction of the log data rather than the original precipitation data, and of assuming that the nonlinearity in response is characteristic of the entire range of precipitation, rather than just at very wet conditions.

Tables 12 and 13 summarize the accuracy of reconstructing extreme droughts. The reconstructions in the South were able to resolve individual years of extreme drought, although not too much importance should be attached to the differences in severity of reconstructed drough in these years, as the ranking of the actual data is not exactly duplicated by the reconstructions. Four of the five driest years in the South were also among the five driest reconstructed years by both the LTR and PWV models. The fifth driest year in the actual data—1904—was seventh driest in both reconstructions.

Comparison of the magnitudes of extreme droughts were more reliable when the reconstructions were interpreted as moving averages of 3 or more years. The driest three-year averages in the LTR reconstruction

Table 12.   Most Severe Reconstructed and Actual Droughts in the
Calibration Period in the South.

| Moving Ave. | Rank | Reconstructed | | | | Actual | |
| | | LTR[a] | | PWV[b] | | | |
		Year[c]	Index	Year	Index	Year	Index
1 year	1	1959	−1.94	1961	−1.74	1961	−1.76
	2	1961	−1.91	1959	−1.69	1959	−1.44
	3	1951	−1.28	1951	−1.39	1963	−1.29
	4	1963	−1.28	1934	−1.20	1904	−1.12
	5	1934	−.97	1963	−1.15	1934	−.99
3 years	1	1961	−1.43	1961	−1.25	1961	−1.34
	2	1963	−1.04	1963	−.85	1963	−1.00
	3	1962	−.76	1951	−.71	1962	−.84
	4	1951	−.76	1949	−.59	1948	−.84
10 years	1	1963	−.58	1963	−.42	1963	−.61

[a]Reconstructed by lagged-tree-ring model.

[b]Reconstructed by prewhitened-variable model.

[c]Year listed is last year of moving average.

Table 13. Most Severe Reconstructed and Actual Droughts in the
Calibration Period in the North — Remainder of legend as
in Table 12.

Moving Ave.	Rank	Reconstructed				Actual	
		LTR		PWV			
		Year	Index	Year	Index	Year	Index
1 year	1	1929	-1.41	1929	-1.15	1939	-1.54
	2	1930	-1.02	1930	-.85	1924	-1.44
	3	1924	-.94	1934	-.84	1929	-1.43
	4	1926	-.93	1933	-.82	1944	-1.37
	5	1922	-.87	1922	-.76	1937	-1.25
3 years	1	1931	-1.07	1931	-.87	1931	-1.15
	2	1930	-.93	1934	-.76	1939	-.96
	3	1932	-.83	1932	-.69	1926	-.90
	4	1934	-.77	1933	-.68	1937	-.84
10 years	1	1935	-.78	1935	-.61	1939	-.66

ranked exactly as the actual data. Both the PWV and the LTR reconstructions also show correctly that 1954-1963 was the driest decade.

The North reconstructions were less accurate than the South in pinpointing extremely dry years. Only two of the 5 driest years in the North were among the 5 driest reconstructed years. The driest year in the actual data--1939--ranked ninth driest in the LTR reconstruction and sixth driest in the PWV reconstruction. As in the South, identification of extreme droughts improved when longer periods were considered.

The year 1934 in the North illustrates an interesting aspect of the "noise." The PWV model reconstructed 1934 as the third driest year in the 1897-1961 calibration period, and the LTR model reconstructed it ninth driest. The year 1934 ranked only twenty-first, however, in the actual data. The discrepancy is probably due to the effect on the trees of the extremely high temperatures in 1934: the mean annual (September-August) temperature was highest on record for Walla Walla, Hood River, and Baker. The high temperature probably affected growth more than did moisture. In other words, excessively high temperatures probably caused reduced growth so that the reconstructed "drought" was more severe than that recorded by the precipitation record. The heat wave of 1934 is a well-known, large-scale climatic anomaly in the western United States, but for the purposes of this study, becomes just another element of the disturbances lumped together as noise.

Independent Verification. The segments of the actual time series of the precipitation index before the calibration period allow verification of the reconstructions on data not used in calibration.

Ideally, the independent data are an extension of the time series of the same variable used in calibration, and cover a period as long as the calibration period. Because of the shortness of available climatic series, these two conditions are not satisfied in this study. The verification series are precipitation indices computed from subsets of the stations forming the calibration series. For example, verification back to 1851 in the South relies solely on the San Diego record. The longest independent data set in the South is 50 years (1851-1900), and 23 years (1874-1896) in the North; the corresponding calibration periods are longer than 60 years. With these qualifications in mind, the independent data plotted in Figures 24 and 25 were compared to the reconstructions.

The South plots (Figure 24) show little noticeable decrease in accuracy from the calibration period to the independent data, and, except for the extremely wet years 1884 and 1890, excellent matchup for the years from about 1865 on. Note that the verification precipitation indices in Figure 24 comprise fewer climatic stations than the calibration-period precipitation index. A simple measure of independent verification is the correlation coefficient r between the verification series and the reconstructed index. An appreciable decrease in r from the calibration period to the independent-check period may indicate that the R^2 for regression overestimates the expected accuracy of long-term reconstructions. Correlation coefficients between the reconstructions and verification series are listed in Tables 14 and 15.

Correlation coefficients in the South decreased very little or not at all from the calibration period to the independent-check periods,

Table 14. Correlation Coefficients Between Reconstructions and Independent[a] Data in South Region.

Actual Recon- struction	Regional Index	3-Station[b] Index		San Diego Index	
	1901–1963	1883–1900	1901–1963	1851–1900	1901–1963
South LTR	.77	.75	.77	.58	.66
South PWV	.75	.80	.75	.62	.66

[a]Correlation with calibration series is also given in first column for comparison. This value is the square root of R from regression (see Appendix C).

[b]Computed as the regional index was, but from fewer stations. Stations for 3-station index were Riverside, San Diego, and Los Angeles.

Table 15. Correlation Coefficients Between Reconstructions and Independent[a] Data in North Region.

Actual Recon- struction	Regional Index	2-Station[b] Index		Walla-Walla Index	
	1897–1961	1885–1896	1897–1961	1874–1896	1897–1961
North LTR	.71	.71	.66	.49	.66
North PWV	.67	.64	.62	.54	.63

[a]As in Table 14.

[b]As in Table 14 except stations are Walla Walla, Washington and Hood River, Oregon.

indicating that the South regression statistics are probably reliable measures of reconstruction accuracy. The independent data check in the North (Figure 25, Table 15) was far less encouraging than in the South. Most notable was the large dropoff in Walla Walla's correlation with the LTR reconstruction from the calibration period to the 1874-1896 period.

Since the correlation coefficient is independent of mean levels and scale of variation, verification by correlation coefficient must be supplemented by information on accuracy of reconstruction of mean levels and variance or standard deviation. The calibration R^2 is verified on independent data only if (1) the correlation coefficient between actual and reconstructed data does not decrease appreciably from the calibration to the independent data, (2) the mean level is reconstructed well in the independent period, and (3) the ratio of variance of reconstructed data to variance of actual data is about the same in the calibration period and the independent period.

The relevant means and standard deviations for the South reconstructions (Table 16) do not appear to invalidate the results suggested by the correlation coefficients in Table 14. The means for the actual San Diego precipitation index are approximately equal to the reconstructed means in the independent-check period, and the ratio of the standard deviation of the reconstruction to the standard deviation of the San Diego series actually increases from the calibration period to the independent-check period (from .70 to .80 for the LTR model and from .74 to .86 for the PWV model).

The ratios of standard deviations in the North similarly change little from the calibration period to the independent-check period, but

Table 16. Means and Standard Deviation Ratios for San Diego Verifica-
tion — Series are South mean regional reconstructions by LTR
and PWV models, and actual precipitation index for San Diego.
$Ratio_1$ is ratio of standard deviation of LTR reconstruction
to standard deviation of San Diego index for period 1901-
1963. $Ratio_2$ is same for period 1851-1900.

Series	Mean	$Ratio_1$	$Ratio_2$
LTR	-.13	.70	.80
PWV	-.09	.74	.86
San Diego	-.09		

the mean level appears to have been reconstructed too low (Table 17).

The shortness of the independent period (1974-1896), however, makes it

difficult to draw conclusions from this result: although the actual

Walla Walla mean was .35, the standard error of the mean was .28.

Nevertheless, this result suggests that the North verification is even

poorer than indicated by the dropoff in r in Table 15.

The poor verification in the North may be due to the general

wetness of the entire independent data period, 1874-1896. In fact, the

two peaks in the plots of actual data (Figure 23) in 1877 and 1894

represent the two wettest September-August rainfall totals in the 1874-

1978 record at Walla Walla. These conditions would probably lead to a

relatively weak relationship between tree-ring indices and precipitation

fluctuations in the 1874-1896 period, considering the difficulty of

reconstructing extreme wetness from tree rings. The best solution to

Table 17. Means and Standard Deviation Ratios for Walla Walla Verification -- $Ratio_1$ and $Ratio_2$ are defined as in Table 16, except that $Ratio_1$ refers to period 1897-1961 and $Ratio_2$ to period 1874-1896.

Series	Mean	$Ratio_1$	$Ratio_2$
LTR	.118	.49	.50
PWV	.132	.45	.45
Walla Walla	.351		

the problem is probably to update the tree-ring data so that a longer, more representative period could be held back for independent check.

Interestingly, in the North and the South, the PWV reconstruction correlated higher than the LTR reconstruction with the longest independent data series. In addition, the PWV model reconstructed the mean levels in the independent period more accurately than the LTR models (Tables 16 and 17). These results contradict the implication given by the calibration period values of R^2 than the LTR is superior to the PWV model. This reversal in model accuracy may be due to the problem mentioned earlier of calibration of the LTR model to the particular sequence of wet and dry years in the calibration period.

Major Features of Long-Term
Reconstructions

Effects of Choice of Model. The long-term time series of the mean regional reconstructions are plotted in Figure 27. The noticeable differences due to type of reconstruction model are small, especially in
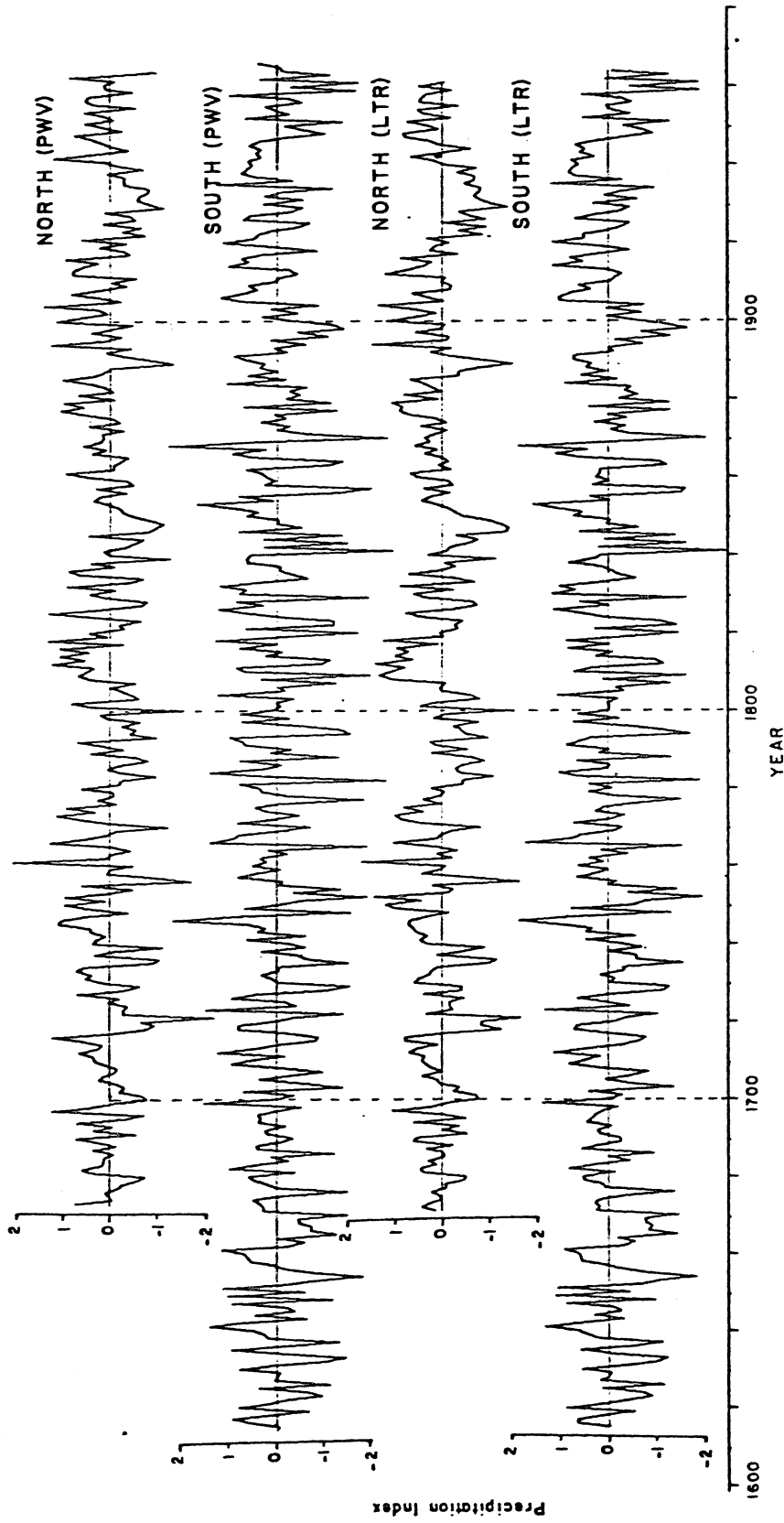
Figure 27. Time Series of Long-Term Reconstructed Precipitation Indices for the South Region and the North Region — Plots are mean regional reconstructions by the lagged-tree-ring model (bottom two plots) and the prewhitened-variables model (top two plots).

the South. The correlation coefficient is .90 between the two North

reconstructions and .97 between the two South reconstructions. The two

North reconstructions differ occasionally in the sizes of peaks, high-

frequency features, and deepness of some extended droughts (e.g.,

1930's, 1840's). The reasons for these differences were discussed

earlier regarding the single-site reconstructions. In the South, the

two plots in Figure 27 are so similar that it is difficult to pick out

differences by eye. The following discussion will refer to LTR recon-

structions unless noted otherwise.

North-South Contrasts. The North-South differences in Figure 27

are striking. Periods of drought or wetness in the two regions do not

coincide; this is true both for individual years and for extended dry or

wet periods. The correlation coefficients between North and South re-

constructions for different periods are as follows:

1897-1961	-.109
1832-1896	-.106
1767-1831	-.015
1702-1766	+.144
1673-1961	-.027

For comparison, the correlation coefficient between the actual precipi-

tation indices in the two regions for the 1897-1961 period is .001.

There is no evidence, therefore, of coupling of precipitation anomalies

in the two regions.

The lack of coherence of drought between the two regions is

shown more clearly in Figure 28, which delineates the 10 driest periods

in the regions in terms of moving averages of the reconstructed precipi-

tation index. Only in the mid-1840's, when the South was just pulling
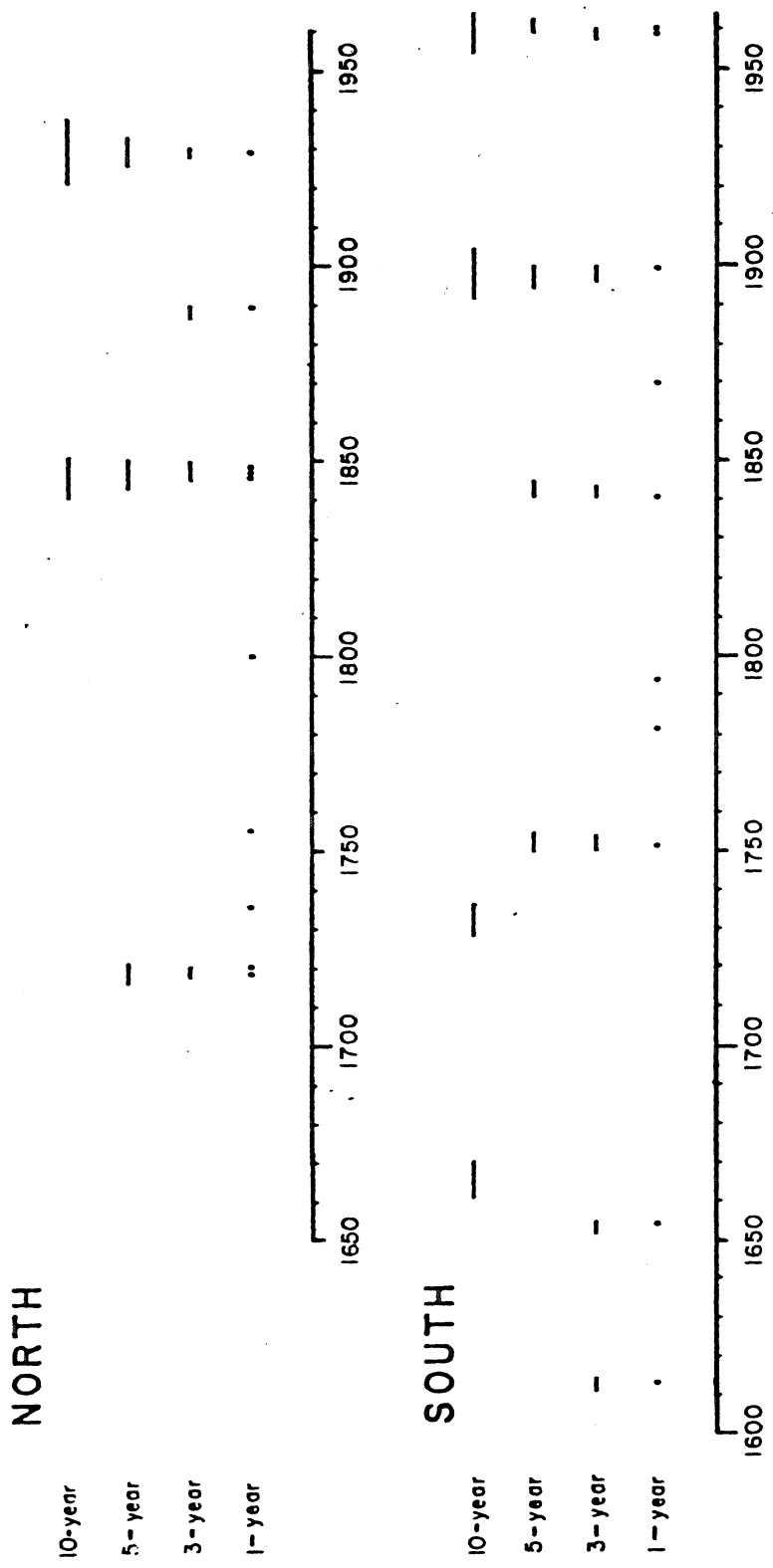
Figure 28. Driest Reconstructed Periods in the South and North Regions — Dots mark 10 driest single years of mean regional reconstruction (LTR model). Line segments mark 10 driest moving averages of various length. Number of line segments for a given moving average is fewer than 10 because some droughts overlap.

out of a drought and the North was entering a drought, did droughts overlap.

Reconstructed Drought History in the South. Figure 28 indicates that the droughts centered around 1900 and 1961 were outstanding in the context of the past several hundred years. The worst droughts of the calibration period 1901-1963 are compared with those of the entire 1612-1964 record in Tables 18 and 19. Two droughts--1959-1961 and 1895-1904--within the last hundred years were apparently representative of the worst droughts to hit the South region since 1612. The only 10-year period reconstructed drier than 1895-1904 was 1662-1671. Some historical evidence for a drought around 1670 is found in written records kept by missionaries, which indicate that the Pueblo Indians in New Mexico suffered greatly at this time. A great famine killed off half the population of the Indian village of Tesque, near Santa Fe in 1670 (Page 1980).

The general downward trend in rainfall (Figure 24) culminating in the severe drought of the early 1960's might tempt a hypothesis of changing climate in the Southwest. The long-term reconstruction does not seem to justify this hypothesis, however. Similar trends have occurred in the past, and the single-year extremes in 1961 or 1959 have been surpassed in the long-term record. Most important, the actual precipitation index (Figure 24) swung upward after 1961, and eventually reached a wet peak in 1978.

Reconstructed Drought History of the North. The long drought centered around 1930 is a conspicuous feature both in the actual data

Table 18. Worst Droughts in Long-Term Reconstruction in the South Region Compared to Worst Droughts in 1901-1963.

Moving Ave (years)	Model	Driest 1901-1963		N[a] 1615-1964	Driest 1615-1964	
		Year[b]	Index		Year[b]	Index
1	LTR	1959	-1.94	4	1841	-2.49
	PWV	1961	-1.74	11	1841	-2.81
3	LTR	1961	-1.43	0	1961	-1.43
	PWV	1961	-1.25	0	1961	-1.25
10	LTR	1963	-.58	9	1671	-.71
	PWV	1963	-.42	15	1671	-.59

[a]Number of years in the period 1615-1964 that were drier than the driest year in the period 1901-1963.

[b]Year given is last year of sequence for moving averages.

Table 19. Worst Droughts in Long-Term Reconstruction in the North Region Compared to Worst Droughts in the Period 1897-1961.

Moving Ave (years)	Model	Driest 1897-1961		N[a] 1673-1961	Driest 1673-1961	
		Year[b]	Index		Year	Index
1	LTR	1929	-1.41	5	1721	-1.67
	PWV	1929	-1.15	6	1721	-2.20
3	LTR	1931	-1.07	3	1848	-1.35
	PWV	1931	-.87	6	1721	-1.28
10	LTR	1935	-.78	0	1935	-.78
	PWV	1935	-.61	0	1935	-.61

[a]Number of years in period 1673-1961 that are drier than the driest year in period 1897-1961.

[b]Year given is last year of sequence for moving averages.

(Figure 25) and in the long-term reconstruction (Figure 27). The
drought is most notable for its duration rather than for severity in
individual years. A more intense drought occurred in the 1840's: three
of the 10 driest years of the entire reconstruction were 1846, 1847, and
1848.

Table 19 indicates that the 1840's and 1930's droughts dominated
the drought history of the North region. Both droughts included at
least one extremely dry year: 1929 was the sixth driest of the LTR
reconstruction, and 1847 was the seventh driest. Both droughts were
also long-lasting: the four driest 10-year moving averages were in the
1930's, and the fifth driest was 1842-1851.

The reconstructions support a conclusion arrived at by Keen
(1937, p. 184) in a study of tree stumps from logging operations in
eastern Oregon:

> The tree-ring record shows that between 1839 and 1854, when
> the emigrant trains were trekking into Oregon, the country was
> suffering from severe drought. Evidently, Goose Lake, Harney
> Lake, and many other lakes in the region were dry at that time,
> for when Goose Lake dried up in 1925 for the first time in the
> memory of present settlers, the ruts of a wagon road were
> clearly seen crossing the bed of the lake, indicating that in
> the 1840's there was no water in this lake to impede the
> progress of the early settlers. The tree-ring record indicates
> that this was undoubtedly the case, for the depression of
> growth rate during the 1840's and early 1850's was almost as
> severe as the present one.

The great 1930's drought was nearing its end at the time of
Keen's writing (see Figure 23). Wetter conditions returned after 1939,
and drought did not return through the end of the period covered by
the tree-ring data in this study. Extreme drought hit the region again

in 1973 and 1977, when the precipitation index was lower than in any other year in the 1897-1961 calibration period (see Figure 23).

The 1977 drought has been studied with great interest (Namias 1978, Buchanan and Gilbert 1977, Shelton 1978, and others) because of its effect on water supply. A rough estimate of the historical significance of the 1977 drought can be gained by comparing the precipitation index for that year (-2.02) with the index for the driest reconstructed years. Both the LTR and the PWV reconstructions showed 1721 as the driest year, but the reconstructed values differed:

	LTR model	PWV model	Actual
1721	-.1.67	-2.20	-
1977	-	-	-2.02

Even adopting the PWV value as representative of the driest conditions, 1977 would appear to approximate the worst single-year drought since 1673. Future tree-ring collections covering the year 1977 are needed for a more definite conclusion.

CHAPTER 4

CONCLUSIONS AND RECOMMENDATIONS

Conclusions

Nonclimatic persistence in tree rings can lead to errors in reconstructions of annual climatic or hydrologic time series. Non-climatic persistence can be properly adjusted for only if the lagged response of each tree-ring series to the variable to be reconstructed is understood.

Box-Jenkins methods can effectively be used to study the lagged response, and to select an appropriate lagging scheme for a reconstruction model. The number of past rings, or negative lags, in the reconstruction model can be selected by transfer-function modeling, assuming a linear system in which the climate or hydrologic series is regarded as input and the tree-ring index as output. The estimated impulse-response function of the system indicates the relative importance of past years' climate to the current ring; the decay pattern of the impulse response weights allows dependence on past year's climate to be reformulated as dependence on past years' tree-ring index. The lagged relationship can be further clarified by autoregressive-moving-average (ARMA) modeling. The crosscorrelations between residuals from ARMA models fit to the climatic or hydrologic series and the tree-ring index give the lagged relationship minus the possible masking effects of autocorrelation in the individual series. These crosscorrelations can be used to screen

out insensitive tree-ring series, and to select positive lags for the reconstruction model.

Transfer-function analysis of tree-ring indices and regional precipitation indices revealed at least two distinct forms of dependence on past years' rainfall. In the first form, dependence dropped off roughly as a simple exponential with time. The implied reconstruction model included the tree-ring index lagged t-1 to adjust for past years' climate. In the second form, dependence did not drop off as a simple exponential, but in a pattern resembling a damped sine wave or a mixture of exponentials. The implied reconstruction model included tree-ring indices lagged t-1 and t-2 to adjust for past years' climate. Climatically sensitive tree-ring series were represented by both forms. The general implication of this result is that the lagged response may vary from site to site, so that wholesale treatment of tree-ring indices by a single lagged model is inappropriate.

A useful conceptual model of the tree-ring response is that random shocks of climate deviations induce random shocks of tree-ring index deviations, with autocorrelation in the tree-ring index resulting from inertia in the system. The model was supported by the results of the crosscorrelation analysis on prewhitened series: when autocorrelation was removed from the rainfall index and the tree-ring indices, no lag was indicated in the response. The following reconstruction procedure consistent with the random-shock concept was devised.

1. The climate variable y_t and the tree-ring index x_t for a common period are fit to ARMA models. The residuals, or the prewhitened series from the models, represent the random shocks.

2. The prewhitened y_t is regressed against prewhitened x_t. No
    lags are included in the regression.

3. The prewhitened y_t is reconstructed by substituting the long
    term record of prewhitened x_t into the regression equation.

4. Autocorrelation is built back into the reconstruction with the
    original ARMA model used to prewhiten y_t.

Tree rings for years after year t do not enter explicity or im-
plicitly into the reconstruction for year t by this method when the ARMA
models are pure autoregressive, as for all the trial series. The
method therefore differs inherently from reconstruction models that
include positively lagged tree ring as predictors. Trial regressions
and reconstructions by the proposed method (PWV model) and by a model
using positively lagged tree rings (LTR model) indicated that each model
has its advantages and disadvantages. The LTR model generally yielded a
higher per cent variance explained (R^2) in calibration than the PWV
model. This higher R^2 was manifested by more accurate reconstruction of
the depths of troughs and peaks (low frequency variation), and of the
intensity of dryness in very dry years.

On the other hand, the PWV model has a more even frequency
response than the LTR model; the PWV model may therefore be preferable
when spectral properties of the reconstructed climatic or hydrologic
variable are of interest. In addition, the PWV model performed much
better relative to the LTR model on independent data than on calibration-
period data. This result may be due to calibration of the LTR model to
the particular <u>sequence</u> of wet and dry years in the calibration period.

If so, the calibration statistics of the LTR model may be misleading as indicators of expected accuracy of long-term reconstructions. The PWV model may therefore yield less impressive calibration statistics, yet more reliable reconstructions than the LTR model.

Although emphasis in this study was on methods, the resulting long-term mean regional reconstructions were interesting in themselves for their implications on the drought history of the South and North regions. Droughts in the two regions did not tend to coincide. The worst droughts since 1615 in the South were centered around 1665 and 1960. The unusual proximity of the two extremely dry years 1959 and 1961 caused the period 1959-1961 to be the driest 3-year moving average in the reconstructed series. The 1660's drought, on the other hand, was notable for its extent: the driest 10-year moving average of the South reconstruction was 1669-1671.

The drought history of the North was dominated by the droughts centered around 1847 and 1930. The years 1846, 1847, and 1848 were all among the 10 driest years of the North (LTR) reconstruction. The 49ers' bleak perception of the area at that time may therefore have been justified. The drought centered about 1930 was exceptional for its combined persistence and intensity. Seven of the ten driest 10-year moving averages of the North reconstruction overlapped the year 1935. Though 1977 was outside the period covered by the tree-ring reconstruction, comparison of the actual precipitation index for 1977 with the long-term reconstructions indicated that 1977 was possibly the driest single year since at least 1673.

<u>Recommendations</u>

The accuracy of the regional reconstruction could probably be improved with additional tree ring collections. A denser spatial grid of climatically sensitive sites in each region, especially the North, would provide more representative sampling of the regional climatic signal. In addition, the 15 to 20 years additional tree-ring data would allow either for longer calibration periods or longer independent verification. Tree-ring data for recent years would also allow the 1976-1977 drought to be viewed in the context of the past several hundred years more accurately than was possible with the present data base.

The effects of annual, large scale fluctuations of climate variables other than precipitation on tree rings should be studied. The reconstruction for 1934 in the North pointed out that precipitation along may be inadequate as a measure of drought stress on the trees, at least in some years. One possible approach is to reconstruct precipitation, and compare the time series of reconstruction residuals, or errors, to large scale anomaly patterns in various components of the energy balance—temperature, relative humidity, solar radiation, and wind speed. Even if this approach does not yield an optimum drought variable for calibration with tree rings, it may provide insight into the sources of errors in reconstructions.

Considerable work remains to be done on the problem of departure from non-linearity of the tree rings' response to moisture under very wet conditions. The accuracy in reconstructing extremely wet years could possibly be improved by calibrating with less positively skewed,

higher elevation precipitation series more representative of the rain-fall received by the trees, or with annual streamflow. Even these measures may not be sufficient, however, when the error in wet years is due to nonlinearity in the trees' response to moisture. Is the typical response linear up to some moisture level and nonlinear beyond, or is it nonlinear over the entire range of moisture conditions? How does this deviation from linearity vary from one location to another? Can nonlinearity be dealt with effectively by log-transforming the climate or hydrologic data? These questions are all important because nonlinearity limits the usefulness of methods such as those used in this study, which assume a linear system.

Transfer-function modeling should be applied to tree-ring systems using different types of input series. For example, for upper tree-line sites, mean annual temperature could serve as input; or for large watersheds, annual streamflow would serve as input. Transfer-function modeling would be especially applicable to these systems since the input variables may be appreciably autocorrelated. Seasonal rather than annual climatic inputs may also be appropriate for some series.

Extension to Large-Scale Studies

To focus on the lag in response of tree rings to climate, this study deferred consideration of spatial covariance among tree-ring sites until the step of averaging single-site reconstructions into regional mean reconstructions. Most modern tree-ring studies (see Chapter 1), on the other hand, emphasize spatial covariance much more strongly, and treat it more elaborately than by simple averaging.

The described methods can be adapted to such studies by breaking the reconstruction problem down into the sequential steps of filtering in time followed by filtering in space. Single-site reconstructions are nothing more than a time-filtered tree-ring index, where the filter is designed to amplify the annual climatic signal. For large-scale reconstructions using a grid of tree-ring sites, the time filtering could be accomplished for individual tree-ring series by single-site reconstruction of some regional climate variable, and the remainder of the large-scale reconstruction model could be done as before. The only changes are therefore as follows.

1. The original tree-ring indices are replaced with the time-filtered series (single-site reconstruction).

2. The lags are omitted from the large-scale reconstruction model.

Whether this approach is practical for any particular study depends on the resources available, since the single-site reconstructing requires transfer-function analysis and ARMA modeling of each tree-ring series separately. The extra effort, however, must be weighed against the increased understanding of the lagged response of the data and the possibility of more reliable long-term reconstructions.

APPENDIX A

COMPUTATION FORMULAS FOR AUTOCORRELATIONS
AND CROSSCORRELATIONS

Formulas for the sample autocovariance, autocorrelation, cross-covariance, and crosscorrelation are given in this appendix, along with formulas for the corresponding variances which may be used to set confidence limits on the sample functions.

Sample Autocovariance and Autocorrelation

The sample autocovariance $c_x(k)$ of time series x_t at lag k is given by

$$c_x(k) = \frac{1}{N-k} \sum_{t=1}^{N-k} (x_t - \bar{x})(x_{t+k} - \bar{x}) \qquad (A.1)$$

where N is the sample size, and $\bar{x}$ is the sample mean (Chatfield 1975, p. 25). The sample autocorrelation $r_x(k)$ is given by

$$r_x(k) = c_x(k)/c_x(0) \qquad (A.2)$$

where $c_x(k)$ and $c_x(0)$ are as in Equation (A.1) (Chatfield 1975, p. 25).

Variance of Autocorrelations

The variance of the estimated autocorrelation at lag k is given by

$$Var[r_x(k)] \simeq \frac{1}{N} (1 + 2 \sum_{i=1}^{k} r_x^2(i)), \qquad (A.3)$$

where terms are defined as in Equations (A.1) and (A.2), and the theoretical autocorrelations beyond lag k are deemed to have "died out" (Box and Jenkins 1976, p. 35).

Box and Pierce (1970) show that Equation (A.3) may greatly overestimate variances when the autocorrelations are of the residuals from an ARMA (p,q) model

$$x_t - \phi_1 x_{t-1} - \cdots - \phi_p x_{t-p} = a_t - \theta_1 a_{t-1} - \cdots - \theta_q a_{t-q} \qquad (A.4)$$

where

x_t = time series (mean subtracted),

a_t = ARMA residuals,

p,q = autoregressive and moving average orders of the model, and

$\phi_1, \phi_2 \cdots \phi_p, \theta_1, \theta_2 \cdots \theta_q$ are the model parameters.

If (A.4) is rewritten in infinite moving average form

$$x_t = a_t - \psi_1 a_{t-1} - \psi_2 a_{t-2} - \psi_3 a_{t-3} - \cdots \qquad (A.5)$$

where the ψ weights die out quickly, the variances of the sample auto-correlations of a_t are given approximately by

$$\mathrm{Var}[r_a(k)] \simeq \frac{1}{N} [\overleftarrow{I} - \overleftarrow{Q}]_k \qquad (A.6)$$

where N is the sample size, $\overleftarrow{I}$ is the identity matrix of rank p+q, and $[\overleftarrow{I} - \overleftarrow{Q}]_k$ is the kth diagonal element of the array $[\overleftarrow{I} - \overleftarrow{Q}]$. The array $\overleftarrow{Q}$ in Equation (A.6) is computed from the ψ weights of Equation (A.5) by the formula

$$\overleftarrow{Q} = \overleftarrow{\psi}(\overleftarrow{\psi}^T\overleftarrow{\psi})^{-1}\overleftarrow{\psi}^T \qquad (A.7)$$

where $\overleftarrow{\psi}$ is the p+q column matrix:

$$\overline{\psi} = \begin{bmatrix} 1 & & & & \\ \psi_1 & \cdot & \cdot & & \\ \cdot & \cdot & & \cdot & \\ \cdot & & \cdot & & \cdot \\ \cdot & & & \cdot & \\ \psi_m & & & & 1 \\ & & & & \psi_1 \\ & \cdot & & & \cdot \\ & & \cdot & & \cdot \\ & & & \cdot & \\ & & & & \psi_m \end{bmatrix} \qquad (A.8)$$

The ψ_i weights are assumed to be negligible for all $j >$ some m.

Sample Cross-Covariance and Crosscorrelation

The sample cross-covariance $Cov_{xy}(k)$ between time series x_t and y_t at lag k is given by

$$Cov_{xy}(k) = \begin{cases} \dfrac{1}{N} \sum\limits_{t=1}^{N-k} (x_t - \overline{x})(y_{t+k} - \overline{y}), & k = 0, 1, \ldots, N-1 \\[2em] \dfrac{1}{N} \sum\limits_{t=1-k}^{N} (x_t - \overline{x})(y_{t+k} - \overline{y}), & k = -1, -2, \ldots, -(N-1) \end{cases} \qquad (A.9)$$

where N is the sample size, and $\overline{x}$ and $\overline{y}$ are the sample means (Chatfield 1975, p. 173).

The sample crosscorrelations $r_{xy}(k)$ are given by

$$r_{xy}(k) = Cov_{xy}(k)/\sqrt{C_x(0) \cdot C_y(0)} \qquad (A.10)$$

where $C_x(0)$ and $C_y(0)$ are defined in Equation (A.1) (Chatfield 1975, p. 137.

Variance of Crosscorrelations

The variances of the sample crosscorrelations depend on the sample autocorrelations of the two component series. If the two series x_t and y_t are white noise, the variances may be estimated by

$$\text{Var}[r_{xy}(k)] \simeq \frac{1}{N} \tag{A.11}$$

where N is the sample size (Chatfield 1975, p. 173).

If either series is not white noise, the variance is given by

$$\text{Var}[r_{xy}(k)] \simeq \frac{1}{N-k} \sum_{i=-\infty}^{\infty} [r_x(i)r_y(i) + r_{xy}(k+i) \cdot r_{xy}(k-i)$$
$$+ r_{xy}^2(k)\{r_{xy}^2(i) + \frac{1}{2}r_x^2(i) + \frac{1}{2}r_y^2(i)\}$$
$$- 2r_{xy}(k)\{r_x(i)r_{xy}(i+k) + r_{xy}(-i)r_y(i+k)\}] \tag{A.12}$$

where N is the sample size, and $r_{xy}(i)$, $r_x(i)$, $r_y(i)$ are defined as in Equations (A.2) and (A.10). In practice, the sample autocorrelations and crosscorrelations are first computed, inspected, and assumed to be nonzero only over some small range of lags, so that the summation in Equation (A.12) is finite.

APPENDIX B

BACKWARD SHIFT NOTATION

Extensive use is made of backward shift notation (Box and Jenkins 1976, p. 8) in this paper. The notation is convenient for describing linear operations in a condensed form.

Backward Shift Operator

The backward shift operator B is defined by

$$Bx_t = x_{t-1}, \quad B^2 x_t = x_{t-2}, \quad \ldots, \quad B^i x_t = x_{t-i} \tag{B.1}$$

where x_t is a time series (mean subtracted).

Autoregressive Operator

The autoregressive operator $\phi(B)$ of order p is defined as

$$\phi(B) = 1 - \phi_1 B - \phi_2 B^2 - \ldots - \phi^p B^p \tag{B.2}$$

where $\phi_1, \phi_2, \phi_2, \ldots, \phi_p$ are the autoregressive parameters, and B, B^2, $\ldots$, B^p are defined as in Equation (B.1). The operator $\phi(B)$ applied to time series x_t yields

$$\phi(B)x_t = x_t - \phi_1 x_{t-1} - \phi_2 x_{t-2} - \ldots - \phi_p x_{t-p} \tag{B.3}$$

Moving Average Operator

The moving average (MA) operator $\theta(B)$ of order q is defined as

$$\theta(B) = 1 - \theta_1 B - \theta_2 B^2 - \ldots - \theta_q B^q \tag{B.4}$$

137

where $\theta_1, \theta_2, \ldots, \theta_q$ are the moving average parameters. The operators $\phi(B)$ and $\theta(B)$ are used together to represent the general ARMA (p,q) model:

$$\phi(B)x_t = \theta(B)a_t, \tag{A.5}$$

or equivalently,

$$x_t - \phi_1 x_{t-1} - \ldots - \phi_p x_{t-p} = a_t - \theta_1 a_{t-1} - \ldots - \theta_q a_{t-q} \tag{A.6}$$

where a_t are the ARMA residuals, and other terms are defined as in Equations (A.3) and (A.4).

Transfer-Function Operators

Transfer-function modeling makes use of an input operator

$$\omega(B) = \omega_0 - \omega_1 B - \ldots - \omega_s B^s, \tag{A.7}$$

and an output operator

$$\delta(B) = 1 - \delta_1 B - \delta_2 B^2 - \ldots - \delta_r B^r \tag{A.8}$$

such that the transfer function

$$y_t - \delta_1 y_{t-1} - \ldots - \delta_r y_{t-r} = \omega_0 x_t - \omega_1 x_{t-1} - \ldots - \omega_s x_{t-s} \tag{A.9}$$

can be written in the condensed form

$$\delta(B)y_t = \omega(B)x_t \tag{A.10}$$

Impulse Response Operator

The impulse response operator

$$V(B) = v_0 + v_1 B + v_2 B^2 + \ldots \tag{A.11}$$

allows the general linear input-output system

$$y_t = \sum_{i=0}^{\infty} v_i x_{t-i} + N_t \qquad\qquad (A.12)$$

to be written as

$$y_t = V(B)x_t + N_t \qquad\qquad (A.13)$$

where x_t and y_t are the input and output series (means subtracted), N_t is the noise, and v_0, v_1, v_2, v_3, ... are the impulse response weights.

APPENDIX C

REGRESSION STATISTICS

Regression were run with the SPSS (Nie et al. 1975) computer package. Equations listed below are from the indicated pages of the SPSS user's manual.

Per Cent Variance Explained, $R^2 \times 100$

The proportion of variance explained by regression is evaluated by the square of the multiple correlation

$$R^2 = \frac{\sum\limits_{t=1}^{N} (\hat{y}_t - \bar{y})^2}{\sum\limits_{t=1}^{N} (y_t - \bar{y})^2} \qquad (C.1)$$

where y_t is the observed time series of the predictand, $\hat{y}_t$ is the predicted series of y_t, $\bar{y}$ is the mean of y_t, and N is the sample size, or the number of years of data used in estimating the regression equation (Nie et al. 1975, p. 331).

F-Test for Significance of R^2

The test statistic for the null hypothesis of zero multiple correlation is given by

$$F = \frac{R^2/k}{(1-R^2)(N-k-1)} \qquad (C.2)$$

where k is the number of predictors, R^2 and N are defined as in Equation

(C.1), and the computed F is tested against an F-distribution with degrees of freedom k and $N-k-1$ (Nie et al. 1975, p. 335).

Adjusted R^2

Adjusted R^2 is the value of R^2 from Equation (C.1) for the number of predictors in the regression equation:

$$\text{Adjusted } R^2 = R^2 - \frac{(k-1)}{(N-k)} (1-R^2) \qquad (C.3)$$

where k is the number of independent variables, or predictors; and N is the sample size (Nie et al. 1975, p. 358).

Standard Error of Regression Coefficients

The estimated standard error of a regression coefficient B is given by

$$SE_B = \sqrt{\frac{\sum\limits_{t=1}^{N} (\hat{y}_t - y_t)^2 / (N-2)}{\sum\limits_{t=1}^{N} (x_t - \bar{x})^2}} \qquad , \qquad (C.4)$$

where x_t is the corresponding predictor variable with sample mean $\bar{x}$, and other terms are defined as before (Nie et al. 1975, p. 325).

APPENDIX D

FREQUENCY RESPONSE FORMULAS

Computational formulas for estimating the gain, phase, squared coherency, and intermediate spectral and cross-spectral quantities are given here, along with details relevant to the plotted functions in Figures 22 and 23.

Formulas for the various functions are taken from Chatfield (1975, pp. 139-140 and 180-182). Computations were carried out with the SPSS statistical package (Nie et al. 1975). Formulas for the confidence intervals on the gain, phase, and squared coherency are from Jenkins and Watts (1968).

The Parzen window with a truncation point of 15 lags was used for the plotted functions, although analyses were initially run with 10, 15, and 30 lags following the window-closing procedure recommended in Jenkins and Watts (1968, p. 280). The plotted bandwidth was computed as in Jenkins and Watts (1968, p. 152) by dividing the standardized bandwidth by the truncation point. All functions were evaluated at the frequencies

$$\omega = \pi j/M, \qquad j = 0,1,2, \ldots, M \qquad (D.1)$$

Spectral density function $f(\omega)$ of time series x_t.

$$\hat{f}_x(\omega) = \frac{1}{\pi}[\lambda_0 r_0 + 2 \sum_{k=1}^{M} \lambda_k r_k \cos(\omega k)] \qquad (D.2)$$

142

where r_k is the sample autocorrelation of x_t at lag k, and λ_k, k = 1,2,3, ..., M are the Parzen lag-window weights, with truncation point M.

Co-spectrum $\hat{c}(\omega)$:

$$\hat{c}(\omega) = \frac{1}{\pi} \left[\sum_{k=-M}^{M} \lambda_k r_{xy}(k) \cos(\omega k) \right] \tag{D.3}$$

where $r_{xy}(k)$ is the crosscorrelation at lag k between x_t and y_t.

Quadrature spectrum $\hat{q}(\omega)$:

$$\hat{q}(\omega) = \frac{1}{\pi} \left[\sum_{k=-M}^{M} \lambda_k r_{xy}(k) \sin(\omega k) \right] \tag{D.4}$$

Cross-amplitude spectrum $\hat{A}_{xy}(\omega)$:

$$\hat{A}(\omega) = \sqrt{\hat{c}^2(\omega) + \hat{q}^2(\omega)} \tag{D.5}$$

Phase $\hat{F}_{xy}(\omega)$:

$$\text{Tan } [\hat{F}_{xy}(\omega)] = -\hat{q}(\omega)/\hat{c}(\omega) \tag{D.6}$$

Squared coherency $\hat{C}(\omega)$:

$$\hat{C}(\omega) = \hat{A}_{xy}^2(\omega)/[f_x(\omega) \cdot f_y(\omega)] \tag{D.7}$$

Gain $\hat{G}(\omega)$:

$$\hat{G}(\omega) = \hat{A}_{xy}(\omega)/\hat{f}_x(\omega) \tag{D.8}$$

Confidence interval for gain (Jenkins and Watts 1968, p. 434): The 100 (1 − α) per cent confidence interval on the gain estimate is given by

$$\hat{G}(\omega) \left\{ 1 \pm \sqrt{\frac{2}{v-2} \, F_{2,v-2}^{(1-\alpha)} \, (\frac{1 - \hat{C}(\omega)}{\hat{C}(\omega)})} \right\} \qquad (D.9)$$

where $F_{2,v-2}$ refers to an F distribution with degrees of freedom 2 and $v - 2$, and

$$v = 3.71 \frac{T}{M}$$

is the number of degrees of freedom of a Parzen window with truncation point M, when the sample size is T years.

Confidence interval for phase:

The 100 $(1 - \alpha)$ per cent confidence interval for the phase (Jenkins and Watts 1968, p. 435) is given by

$$\hat{F}_{xy}(\omega) \pm \arcsin \sqrt{\frac{2}{v-2} \, F_{2,v-2}(1-\alpha) \, (\frac{1 - \hat{C}(\omega)}{\hat{C}(\omega)})} \qquad (D.10)$$

where terms are defined as in previous equations.

Confidence interval for squared coherency:

The two-standard-error confidence level for the squared coherency (Jenkins and Watts 1968, p. 379) is given by

$$c^*(\omega) \pm 1.96 \sqrt{\frac{.539M}{2T}} \qquad (D.11)$$

where $c^*(\omega)$ is the transformed variable

$$c^*(\omega) = \frac{1}{2} \ln \frac{1 + |\sqrt{\hat{C}(\omega)}|}{1 - |\sqrt{\hat{C}(\omega)}|} \qquad (D.12)$$

and T is the sample size or length of record.

REFERENCES CITED

Akaike, H. 1974. A new look at statistical model identification. *IEEE Transactions on Automatic Control*, AC-19(6), 716-723.

Blasing, T. J., and H. C. Fritts. 1976. Reconstruction of past climatic anomalies in the North Pacific and western North America from tree-ring data. *Quaternary Res.*, 6, 563-579.

Box, G. E. P., and G. M. Jenkins. 1968. Some recent advances in forecasting and control: part I. *Applied Statistics*, 17(2), 91-109.

Box, G. E. P., and G. M. Jenkins. 1976. *Time Series Analysis: Forecasting and Control*. Holden-Day, San Francisco.

Box, G. E. P., and D. A. Pierce. 1970. Distribution of residual autocorrelations in autoregressive integrated moving average time series models. *J. of the American Statistical Association*, 65(332), 1509-1525.

Bruce, J. P., and R. H. Clark. 1966. *Introduction to Hydrometeorology*. Pergamon Press, New York.

Bruggeman, W., and D. E. O'Neill. 1980. Comparison of classical econometric methods and multivariate time series analysis in assessing the relationship between consumption and income. In *Time Series*, edited by O. D. Anderson, North Holland Publishing Company, 182-207.

Buchanan, T. J., and B. K. Gilbert. 1977. The drought. *Water Spectrum*, 9(3).

Chatfield, C. 1975. *The Analysis of Time Series: Theory and Practice*. John Wiley & Sons, New York.

Cook, E. R. 1981. Lamont Doherty Geological Obs., Palisades, New York, personal communication.

Cooley, W. W., and P. R. Lohnes. 1971. *Multivariate Data Analysis*. John Wiley & Sons, Inc., New York.

Dawdy, D. R., and N. C. Matalas. 1964. Statistical and probability analysis of hydrologic data, Part III: analysis of variance, covariance, and time series. In *Handbook of Applied Hydrology*, edited by V. T. Chow, McGraw-Hill.

145

Douglas, A. V. 1976. Past Air-Sea Interactions over the Eastern North Pacific Ocean as Revealed by Tree-ring Data. Ph.D. dissertation, University of Arizona.

Douglas, A. V. 1980. Geophysical estimates of sea-surface temperatures off western North America since 1671. California Cooperative Ocean Fisheries Investigations Rep., XXI, 102-112.

Draper, N. R., and H. Smith. 1966. Applied Regression Analysis. John Wiley & Sons, Inc., New York.

Fritts, H. C. 1962. An approach to dendroclimatology: screening by means of multiple linear regression techniques. J. of Geophysical Research, 67(4).

Fritts, H. C. 1965. Tree-ring evidence for climatic change in western North America. Monthly Weather Review, 93(7), 421-443.

Fritts, H. C. 1974. Relationships of ring widths in arid-site conifers to variations in monthly temperature and precipitation. Ecological Monographs, 44(4), 411-440.

Fritts, H. C. 1976. Tree Rings and Climate. Academic Press.

Fritts, H. C., T. J. Blasing, B. P. Hayden, and J. E. Kutzbach. 1971. Multivariate techniques for specifying tree-growth and climate relationships and for reconstructing anomalies in paleoclimate. J. of Applied Meteorology, 10(5), 845-864.

Fritts, H. C., G. R. Lofgren, and G. A. Gordon. 1979. Variations in climate since 1602 as reconstructed from tree rings. Quaternary Research, 12, 18-46.

Glahn, H. R. 1968. Canonical correlation and its relationship to discriminant analysis and multiple regression. J. of the Atmospheric Sciences, 25, 23-31.

Harlow, W. M., and E. S. Harrar. 1968. Textbook of Dendrology. McGraw-Hill.

Henry, W. P., and J. J. Cassidy. 1978. What the design engineer needs from the hydrometeorologist. J. of Applied Meteorology, 17(10), 1558-1563.

Hipel, K. W., and A. I. McLeod. 1978. Preservation of the rescaled adjusted range, 2: simulation studies using Box-Jenkins Models. Water Resources Research, 509-516.

IMSL, International Mathematical and Statistical Libraries, Inc. 1980. Reference Manual, IMSL LIB-0008.

Jenkins, G. M., and D. G. Watts. 1968. Spectral Analysis and Its Applications. Holden-Day, San Francisco.

Keen, F. P. 1937. Climatic cycles in eastern Oregon as indicated by tree rings. Monthly Weather Review, 65(5), 175-188.

Kilmartin, R. 1976. Hydroclimatology: a needed cross-discipline. EOS Trans. AGU, 57(12), 920.

Kuehl, R. O., D. R. Buxton, and R. W. Briggs. 1976. Application of time series analysis to investigate crop and environment relationships. Agronomy J., 68, 491-495.

Lettenmaier, D. P., and S. J. Burges. 1978. Climate change: detection and its impact on hydrologic design. Water Resources Research, 14(4), 679-687.

Mandelbrot, B. B., and J. R. Wallis. 1968. Noah, Joseph, and operational hydrology. Water Resources Res., 4(5), 909-918.

Matalas, N. C. 1962. Statistical properties of tree-ring data. Bull. Int. Assn. Sci. Hydrol., 9(2), 39-47.

Meko, D. M., C. W. Stockton, and W. R. Boggess. 1980. A tree-ring reconstruction of drought in Southern California. Water Resources Bulletin, 16(4), 594-600.

Murrow, P. A., and V. C. La Marche, Jr. 1978. Tree-ring evidence for chronic insect suppression of productivity in subalpine Eucalyptus. Science, 201, 1244-1246.

Namias, J. 1978. Recent drought in California and western Europe. Reviews of Geophysics and Space Physics, 16(3), 435-458.

Nie, N. H., C. H. Hull, J. G. Jenkins, K. Steinbrenner, and D. H. Bent. 1975. SPSS: Statistical Package for the Social Sciences. McGraw-Hill.

O'Connell, P. E. 1971. Stochastic modeling of long-term persistence in streamflow sequences. Ph.D. thesis, Dept. of Civil Eng., Imperial Coll., London.

Page, J. K. 1980. Rebellious Pueblos outwitted Spain three centuries ago. Smithsonian, 86-95.

Pike, C. B. 1972. Some Meteorological Aspects of the Seasonal Distribution of Precipitation in the Western United States and Baja California. Univ. of California Water Resources Center, Contribution No. 139.

Rencher, A. C., and F. C. Pun. 1980. Inflation of R^2 in best subset regression. Technometrics, 22(1), 49-53.

Rodriguez-Iturbe, I., J. M. Mejia, and D. R. Dawdy. 1972. Streamflow simulation I: a new look at Markovian models, fractional guassian noise, and crossing theory. Water Resources Res., 8(4), 921-974.

Schulman, E. 1956. Dendroclimatic Changes in Semiarid America. University of Arizona Press, Tucson.

Sharma, T. C. 1980. Response functions applied to a drainage system. J. of Hydrology, 45, 279-287.

Shelton, M. L. 1978. Drought to flood, a sudden moisture reversal in California. Weatherwise, 31(3), 92-100.

Stockton, C. W. 1971. The feasibility of augmenting hydrologic records using tree-ring data. Ph.D. dissertation, University of Arizona., Tucson.

Stockton, C. W. 1975. Long-term Streamflow Records Reconstructed from Tree-rings. University of Arizona Press, Tucson.

Stockton, C. W., and W. R. Boggess. 1979. Augmentation of hydrologic records using tree rings. Proceedings of the Engineering Foundation Conference, Improved Hydrologic Forecasting--Why and How, ASCE, Pacific Grove, Calif., March 25-30, 239-265.

Stockton, C. W., and D. M. Meko. 1975. A long-term history of drought occurrence in western United States as inferred from tree rings. Weatherwise, 28(6), 245-249.

Stokes, M. A., and T. L. Smiley. 1968. An Introduction to Tree-ring Dating. University of Chicago Press, Chicago.

U. S. Weather Bureau, ESSA, and NOAA. Local Climatological Data, with Comparative Data, selected stations in the western United States. Washington, D. C., U. S. Weather Bureau to 1965, ESSA to 1970, and NOAA 1970 et seq.

Wallis, J. R., N. C. Matalas and J. R. Slack. 1974. Just a Moment: Article and Appendix of Graphs. U. S. Geological Survey. Reproduced by National Technical Information Service.

Wallis, K. F. 1977. Multiple time series analysis and the final form of econometric models. Econometrika, 45(6), 1481-1497.

Walpole, R. E., and R. H. Myers. 1972. Probability and Statistics for Engineers and Scientists. The Macmillan Company.

Whitehead, P. G. 1979. Applications of recursive estimation techniques
     to time variable hydrologic systems. J. of Hydrology, 40(1),
     1-16.

Zellner, A., and F. Palm. 1974. Time series analysis and simultaneous
     equation econometric models. J. of Econometrics, 2, 17-54.